PERFORMANCE BOUNDS ON THE LOCALIZATION OF CELLULAR PHONES USING RSS MEASUREMENTS WITH UNKNOWN PATHLOSS EXPONENTS

by

Veli Sari

B.S., Electronics and Communication Engineering, Istanbul Technical University, 2004

Submitted to the Institute for Graduate Studies in
Science and Engineering in partial fulfillment of
the requirements for the degree of
Master of Science

Graduate Program in Electrical and Electronics Engineering
Boğaziçi University

2010

ACKNOWLEDGEMENTS

I am heartily thankful to my thesis supervisor, Assist. Prof. Kerem Harmancı, whose encouragement, guidance and support from the initial to the final level enabled me to complete this thesis. I also would like to thank Prof. Emin Anarım and Assoc. Prof. Mehmet Akar for his valuable ideas and advices.

I offer my regards and blessings to all of those who supported me in any respect during the completion of thesis.

Finally, I am grateful to my family for their support and encouragement during my whole educational life.

ABSTRACT

PERFORMANCE BOUNDS ON THE LOCALIZATION OF CELLULAR PHONES USING RSS MEASUREMENTS WITH UNKNOWN PATHLOSS EXPONENTS

In this thesis, performance of an Received Signal Strength (RSS) based location estimation model, which incorporates the antenna radiation pattern information into log-normal path loss the signal model is evaluated. Performance bounds evaluated with most common technique called Cramer-Rao Lower Bound(CRLB) which puts a lower bound on the variance of a parameter estimate that can be achieved by any unbiased estimator. Being able to place a lower bound on the variance of any unbiased estimator proves to be extremely useful in practice. It provides a benchmark against which we can compare the performance of any unbiased estimator. Furthermore, it alerts us to the physically impossibility of finding an unbiased estimator whose vairance is less than the bound.

The Performance analyzing is done under various scenarious and solutions showed that this model is very robust against the variations in the signal propagation characteristics and it can be very useful in radio planning of cellular networks.

ÖZET

YOL KAYBI ÜSSELERİNİN BİLİNEMEDİĞİ DURUMLARDA RSS ÖLÇÜMLERİ İLE KONUMLANDIRMA PERFORMANS SINIRLARINI BELİRLEME

Bu çalışmada, standart log-normal yol kaybı modeline anten ışınım örüntüsünü dahil ederek Sinyal ölçümlerine (RSS) dayanan konum belirleme modelinin performans sınırları hesaplanmıştır. Bu modelin performansı en yaygın teknik olan Cramer-Rao alt sınırı (CRLB) ile değerlendirilmiştir. CRLB yansız bi kestirici ile elde edilebilecek parametrenin varyansı üzerinde en düşük alt sınırı verir. Yansız bir kestiricinin varyansı üzerine en düşük alt sınırı verebilmek pratikte oldukça faydalı olmaktadır. Başka bir kestirici performansı ile kıyaslama yapabilmesi önem kazanmaktadır. Ayrıca, fiziksel olarak verilen sınırdan daha düşük bir varyansı verebilecek yansız bir kestirinicinin bulunma ihtimalinin imkansızlığını otaya koyar.

Sinyal modelimizin performansı çeşitli senaryolar altında analiz edilmiş ve ortaya konulan sonuçlara dayanarak, geliştirilen modelin ortam parametrelerindeki değişimlere karşı dayanıklı olduğu ve anten ışınım bilgisinin hücresel iletişim ağlarının radyo planlamasında kullanılmasının yararlı olacağı gösterilmiştir.

TABLE OF CONTENTS

LIST OF FIGURES

LIST OF TABLES

LIST OF SYMBOLS/ABBREVIATIONS

A	Radiation Pattern
c	Speed of Light
d_0	Free Space Reference Distance
G	Antenna Gain
k	Representing Base Station Index
P	Transmitted Power
R	Received Power
s	Sectoral Indetifier
α	Path Loss Exponent
λ	Wavelength
ϕ	Azimuth Angle of BS
σ_v	Shadow Fading Standard Deviation
θ	Unknown Parameters
v	Random Variable Shadow Fading
AOA	Angle of Arrival
ALI	Automatic Location Identification
BS	Base Station
CI	Cell Identification
CPICH	Common Pilot Channel
CRLB	Cramer-Rao Lower Bound
E-911	Enhanced 911
E-112	Enhanced 112
ECR	Enhanced Call Routing
EM	Expectation Maximization
EOTD	Enhanced Observed Time Difference
FCC	Federal Communications Commission

F/S	Front to Side Ratio
GPS	Global Positioning System
LBS	Location Based Services
LMU	Location Measurement Unit
LOS	Line of Sight
LTE	Long Term Evolution
MLE	Maximum Likelihood Estimate
MS	Mobile Station
OTDOA	Observed Time Difference Of Arrival
PLE	Path Loss Exponent
PSAP	Public Safety Answering Point
RMSE	Root Mean Square Error
RSCP	Received Signal Code Power
RSS	Received Signal Strength
RSS-UPLE	RSS Unknown Path Loss Exponent Algorithm
SMLC	Serving Mobile Location Center
SMS	Short Message Service
TA	Timing Advance
TOA	Time of Arrival
TDOA	Time Difference of Arrival
TDMA	Time Division Multiple Access
TTFF	Time to First Fix
UMTS	Universal Mobile Telecommunication System

1. INTRODUCTION

Recently, location estimation has been among the most active research topics in the cellular communication systems. In a next-generation cellular phone, there is greatly a possibility that the service associated with the position information on a cellular phone will be developed. Therefore, the location estimation method using the cellular phone has been extensively studied. In the case of the system of a network base, location aware computing concept has gained considerable attention where devices are located or locate themselves and get services based on the location information.

With accurate position estimation, a variety of applications and services such as emergency services, monitoring and tracking for security reasons, location sensitive billing, fraud protection, asset tracking, fleet management, intelligent transportation systems, mobile yellow pages, and even cellular system design and management can become feasible for cellular networks [1]. These potential applications of wireless positioning have also been recognized by the IEEE, which set up a standardization group 802.15.4a for designing a new physical layer for low-data rate communications combined with positioning capabilities [2]. Also, the Federal Communications Commission (FCC) in the US has required wireless providers to locate mobile users within tens of meters for emergency 911 calls [3].

In fact, the Global Positioning System (GPS) is widely used for location estimation which is based on signals transmitted from satellites. Currently the best positioning acccuracy in cellular systems are provided by A-GPS(Assisted-GPS) at the cost of significant increase of network and handset complexity [4]. However, still GPS may not provide accurate result in urban areas, like Istanbul. This is because satellite signals are often reflected, deflected or blocked by high rise buildings and thus causing inaccurate estimations. In addition, in a city or a building there is often no direct line of sight between GPS satellite and terminal, which causes a severe degradation of accuracy. On the other hand, cellular radio network have good coverage in most of the populated areas. Hence using existing cellular network for location estimation could

be an alternative method for mobile location estimation and is a more economical as well as relatively less complex solution. Moreover, using existing cellular network can be used in such a case where GPS method cannot be applied, i.e. indoor positioning, but generally with a degradation in the accuracy.

Improving the accuracy of location estimation systems based on the existing cellular network infrastructure is the main goal of the positioning techiques which are widely discussed in literature [5], including time of arrival (TOA),time difference of arrival (TDOA), enhanced observed time difference (EOTD), angle of arrival (AOA), assisted global positioning system (AGPS), and received signal strength (RSS), where many of them are based on timing information [6–12].

Time-based solutions measure either the absolute or relative arrival times of several signals, backsolving the location of a handset through triangulation. Time-based solutions require precise synchronization for all base station clocks. Both TDMA and GSM (the most often deployed wireless system in the world) do not include the precise time synchronization of measurement in their original air interface standards. Thus, additional equipment is required for each base station. Because of the new hardware requirements, the deployment of time-based and angle-based schemes would cost at least several million dollars for a metropolitan area like istanbul. Furthermore, these schemes require a line-of-sight (LOS) link from the base station antenna to the handset in order to work well. In rural areas, these technologies have difficulty reaching enough base stations to perform triangulation; in urban areas, the absence of LOS degrades the performance of this technology [13].

Angle-based solutions use the precise measurement of the direction along the line of maximum signal strength at two or more base stations to triangulate the location of a handset. These techniques require high signal fidelity for super-resolution array processing. Therefore, sophisticated and expensive antenna array hardware is required for each base station.

RSS-based solutions use RSS measurements of the forward control channel, trans-

mitted by all base stations to find handsets. In TDMA (IS-136) systems, the mobile station can measure the power of up to 24 neighboring control channels. Unlike voice channels, the forward control channel is transmitted at a constant power and yields a reliable, repeatable measurement. In GSM systems, handsets report the measured powers of the six strongest control channels. In an RSS location scheme, no additional base station hardware is required because RSS measurements are all the information needed from the handset hardware. Furthermore, the RSS signature method does not require the existence of a LOS signal, which makes it an excellent solution for suburban, urban, and indoor environments.

The positioning method used in this thesis is based on received signal strength measurements and the main goal of this thesis to derive Cramer-Rao lower bound for performance evaluation of RSS positioning model and also compare with accuracy results given in [14], which claims that it resolves major shortcomings of the existing techniques which are assuming a perfect free space channel or known as a priori the channel conditions [15–20] and gives better accuracy in positioning evaluation, So, The CRLB results will be a key performance measure in positioning and give ideas about location accuracy evaluation.

In the first chapter, a short introduction to cellular location services is given. We presented the main forces for implementing location services and briefly discuss variety of applications that can be feasible for cellular networks. In chapter 2, wireless positioning methods are discussed and we describe most common existing location estimation technologies. In Chapter 3, it is presented the detailed literature survey on RSS based positioning. In chapter 4, RSS based location model is given with pathloss log-normal model as well as antenna radiation model. In chapter 5, which is main contribution of the thesis, Cramer-Rao bound analysis is presented and derivation for accuracy measurement given analytically. In Chapter 6, numerical analysis of Cramer-Rao bound and performance evaluation are given for different scenarious. The conclusions remarks are given in the last chapter.

2. AN INTRODUCTION TO LOCATION SERVICES

Location related services are described as the next revolution on services and functionality in the cellular network. A variety of applications such as [1]:

- Location emergency services
- Driving directions and assistance
- Location sensitive billing
- Tracking (packages, cars, people, asset etc.)
- Mobile yellow pages
- Cellular system design and management

can be feasible for cellular networks. The quality of services will all depend on the accuracy of the location estimates. This accuracy depends on the location technologies used, and on the network topology. However not all services requires the same accuracy on the location estimate.

This chapter will focus on the two main forces for implementing location services for the operator, government requirements and commercial services.

2.1. Government Requirements

Some regulations have accelerated the research of the location technologies.

2.1.1. Enhanced 911

The Enhanced 911(E-911) regulative by the US Federal Communications Commission (FCC) pushes location technologies in the USA [3]. In a series of orders since 1996, the FCC has taken action to improve the quality and reliability of 911 emergency services for wireless phone users, by adopting rules to govern the availability of basic 911 services and the implementation of E-911 for wireless services.

The Federal Communications Commission has several requirements applicable to wireless or mobile telephones [3]:

- Basic 911: All 911 calls must be relayed to a call center, regardless of whether the mobile phone user is a customer of the network being used.
- E911 Phase 1: Wireless network operators must identify the phone number and cell phone tower used by callers, within six minutes of a request by a PSAP.
- E911 Phase 2: Wireless carriers are required to provide Automatic Location Identification(ALI) as part of phase II E-911 implementation October1,2001 [21], as detailed given in Table 2.1.

Table 2.1. Accuracy required for locating mobile terminals in PII E-911

Solutions	67% of calls	97% of calls
Handset based	50 m	150 m
Network based	100 m	300 m

2.1.2. Enhanced 112

In Europe, the European Commission in 1998 established a universal 112 call number to support emergency services to both landline and mobile users. 112 calls will enable wireless and landline telephone callers in countries that are members of the European Union (EU) to dial a single number, 112, for fire, medical, and police emergencies. 112 calls are the European equivalent of the US 911 call. On July 12, 2000 the Commission of European Communities issued a proposal for a directive on universal service and users' rights relating to electronic communications networks. The proposed requirements for location accuracy in E-112 is given in Table 2.2. The caller's position must be available within 30 seconds of call initiation.

Table 2.2. Proposed requirements for location accuracy in E-112

	Highways	Rural	Suburban	Urban	Indoor
Caller can provide general information,	100-500 m	100-500 m	50-500 m	25-150 m	10-50 m

2.2. Location Based Services

A location-based service (LBS) is an information and entertainment service, accessible with mobile devices through the mobile network and utilizing the ability to make use of the geographical position of the mobile device [22].

2.2.1. Safety

A wide range of safety solutions open up by use of location technology:

- *Emergency alert services*, In public safety, a location system needs to track the emergency calls, provide the emergency dispatch team accurate location information, and send the team to its task quickly and safely.
- *Roadside assistance*, in the same way as with emergency alert services, if your car has a breakdown, it would be very useful to know exactly where the car is placed, saving both time and money.
- *Safety alarm*, social workers, watchmen and alone-working people like forestry workers, can send out a distress signal with an exact position, just by using the MS.

2.2.2. Location Based Charging

Location based charging allows a subscriber to be charged different rates depending on the subscriber's location or geographic zone, or changes in location or zone. The rates charged may be applicable to the entire duration of the call, or to only a part of the call's duration. This service may be provided on an individual subscriber basis, or on a group basis. E.g. when provided on an individual basis, this service could apply reduced rates to those areas most often frequented by the subscriber by taking into consideration the subscriber's daily route and life style. Different rates may be applied at country clubs, golf courses, or shopping malls. E.g. a "home" zone may be defined centred around a user's home, an agreed larger area, work or travel corridor or some unrelated zone. Additionally, different rates may be applied in different zones

based on the time of day or week.

In addition to being applicable on an individual basis, this service may be applicable on a group basis, which may be desirable e.g. for business groups. Locations may be defined for business groups to include corporate campuses, work zones or business zones with different charging rates. Individual and group subscribers should be notified of the zone or billing rate currently applicable, and be notified when the rate changes. Location based charging may be invoked upon initial registration. A charging zone would then be associated with the subscriber's location. When the subscriber moves to a different zone, the subscriber would be notified.

2.2.3. Fleet and Asset Management / Tracking Services

Fleet and asset management services allow the tracking of location and status of specific service group users. Examples may include a supervisor of a delivery service who needs to know the location and status of employees, parents who need to know where their children are, animal tracking, and tracking of assets. The service may be invoked by the managing entity, or the entity being managed, depending on the service being provided.

Fleet management may track the location of vehicles (cars, trucks, etc.) and use location information to optimize services.

Asset management services, for example, may range from asset visualisation (general reporting of position) to stolen vehicle location and reporting of location when an asset leaves or enters a defined zone.

2.2.4. Military Applications

In military applications, a geolocation system can help troops locate the enemies, provide maps for making attack plans, and navigate troops [23].

2.2.5. Traffic Monitoring/Tracking

Mobiles in cars could be anonymously sampled to determine average velocity of vehicles and detect and report congestion.

Congestion, average flow rates, vehicle occupancy and related traffic information can be gathered from a variety of sources including roadside telemetric sensors, roadside assistance organisations and ad-hoc reports from individual drivers.

2.2.6. Enhanced Call Routing

Enhanced Call Routing (ECR) allows subscriber or user calls to be routed to the closest service client based on the location of the originating and terminating calls of the user. The user may optionally dial a feature or service code to invoke the service. In addition to routing the call based on location, ECR should be capable of delivering the location information to the associated service client. For example, this capability may be needed for services such as Emergency Roadside Service. This could be used for the purpose of dispatching service agents for ECR service clients that can make use of this information.

2.2.7. Location based information services

Location based information services allow subscribers to access information for which the information is filtered and tailored based on the location of the requesting user. Service requests may be initiated on demand by subscribers, or automatically when triggering conditions are met, and may be a singular request or result in periodic responses. Examples of location based information services are described below [22].

City sightseeing: This would enable the delivery of location specific information to a sightseer. Such information might describe historical sites, providing navigation directions between sites, facilitate finding the nearest restaurant, bank, airport, bus terminal, restroom facility, etc.

Location dependent content broadcast: The main characteristic of this service category is that the network automatically broadcasts information to terminals in a certain geographical area. The information may be broadcast to all terminals in a given area or only to members of a specific group (perhaps only to members of a specific organization). The user may disable the functionality totally from the terminal or select only the information categories that the user is interested in. An example of such a service may be localized advertising. E.g. merchants could broadcast advertisements to passers-by based on location information.

Mobile Yellow Pages. The Internet has also changed how people find phone numbers. Instead of thumbing through the yellow pages or calling directory assistance you simply could go online and search the number. Wireless takes this one step further by adding the location of the subscriber to the search. Now the phone number of the nearest location can be ascertained as opposed to all locations within the nearest area. Mobile Yellow Pages services provide the user with the location of the nearest service point, e.g. Italian restaurant. The result of the query may be a list of service points fulfilling the criteria (e.g. Italian restaurants within three kilometres). The information can be provided to the users in text format (e.g. name of the restaurant, address and telephone number) or in graphical format (map showing the location of the user and the restaurants).

Finding friends: Friend finders services are now available that allow users to find the locations of their friends or family. The service uses Short Message Services (SMS), it operates in Europe and Southeast Asia and has become extremely popular. The service automatically notifies a user when a selected person (who also has a wireless device) is nearby or has entered into a specified area. Such a service could be designed to notify a parent when a child has arrived at home, school, or other specified location.

Driving directions and navigating: Another industry that is working at exploiting location technology is the automotive market. An application can be dynamic route guidance.

Dynamic route guidance can be described as a 'traffic-aware' turn-by-turn navigation system. A dynamic route guidance system would incorporate information or knowledge of road conditions in order to provide instructions on the quickest route to an end destination. Many factors can affect road conditions such as road closures, accidents, lane closures, construction, heavy congestion, major events, etc, and this information could be used by the system. Another alternative approach to providing dynamic route guidance would be to use speed information as the most important information element. Vehicle speed or how fast vehicles are travelling on a particular segment of a highway would be very useful in determining the shortest travel time to a destination and the availability of speed information would make a system more traffic-aware.

3. WIRELESS POSITIONING METHODS

Positioning systems operate by measuring radio signals traveling between a set of fixed stations and a mobile station. The mobile station's position is derived from known geometrical relationships of fixed stations, and measurements of the direction and/or length of the radio paths. In *self-positioning* techniques a positioning receiver placed in the mobile station makes the appropriate signal measurements and uses these measurements to determine its position. In *remote-positioning* methods a transmitter for the mobile station is required and receivers at more locations measure a signal from the object to be positioned. These measurements are collected at a central site where an estimate of the position of the object is determined.

Finding the position of a mobile device in relation to its cell site is a way to find out the location of a user. The cells in mobile radio communications vary considerably in size and shape. Their size can be up to 35 km radius in rural areas with good line-of-sight (LOS) between the base station and mobile users. In urban areas microcells have been proposed with some few hundred of meters in radius, sometimes covering only a small segment of a highway, a street along the side of a city block or a part of the park.

Table 3.1. Different cell types and dimensions

Cell type	Cell radius (m)
Large macrocell	3000-30000
Small macrocell	1000-3000
Microcell	100-1000
Picocell	10-100
Nanocell	1-10

The presence of LOS has a deep effect on radio propagation characteristics, and the size and shape of the cells should be adapted to ensure acceptable quality of communication in the whole area. Table 3.1 presents different types of cells, and their sizes. Various methods are adopted to determine the location of the mobile user [24]- [25].

Network based positioning relies on various means of triangulation of the signal from cell sites serving a mobile phone.

Positioning technologies of the mobile device can be divided into three main categories: Network and handset based technologies, and hybrid technology. In this chapter these three categories are briefly discussed, and important capabilities are identified and evaluated. This is done in order to give the reader an overview of the most common methods.

The position of a user can be determined using various techniques:

- Cell identification (CI)
- Angle of Arrival (AoA)
- Time of Arrival (ToA)
- Enhanced Observed Time Difference (E-OTD)
- Assisted GPS (A-GPS)

3.1. Network Based Technologies

Network based technologies have the advantage that they can be used with old mobile terminals. All the required updates for these methods to work, will be in the network.

3.1.1. Cell Identification and TA

Cell identification (CI) is the basic positioning method to start offering LBS, since all handsets support this technology. CI uses the network base transceiver station (BTS) to identify the user in the cell area. CI positioning can support all mobile users. CI can be used alone, or together with timing advance (TA) and network measurements reports, to improve the performance. GSM employs a timedivision multiple access (TDMA) scheme, and the successful operation requires that all signals arrive at the base station at the appropriate time. The time at which the signal from the handset is

sent must be varied depending of the distance to the base station. This is achieved by having each base station sending to each handy connected to it a timing advance (TA) report. TA is the amount by which the mobile station (MS) must advance the timing of its transmission to ensure that it arrives in the correct time slot. TA is reported in units of a bit period, which equates to an accuracy of 554 m [26].

Table 3.2. Accuracy of CI positioning

	Rural	Suburban	Urban	Indoor
Accuracy	1 km- 35 km typically 15 km	1 km - 10 km typically 5 km	500 m - 5 km for macro cells, 50 m - 500 m for microcells	10 m - 50 m for pico cells

The accuracy is dependent on cell size [24], [27] and it can be up to 250 m for an urban area to 35 km in rural areas, where network transmitters are widely separated, as shown in Table 3.2. The measurement only puts the user in a particular cell's circle of coverage. If the user is within reach of more than one cell, the ambiguity of position can be significantly reduced. Although the accuracy is not high, it is popular amongst the operators, as it does not require any modifications in the handset or the network. For that reason it is comparatively cheap to deploy. Figure 3.1 shows the positioning performance with cell identification and timing advance.

As in cellular systems handsets make measurements on the air interface and send them to the network for hand-over decisions, these measurement reports contain the estimated power level at the handset [24]. The power level can be used to estimate the distance between the base station and a handset, based upon simple propagation models and network planning tools. Accuracy is dependent on cell density, network configuration and radio environment. Enhanced cell identification performs poorly indoors and in rural areas with low base station density. The accuracy of the enhanced CI technique is presented in Table 3.3.

Especially in case of macro cells, there is a very poor positioning performance compared to other radio navigation techniques. Applying multisector antennas at the base station can improve the performance reducing the ambiguity of the position within

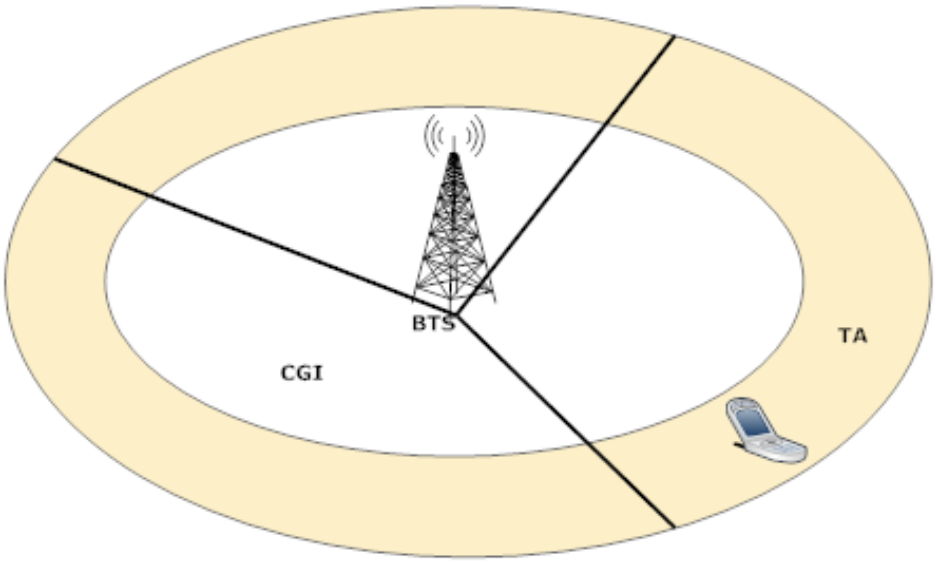

Figure 3.1. CI positioning with timing advance

Table 3.3. Accuracy of Enhanced CI positioning

	Rural	Suburban	Urban	Indoor
Accuracy	250 m - 35 km	250 m - 2,5 km	50 m - 550 m	variable

the cell.

3.1.2. Angle of Arrival

Angle of Arrival Method (AoA) is a technique that calculates the angles (directions) at which a signal arrives at two base stations from a handset, using triangulation to find the location [26], [28]. AoA requires a complex antenna array at each cell site. These antennas in principle work together to determine the angle relative to the cell site, from which a cellular signal originated. Simple geometric relationships are then used to determine the location by finding the intersections of the lines-of-position, if at least two base stations are able to determine the AoA of the signal.

AoA technique is more suitable for macrocells with higher elevations of antennas, reducing the problem of scattering environment. AoA method works poorly in ur-

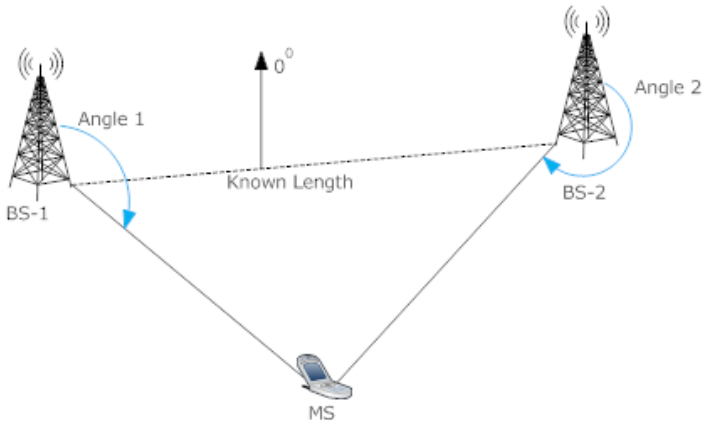

Figure 3.2. Angle of Arrival Method

ban settings with multipath reflections of the radio signals, where buildings and other obstacles interrupt radio signals.

3.1.3. Time of Arrival

Time of Arrival Method (ToA) is an enhanced positioning method. ToA technique measures the time of arrival of the signal from the mobile user to a number of base stations located at quite accurately known positions. Usually, the clock of the mobile station is not synchronized with the network stations. ToA method requires timing information obtained from the signals transmitted by a MS, which may be implemented in different ways for each cellular system. From measuring the time it has taken a signal to travel from transmitters to the user (self-positioning) or vice versa (remote-positioning), the range between those points can be determined and the user position can be calculated. The ToA technique requires a high degree of synchronism within the network of base stations, and the transmitted signals have to be time-tagged to enable range measurements. Where very accurate synchronisation of the network can be achieved, this technique can offer accuracy of location of around 125 to 200 m [27]. The cost benefit analysis is not very much in favour of the usage of this technology, as the cost of implementing this is very high as compared to the enhancement in the performance. It is expensive because of the large number of location measurement units (LMUs) required. The accuracy of ToA is definitely better than CI, but it is dependent on the visibility of the transmitter at LMU sites, as non-line-of-sight propagation with

signal reflections has a significant influence on the accuracy.

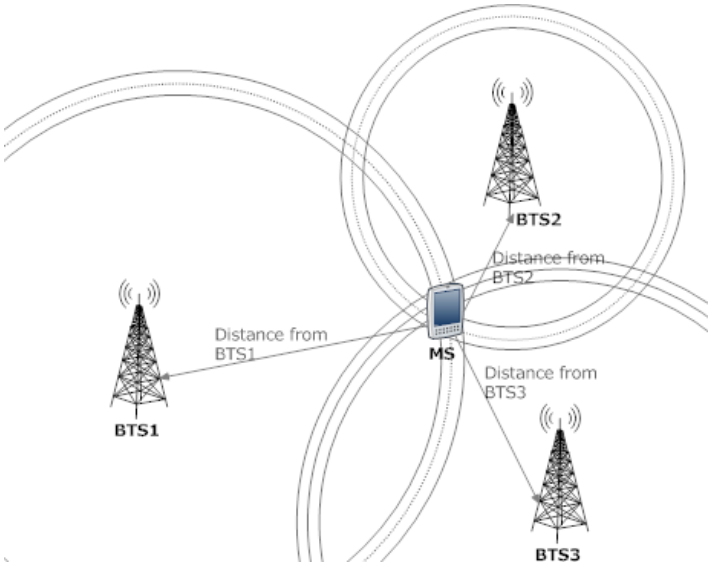

Figure 3.3. Time of Arrival Method

3.2. Handset Based Technologies

Handset based technologies have the best accuracy, but need new or upgraded mobile terminals.

3.2.1. Assisted GPS

Assisted GPS Method (A-GPS) is an advanced positioning method combining mobile technology and GPS. This technology is expensive for the endusers, as they have to invest in a GPS-equipped handset. Adding GPS functionality has a high impact on the handset with new hardware and software required. By itself, GPS can achieve the most accurate positioning, but this technology is often enhanced by the network. GPS receiver needs to be in sight of four or more satellites to estimate a three-dimensional position. Its implementation is therefore difficult in urban areas and indoor, where people spend most of their time. A-GPS uses techniques that enhance the sensitivity of the GPS receiver when it operates under unfavourable conditions (under foliage, in urban canyons or even inside a building) [27]. The process of getting the first fix from a GPS receiver - Time to First Fix (TTFF) - after it has been out of sight of any satellites for more than about three hours can take more than 10 minutes.

During this initial period the receiver has to acquire the signal and then download the navigation message with ephemeris data. The navigation message is transmitted at 50 bit/s, and the complete message is sent within a 12.5 minute period. If there is any fading of the signal during this period, it may be necessary to wait until the part of the message is broadcast again before the user's receiver obtains the satellites' accurate positions. In a poor reception area a GPS receiver could be unable to decode the vital part of the message if there are some interruptions in the received signal. In A-GPS technology a GPS reference receiver should be used connected to the network in such a way as to make available the ephemeris data from all of the satellites in view. This transmitted information brings improvements in time to first fix and battery life, as the handset no longer needs to search for and decode signals from each satellite. Accuracy of the A-GPS technique is shown in Table 3.4.

Table 3.4. Accuracy of Assisted GPS

	Rural	Suburban	Urban	Indoor
Accuracy	10 m	10 m - 20 m	10 m - 100 m	variable

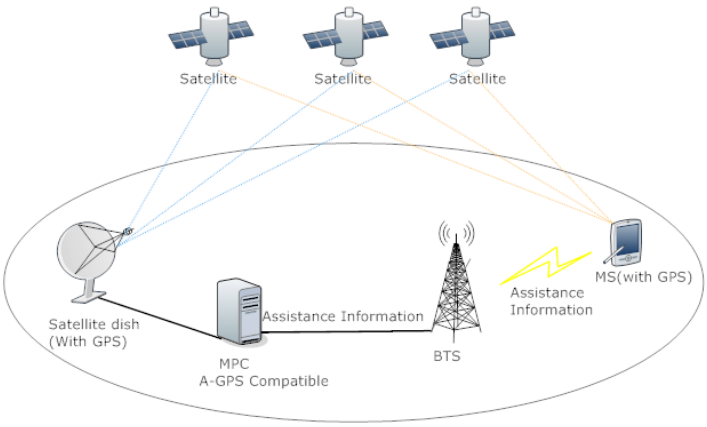

Figure 3.4. A-GPS Positioning

3.2.2. Received Signal Strength

RSS (Received Signal Strength) method is also known as signal-attenuation method to estimate the distance. As signals are prone to attenuation, signal attenuation-based methods attempt to calculate the signal path due to propagation. It is known

that the RSS value is directly related to the distance between MS and BS given by standart log-normal propagation model [1]. Since each radial distance estimate represents a circle with the corresponding BS in the center, intersections of the circles obtained from RSS measurements are chosen as candidate MS locations. More information will be found in Chapter 4 about RSS based positioning method.

3.3. Hybrid Technologies

3.3.1. Enhanced Observed Time Difference

Enhanced Observed Time Difference (E-OTD) is also an enhanced positioning method. This technique is a modification of the ToA method, and in E-OTD the handset measures the differences of arrival time of signals transmitted from at least three synchronized base stations. This time measurement capability is a new function in the handset. Timing measurements made by the handset are transfered to the Serving Mobile Location Center (SMLC). The measurements returned are related to the distance from each Base Transceiver Station (BTS) to the mobile station [24]. If the network is not synchronized the base station transmission time must be measured using a network with separate location receivers overlaid on the cellular network as location measurement units (LMUs) placed in fixed positions with the capability to perform E-OTD measurements and return them to the SMLC. Each of these LMU has an accurate timing source. Typically, one LMU is needed per 3 to 5 base stations [28]. When a signal from at least three base stations is received by an E-OTD software enabled mobile and the LMU, the time differences of arrival of the signal from each base station at the handset and the LMU are calculated. These time differences are combined to produce intersecting hyperbolic lines from which the location is estimated. E-OTD requires significant network investment and also requires specific software to be installed within the mobile station. The accuracy is dependent on cell density, cell plan, noise, interference, multipath, LMU performance and cell position accuracy, as shown in Table 3.5 [24]. The accuracy does not degrade much indoors, but has poor performance in rural environments with low BTS density [29].

Table 3.5. Accuracy of Enhanced-OTD positioning

	Suburban	Urban	Indoor
Accuracy	50 m - 150 m	50 m - 150 m	10-50 m

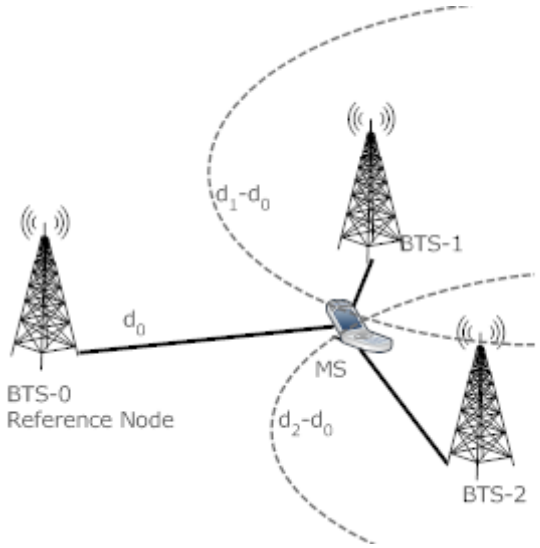

Figure 3.5. Time Difference Of Arrival

The timing measurements in a GSM network are only possible in units of a bit period, as with timing advance TA and observed time difference OTD the resolution is 1 bit. These measurements can be additionally degraded by multipath effects, and therefore the accuracy could be far worse than that indicated by the GSM specification. The accuracy requirement was determined by the needs of voice and data communication services, not for positioning. Both TA and OTD could be used for more precise positioning if the resolution would be increased and multipath rejection algorithms are used, to avoid measurements affected by late-arriving multipath signals.

In UMTS systems with spread-spectrum signalling techniques the main error source (multipath, nonline- of-sight propagation) is strongly reduced compared to GSM. Observed Time Difference Of Arrival (OTDOA) method with network configurable idle periods will offer positioning error typically 50 m or better.

4. RECEIVED SIGNAL STRENGTH IN LITERATURE

The power, or energy, of a signal traveling between two nodes is a signal parameter that contains information related to distance between those nodes. This parameter, commonly referred to as RSS, can be used together with pathloss and shadowing model to provide a distance estimate. Therefore, in the error-free-case, an RSS estimate at a node determines the position of the other node on a circle for two-dimensional positioning as shown in Fig. 4.1.

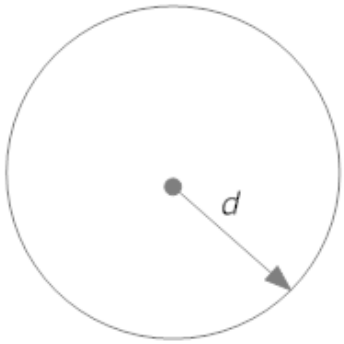

Figure 4.1. One node measures the RSS and determines the distance d between itself and the other node, which defines a circle of uncertainty

It is known that the RSS value is directly related to the distance between MS and BS given by standart log-normal propagation model [1]. Since each radial distance estimate represents a circle with the corresponding BS in the center, intersections of the circles obtained from RSS measurements are chosen as candidate MS locations.

The RSS based localization techniques can be divided into two categories: the distance estimation based and the RSS profiling based techniques. The path loss exponent (PLE) is a key parameter in the distance estimation based localization algorithms, where distance is estimated from the RSS. The PLE measures the rate at which the RSS decreases with distance, and its value depends on the specific propagation environment. Existing techniques on PLE estimation rely on both RSS measurements and distance measurements in the same environment to calibrate the PLE. However, distance measurements can be difficult and expensive to obtain in some environments.

With using directional antennas in cellular networks, measured RSS values also depend on the direction of transmission. A data fusion approach to mobile location estimation based on ellipse propagation model within a cellular radio network is given in [20]. Since BSs have directional transmission properties, i.e, the antenna transmits the largest power in one direction, while transmits small or none power in other directions, the contour line of the signal strength assumed is an ellipse instead of a circle. A statistical estimation of minimum mean square error (MMSE) estimator has been derived.

RSS measurements can be used to construct statistical methods to estimate directly MS location instead of extracting radial distance between the MS and the BS. RSS measurements are used to construct a probability distribution function of the MS location with given RSS observations in [18]. In addition, radiation pattern information of the sectors are included to the signal model to gain benefit from directivity of the antennas and a Maximum Likelihood(ML) estimate of the position is found with Bayesian update scheme as given in in [15]. And in [19], RSS measurements are used in conujunction with the information of MS velocity to obtain the ML estimate of the MS position. The velocity information is used to estimate the relative position of the MS for each RSS measurement.

Correct knowledge of propagation parameters in the path loss model leads accurate estimates of MS by using RSS measurements. In fact, in most of work done in previous researches assumes that propagation parameters are known priori or can be found by performing a training period. In [16], ML estimates of propagation parameters are obtained by employing a training period and measured RSS data is referred as incomplete since the reported RSS measurements are either truncated or quantized. In order to find estimate that minimizes the ML function using incomplete RSS measurements, an algorihtm named Expectation Maximization(EM) is employed in the proposed method.

However, propagation parameters can change depending on MS location or seasonal variations. So, to minimize these errors, propagation paramaters need to be

calibrated in real time. Three environments are classified as urban, suburban and rural in [30]. In the proposed algorithm a neural network scheme is used to estimate environment type and set the parameters of Hata propagation model according to the estimated environment type. Nevertheless, the algorithm is not able to overcome the need for a training period for each base station.

A location estimation problem that is similar to cellular communication networks exits in sensor networks. Generally, sensor networks are deployed randomly. Position of the sensor nodes need to be estimated using the RSS measurements in order to obtain a general picture of the network. In [31], some of the sensor nodes with known location in the network are responsible for obtaining the PLE in log normal path loss model using distance and measured RSS information for indoor localization of mobile nodes. To be able to apply this algorithm to cellular networks, some of the BSs are needed to be elected for PLE calculation. In [32], the PLE and the coordinates of the target node in a sensor network are calculated in real time by using the RSS measurements. Assuming that the number of the RSS measurements are larger than the number of unknowns, both the PLE value and the coordinates of the target node can be estimated simultaneously. An interesting result from this work is that the CRLB for unbiased estimators is outperformed because the proposed algorithm finds a biased estimator of the PLE. Although the algorithms proposed in [31] and [32] aim to adapt the PLE values in real time, they ignore the fact that PLE values for each channel can differ.

Since propagation parameters depend on the environmental characteristics, they can be different for every channel between an MS and BSs located at distinct locations. Thus, it is more appropriate to assume that propagation parameters are different for each channel to mitigate the errors due to errors in propagation parameters.

An algorithm that incorporates different PLEs for each link is proposed for sensor networks in [33]. This algorithm tries to find different PLEs for each channel and the position of the node that minimizes the root mean square (RMS) of the residuals between the measured RSS values and the estimated mean RSS values with a brute force algorithm. However, when the search area for the position of the node becomes

larger, time that is consumed to and a position estimate becomes considerably large.

In [34] it is proposed several techniques for online calibration of the PLE in WSN without relying on distance measurements. In fact, these techniques were proposed which are based on different assumptions about knowledge of distance information, i.e., such as assuming the probability distribution of distance between neighbouring sensors is known, and using some geometric constraints associated with planarity in a wireless sensor network. This technique gives an accurate estimate of α when there is no noise in power measurements, which is not a good assumption in wireless environment, since it has always noise in communication channel.

In [35] it is evaluated the feasibility and quality of self-localization that can be obtained using received signal strength (RSS) measurements from arrays of directional antennas on each sensor node. A suboptimal estimator that using angles of arrial as an intermediate statics has been derived.

Although directional antennas offer many potential performance advantages for sensor networks:e.g., decreased power consumption, reduced intereference, increased range, spatial reuse, and geographic routing. Many of these advantages come at the cost of increased complexity in communication.

Proposed method [36] is based on solving a nonconvex constrained weighted least squares problem. In this method, the propagation path losses from the mobile station (MS) to the BSs are measured, which are then converted to distances between them. For two dimensional positioning, eah RSS measurment will provide a circle centered at the corresponding BS, on which MS lie. In the absence of measurement error, the MS position is given by the intersection of circles from at least three BSs in order to resolve ambiguties from multiple crossings of the lines of position. In practical situation when RSS measurements are in errors, nonlinear LS in appropriate but computatianaly intensive approach for MS positioning. The main idea of the proposed algorithm is to transform the nonlinear equations relating the RSS measurements to the MS location into a set of linear equations by introducing an extra range variable. The linear equ-

ations are then solved by weighted lest squares (WLS) subject to the relation between the range parameter and the MS position coordinates. In fact, there is also assumption made here that a non-line-of-sigth (NLOS) detection algorithm has first been employed to eliminate the measurements with large errors. So, all the measurments that willl be utilized for the MS location assumed come from LOS propagation.

The method [37] relies on the assumption that there is a one-to-one mapping between RSS measurements and location. RSS measurements of the forward control channels, transmitted by cellular base stations, are implemented in IS-136, IS-54B, and other standards (IDEN) as part of mobile assisted (MAHO) procedure. The mobile station can measure the RSS up to 24 forward control channels(IS-136). However, even if the method can be implemented without any hardware requirements, the FCC requirement is not likely met. On the other hand, the mapping of location to RSS measurments needed to be find by calibration runs or by RF engineering tools and these data should be stored in database to find a minimal cost function.

When the statics of the RSS measurement error is known , the Maximum Likelihood (ML) estimator asymtotically optimal. However; due to the nature of the localization problem itself, the formed ML estimator is nonceonvex, causing search for the global minimum very difficult. In addition, its performance highly depends on the initial point provided if a local optimization method is applied to find the solution. To circumvent this problem, it is applied the Semidefinite Programming (SDP) relaxation technique to the RSS based localization problem [38]. The reformulation and relaxation results a convex SDP estimator. Thus, the selection of initial point is not important since any local minimum is also its global minimum. Even it outperforms by means of initial point selection, in case if number of hearable BS resources are greater than 4, the ML estimator gives better location estimation. And it this is the drawback of SDP estimator, since it cannot benefit from resources.

RSS measurements can also be used in conjunction with TAO or TDOA for enhanced estimation accuracy. In [39], two different hybrid schemes: TOA/RSS and TDOA/RSS have been analyzed, the Cramer Rao Bound are derived. It is clearly seen

that the benefits of the use of RSS measurements in conjucntion with TOA and TDOA, are evident for communication ranges below 30 m, which are characteristics for WSN. For longer rangers, hybrid schemes perform esssentialy the same as TOA and TDOA., which means it is not useful for longer rangers such as cellular networks.

An alternative approach derived in [40] to the location estimation problem. In this approach, signal properties, such as received power, angle of arrival, and / or propagation delay, are treated as random variables which are statistically dependent on the locations of the transmitter, the receiver, and the propagation environment. Log normal mathematical model has been used for the transmitter. Firstly, estimate the parameters using maximum likelihood and bayes rule applied and maximum a posterior value selected for location estimation. Even though the estimation results are encouraging, the work does not take into account the effect of the heterogeneity of the propagation environment.

A cooperative mobile positioning algorithm, based on the RSS measurements, is proposed in [41]. It is used a nonlinear least square optimization procedure to calculate the location of the mobile station with and without cooperation. It indicated that cooperation provides more accuracy. The standard log normal path loss model is also considered for MS-MS links addition to MS-BS links. This technique increases the complexity and computational cost and needs more effective data processing methods.

A two step location estimation method based on signal strength and wave scattering models is given in [42]. The Received Signal Level (RSL) method is first used in combination with Maximum Likelihood Estimation (MLE) and triangulation to obtain an estimate of the location of the mobile. Then, scattering 3D multipath channel model of Aulin is employed together with Extended Kalman Filtering (EKF) to obtain improved location estimates with high accuracy. The EKF is initialized at the MLE obtained from the RSL method. In realistic NLOS and multipath conditions the method does not perform well. In addition, it is given that estimation accuracy does not improve as the number of BSs used for triangulation increased, due to Kalman Filter sensitivity.

Another technique that employs RSS measurements is fingerprinting. In fingerprinting methods, a database, which consist of RSS measurements and the corresponding coordinates that the measurements are taken, is used. For indoor and outdoor environments, methods to construct the RSS database differs. For instance, a sliding window is applied on measurements for outdoor database collection, while RSS measurements are averaged for indoor database collection in [7]. Also fingerprinting methods differ on how they apply fingerprint matching. Among fingerprinting methods various signal difference norms are applied to find a match in the database [7]. In [8] a method that uses power delay profiles of CPICHs in UMTS is presented. Power delays of the visible CPICHs are compared with the power delay profiles in the database and the position that corresponds to the highest correlation with the measured signal is chosen as the position estimate. In [10] a database method is combined with a Bayesian method. Employing appropriate measurement models, MS motion models and maps of the predicted average received signal strength over the search area MS position is estimated with a recursive Bayesian Filter. Another method in [4] constructs the database by dividing the search area into grids and storing the most probable situation for visibility of CPICHs with corresponding results of RSCP measurements for each grid location. The method simply calculates the sum of squared residuals between measured values of the pilot carriers and values stored in the database for each grid. As a result, the grid that minimizes the sum of squared residuals is chosen as the MS location.

Among all these methods mentioned above, database techniques give the most accurate results. However the need for substantial amount of training data for each cell make them impractical. On the other hand, accuracy of other methods suffer from misleading propagation parameters. Most of the algorithms disregard the fact that propagation parameters of each channel can be different. Even if a training period is employed, propagation parameters vary depending on the position of the MS. Thus, a method that calibrates the propagation parameters for each channel in real time will significantly improve the accuracy of positioning with RSS measurements. Moreover, such an algorithm will not need preliminary work on site such as training data collection.

5. RSS-BASED LOCATION ESTIMATION MODEL

The received-signal-strength (RSS) based techniques have been proposed by many researches as a low-cost, low-complexity solution for location estimation in wireless networks since the measurement of the RSS is readily available in most of wireless systems without additional hardware components.

Reliable location estimation based on the RSS depends on accurate modeling of the pathloss characteristics of radio propagation channels, that is, the functional relationship between the received signal power and the distance between transmitter and receiver. In the most of existing studies of the RSS-based location estimation techniques in the literature, the channel model is assumed known a priori; that is, the pathloss characteristics of coverage area consider known either by assuming the environment is perfect free-space or by extensive measurement and modeling prior to deployment of location estimation systems. However, the PLE is environment dependent. Even in the same environment, the propagation charactristics may change considerably over a long period of time due to seasonal changes and weather changes [43].Therefore, a reliable wireless network needs to have a capability to accomodate and to adapt to the environment changes.

In this work we study the performance bounds (CRLB) on an RSS based location estimation scenario. In this scenario, the classic narrowband radio propagation model is used together with lognormal path-loss and shadow fading. At least three base-stations are assumed to measure RSS values from an MS. The BSs in this scenario each have three sectors with directional antennas with a known antenna pattern.

In an earlier study [14], the ML estimator that corresponds to this location scenario is implemented and its performance is measured. Note that this ML estimator produces biased estimates and the CRLB of the this work measures the best achievable performance for unbiased estimator. Therefore the MLE RMSE of [14] can be lower than corresponding CRLB in some cases.

In this chapter, short summary of system model is given. Path loss model, Antenna model, and problem formulation will be explained respectively.

5.1. Path Loss Model

Path loss (or path attenuation) is the reduction in power density (attenuation) of an electromagnetic wave as it propagates through space. Path loss is a major component in the analysis and design of the link budget of a telecommunication system.

Path loss may be due to many effects, such as free-space loss, refraction, diffraction, reflection, aperture-medium coupling loss, and absorption. Path loss is also influenced by terrain contours, environment (urban or rural, vegetation and foliage), propagation medium (dry or moist air), the distance between the transmitter and the receiver, and the height and location of antennas. The propagation losses may be caused by the natural expansion of the radio wave front in free space (which usually takes the shape of an ever-increasing sphere), absorption losses (sometimes called penetration losses) when the signal passes through media not transparent to electromagnetic waves or diffraction losses when part of the radiowave front is obstructed by an opaque obstacle, and losses caused by other phenomena.

In wireless communications, path loss can be represented by the path loss exponent, whose value is normally in the range of 2 to 4 (where 2 is for propagation in free space, 4 is for relatively lossy environments and for the case of full specular reflection from the earth surface-the so-called flat-earth model). In some environments, such as buildings, stadiums and other indoor environments, the path loss exponent can reach values in the range of 4 to 6. On the other hand, a tunnel may act as a waveguide, resulting in a path loss exponent less than 2 [44].

The path loss in a cellular communication system shows an increasing trend with distance from the BS. There are various path loss models in the literature, however, these models differ on how they incorporate the environmental characteristics into the model.

As a common approach, *Hata* model is used for signal prediction in macrocellular environments. This model is valid for the frequency range of 100-1500 MHz, distance of 1-20 Km, base station antenna height in between 30-200 m, and vehicular antenna height of 1-10 m [45, 46]. However, Hata model does not address the many new generation communication systems [e.g., UMTS, WiMAX, LTE] that feature smaller cells, shorter base station antenna heights, and higher frequencies. So, there are some modifications to this model and a suitable propagation model hs been given for the real time calibration of propagation parameters is given in Watt units as:

$$R(x,y) = \frac{P}{\beta \left(\frac{d(x,y)}{d_0}\right)^{\alpha}} 10^{-v/10} \tag{5.1}$$

where $R(x,y)$ is the received signal strength and P is the total power being transmitted by the BS on one channel. d_0 is the free space reference distance and $d(x,y)$ is the distance between MS and BS at point (x,y). Variable α is the PLE and it describes how quickly the signal attenuates as a function of distance (i.e. a slope or a steepness of the path loss curve). Variable v is the random variable describing the shadow fading deviation from the mean path loss value (in dB) which is present due to the fact that two spatially different locations having the same MS-BS separation may experience totally different kinds of radio paths. Therefore, measured signals may differ greatly in their mean predicted signal levels. Fast fading is not incorporated in the model since such effects are assumed to be averaged out in the measurements reported by MSs. Finally, β is found from *intercept* and calculated with the Equation 5.2 [47]:

$$\beta = (\frac{4\pi d_0}{\lambda})^2 \tag{5.2}$$

where $\lambda = c/f$ is the wavelength in meters. For GMS and UMTS operation frequencies are considered 900 Mhz and 2100 Mhz respectively, c is speed of light and d_0 is chosen as $1m$ considering microcell environment [45].

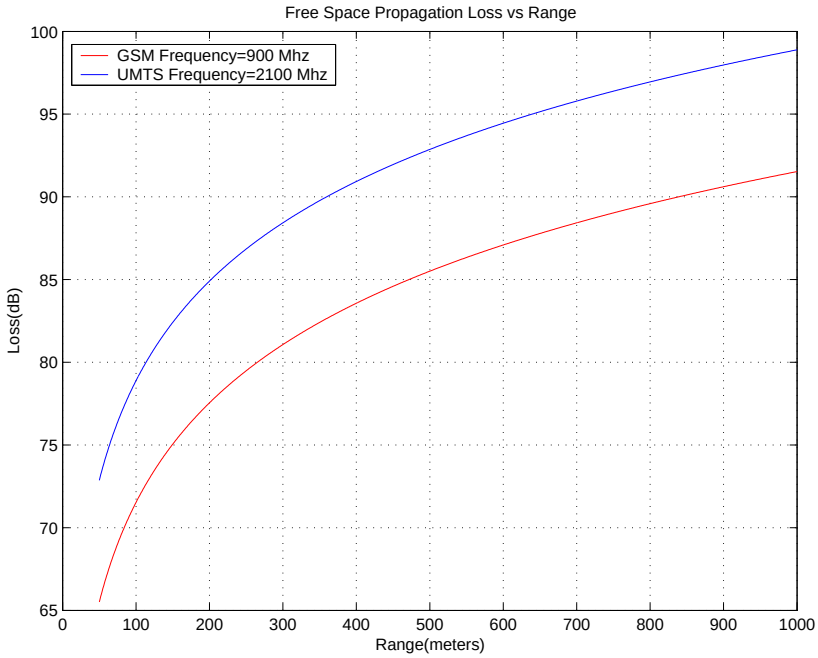

Figure 5.1. Free space propagation loss for both GSM and UMTS cases

The basic stating point for loss calculations is the free space loss, as this represents minimum possible loss. In log-normal propagation model of Eq.5.1, when $\alpha = 2$, it reduces to free-space loss which is $20\log_{10}(4\pi d/\lambda)$. As it is seen in Figure 5.1, the loss in UMTS is greater than the loss in GSM because of operational frequencies they use. The figure shows the phonomenon since RF energy reduces with distance as Maxwell's equations states.

Taking the logarithm of Equation 5.1 and defining received signal power in dB format:

$$R(x,y) = 10\log_{10}\left(\frac{P}{\beta}\right) - 10\alpha\log_{10}\left(\frac{d(x,y)}{d_0}\right) - v, \tag{5.3}$$

5.2. Antenna Radiation Model

A directional antenna or beam antenna is an antenna which radiates greater power in one or more directions allowing for increased performance on transmit and receive and reduced interference from unwanted sources [48]. Power distribution of an antenna

in every direction is given by the *radiation pattern*. Radiation pattern information for an antenna is obtained from the manufacturer [49].

If base stations are used in conjunction with directional (in azimuth) antennas, one base station may serve three cells by using three directional antennas over the designated area. This kind of schemes are commonly applied in GSM and UMTS systems [50]. In this way a better coverage of an area compared to a centrally located base station can be provided. The directivity of a base station antenna provides additional discrimination against signals for neighboring cells, therefore reducing adjacent and co-channel interference. Thus, the accurate knowledge of radiation pattern which can be used to estimate the signal level at every direction is needed to validate the assumptions made in the planning process regarding the coverage area [51]. It is assumed that the network consists of BSs that are operating in a three sector configuration with known radiation patterns where each sector is serving for one cell.

Cellular and point-to-multipoint wireless communication systems commonly use fan-beam antennas for sector coverage from the central station. An approximate formula describing the normalized azimuth radiation pattern of the fan-beam antenna using three parameters is given as [52]:

$$A(\phi) = exp[-a_{3dB}(\frac{|\phi|}{\phi_{HBW}})^{\tau}] \tag{5.4}$$

where a_{3dB}, ϕ_{HBW} and τ are used to adjust the pattern shape. a_{3dB} determines the pattern value at $|\phi| = \phi_{HBW}$ and ϕ_{HBW} is chosen to determine half power bandwidth. Thus,

$$a_{3dB} = -ln(\frac{1}{\sqrt{2}}) = 0.3465 \tag{5.5}$$

τ is used to match the pattern to a second field value, ν, at $|\phi| = |\phi_{\nu}|$ where $0 < \nu < 1$

as in Equation 5.6

$$\tau = \frac{ln(\frac{-ln(\nu)}{a_{3dB}})}{ln(\frac{|\phi_\nu|}{\phi_{3dB}})} \tag{5.6}$$

Then, $A(\phi_\nu) = \nu$. So, the Front-to-Side of the pattern set by an appropriate choice of ν and ϕ_ν. In the proposed algorithm, τ is evaluated at $|\phi_\nu| = \pi/2$, the value of ν is chosen as 0.006 that is the inverse of the front-to-side (F/S) ratio of the normalized pattern and $\phi_{HBW} = \pi/3$ as recommended in [52] according ETSI EN 301 215-2 Class CS 2 requirement in a Local Multipoint Distribution Service (LMDS) point-to-multipoint application.

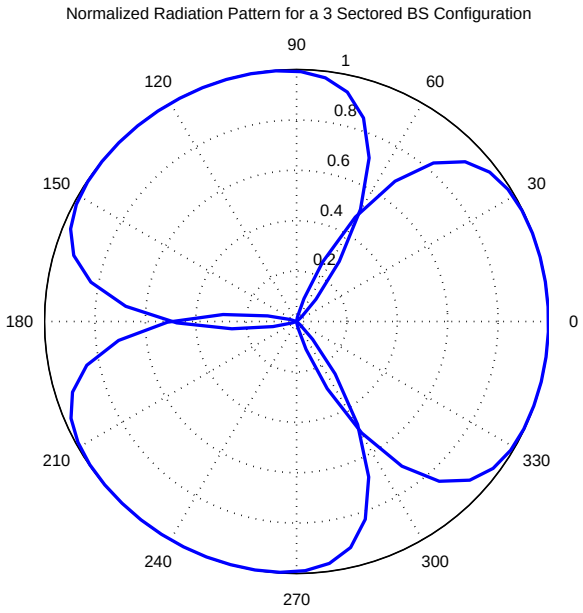

Figure 5.2. Normalized radiation patterns of a 3 sector BS configuration in Magnitude with $\phi_{HBW} = \pi/3$ and $F/S = -44dB$

In Figure 5.2, the radiation pattern with the corresponding parameters is shown for a sectoral BS configuration that employed in the signal model to approximate the radiation pattern of each sector.

Since multi-sector BSs are commonly used in cellular networks, amount of the transmitted power at a direction changes according to the radiation pattern. Therefore,

the path loss model given in previous section can be improved by adding the radiation pattern information which depends on the direction of transmission and antenna characteristic as shown in Equation 5.7.

$$R_{k,s}(x,y) = \frac{PGA_{k,s}^2(x,y)}{\beta\left(\frac{d_{k,s}(x,y)}{d_0}\right)^{\alpha}} 10^{-v_{k,s}/10} \tag{5.7}$$

Where, k and s represent the base station index and the corresponding sector index respectively. Each base station has 3 sectors and each transmitting cell represents one sector. $A_{k,s}(x,y)$ is the normalized radiation pattern that belongs to the base station k and sector s. G is the antenna gain in the azimuth direction and it is assumed that it does not change with each BS. $A_{k,s}(\phi)$ is represented as $A_{k,s}(x,y)$ since it is possible to determine ϕ with the knowledge of MS and BS coordinates. Taking the logarithm of Eq.5.7, we have:

$$R_{k,s}(x,y) = 10\log_{10}\frac{PG}{\beta} - 10\alpha\log_{10}\left(\frac{d(x,y)}{d_0}\right) + 20\log_{10}A_{k,s}(x,y) - v_{k,s}, \tag{5.8}$$

Here, it is assumed that P,G and β are known a priori and the received signal strength measurement into dB unit has been obtained.

5.3. Problem Formulation

It is supposed a target node is located at some unknown location (x,y) and n reference nodes are located at the known locations (x_k,y_k), $1 \le k \le n$.
The problem of RSS-based location estimation is **to estimate the unknown location coordinates of the target node** from RSS measurements of the radio signals transmitted from reference nodes to target node.
The unknown location coordinates can be estimated based on distance measurements by solving for the system of nonlinear equations [1].

$$\sqrt{(x-x_k)^2+(y-y_k)^2} = d_k, \qquad 1 \le k \le n, \tag{5.9}$$

where d_k is the measured distance between the target node and the kth reference node. The nonlinear equations for distance measurements-based location estimation can be related to RSS through the classic narrowband radio propagation pathloss model [53] and the path loss model can be improved by adding the radiation pattern information which depends on the direction of transmission and antenna characteristic $A(\phi)$ as it was given in previous section. Thus,

$$L_p = L_0 + 10\alpha \log_{10} d - 20 \log_{10} A(\phi) + v \tag{5.10}$$

where L_0 is the signal power loss in dB unit at 1m distance and, L_p is the signal power loss at a distance d ($d \geq 1m$), the parameter α is the distance power gradient (Path Loss Exponent, PLE), v is a Gaussian random variable representing log-normal shadow fading effects in multipath environments.

In radio propagation channel studies, the random variable v is considered zero-mean, $i.e., \approx N(0, \sigma_v^2)$, while its standard deviation σ_v^2 depends on the characteristics of a specific environment [53].

For a given wireless system, L_0 can be calculated or measured during the system calibration period and $L_p = P_t - P_r = 10 \log_{10} (PG/\beta) - 10 \log_{10} R(x, y)$ can be determined real-time at receiver node by measuring the received signal power P_r if the transmit signal power P_t is known.
$A(\phi)$ can be written explicitly in terms of base station and sector identifiers, k and s respectively. And since angle ϕ is only dependent on target location (x, y):

$$A_{k,s}(x, y) = exp[-a_{3dB}(\frac{|\Delta\phi_{k,s}(x, y)|}{\phi_{HBW}})^{\tau}]$$

where $\Delta\phi_{k,s}(x, y) = f^*(\phi_k(x, y) - \phi_{k,s})$, function f^* wraps the angle between $-\pi$ and π and is defined with following notation $f(x) = (x + \pi)_{mod2\pi} - \pi$.
ϕ_k:angle defined between kth base station and mobile station,
$\phi_{k,s}$:angle of initial sectoral orientation with respect to the "x" axis).
and angle ϕ notation can be seen explicitly in Figure 5.3.

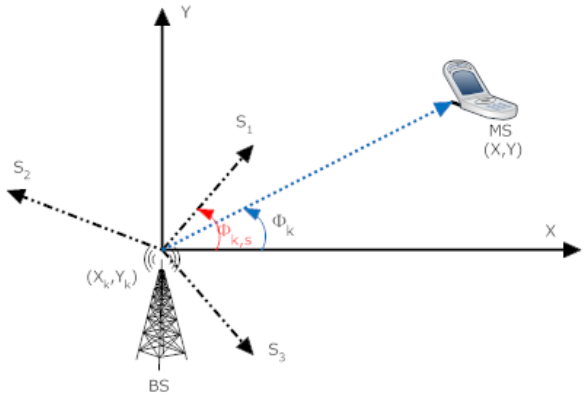

Figure 5.3. Angle ϕ definition on diagram

$\phi_k(x, y)$ is the equivalent of four quadrant-arctangent given below:

$$atan2(y,x) = \begin{cases} arctan(y/x), & \text{if } x > 0 \\ \pi + arctan(y/x), & \text{if } y \geq 0, x < 0 \\ -\pi + arctan(y/x), & \text{if } y < 0, x < 0 \\ \pi/2, & \text{if } y > 0, x = 0 \\ -\pi/2, & \text{if } y < 0, x = 0 \\ undefined, & \text{if } y = 0, x = 0 \end{cases} \tag{5.11}$$

Thus angle ϕ can be expressed analytically as:
$\phi_{k,s}(x, y) = arctan(\frac{y-y_k}{x-x_k}) + \pi sgn(y - y_k)U(x_k - x)$, where sgn is the signum function, and U is unit step function.

If we define $p = L_p - L_0$ which is observed pathloss in dB from 1m distance to d. By substituting (5.9) into (5.10), the system of nonlinear equations for location estimation can be rewritten as:

$$p_{k,s} = g_{k,s}(\theta) + v, \qquad 1 \leq k \leq n, \text{ and } 1 \leq s \leq 3 \tag{5.12}$$

where $g_{k,s}(\theta) = 10\alpha \log_{10} d_k - 20 \log_{10} A_{k,s}(\phi)$ and unknown vector paramater $\theta =$

$[\theta_1, \theta_2, \theta_3]^T = [x, y, \alpha]$, k is the index identifying the base stations while s is the index representing the antenna sector. For each base station k, there are three antenna sectors $s = 1, 2, 3$.

In vector form, it is going to be defined as follows:

$$\mathbf{p} = \mathbf{g}(\theta) + \mathbf{v} \tag{5.13}$$

where $\mathbf{p} = [p_1, ...p_n]^T, \mathbf{g}(\theta) = [g_1(\theta), ...g_n(\theta)]^T$ and $\mathbf{v} = [v_1, ...v_n]^T$
This is the signal model of the problem of RSS based location estimation for a system of BSs with three sector antennas.

In the next chapter it is derived the Cramer-Rao Lower Bound of the problem.

6. CRAMER-RAO BOUND ANALYSIS

6.1. Cramer-Rao Lower Bound

6.1.1. Introduction

The Cramer-Rao Lower Bound(CRLB) places a lower bound on the variance of a parameter estimate that can be achieved by any unbiased estimator. Being able to place a lower bound on the variance of any unbiased estimator proves to be extremely useful in practice. First, it allows us to assert that an estimator is the MVU (Minimum Variance Unbiased) estimator. This will be the case if the estimator attains the bound for all values of the unknown parameter. Second, it provides a benchmark against which we can compare the performance of any unbiased estimator. Furthermore, it alerts us to the physically impossibility of finding an unbiased estimator whose vairance is less than the bound. Although many such variance bounds are exist, the Cramer-Rao lower bound is by far the easiest to determine [54]. Also, the theory allows us to immediately determine if an estimator exists that attains the bound. If no such estimator exists, then all is not lost since estimators can be found that attain the bound in an approximate sense. For these reasons we restrict our discussion to the CRLB.

6.1.2. Derivation of CRB

The CRLB for RSS estimation depends on the strength of signal, Gaussian random variable and pathloss exponent. In radio propagation channel studies, the random variable v in the pathloss model (5.10), which represents shadow fading effects in multipath environments, is considered a zero-mean Gaussian random variable, *i.e.*, $N(0, \sigma_v^2)$, while its standard deviation σ_v^2 depends on the charasteristics of a specific environment [53].

Then the pathloss observation p_k defined in (5.13), has probability density func-

tion:

$$f(p_{k,s};\theta) = \frac{1}{\sqrt{2\pi}\sigma_v} exp(-\frac{(p_{k,s} - g_{k,s}(\theta))^2}{2\sigma_v^2}) \tag{6.1}$$

which is parameterized by unknown vector parameter θ. If we assume that $p_{k,s}$, $1 \leq k \leq n, 1 \leq s \leq 3$, are statistically independent observations, joint distribution of observation vector $\mathbf{p}$ becomes

$$f(\mathbf{p};\theta) = \prod_{k=1}^{n}\prod_{s=1}^{3} f(p_{k,s};\theta) \tag{6.2}$$

The CRB on the covariance matrix of any **unbiased estimator** $\hat{\theta}$ is defined as (in the positive semidefinite sense):

$$cov(\hat{\theta}) - \mathbf{F}^{-1} \geq 0, \tag{6.3}$$

where $\mathbf{F} = -E[\Delta_\theta(\Delta_\theta \ln f(\mathbf{p};\theta))^T]$ is the Fisher information matrix [54].

Given the joint distribution of the observation vector $\mathbf{p}$ in Eq.(6.2), equivalent log-likelihood function can be defined as (see Appendix A.1)

$$l(\theta) = -\frac{1}{2\sigma_v^2}\sum_{k=1}^{n}\sum_{s=1}^{3}(p_{k,s} - g_{k,s}(\theta))^2 \tag{6.4}$$

and the Fisher information matrix can be derived as (see Appendix A.1):

$$F_{ij} = [\mathbf{F}]_{ij} = -E[\frac{\partial^2 l(\theta)}{\partial\theta_i \partial\theta_j}] \tag{6.5}$$

$$= \begin{cases} \frac{1}{\sigma_v^2}\sum_{k=1}^{n}\sum_{s=1}^{3}(\frac{\partial g_{k,s}(\theta)}{\partial\theta_i})^2 & \text{if } i = j; \\ \frac{1}{\sigma_v^2}\sum_{k=1}^{n}\sum_{s=1}^{3}\frac{\partial g_{k,s}(\theta)}{\partial\theta_i}\frac{\partial g_{k,s}(\theta)}{\partial\theta_j} & \text{if } i \neq j. \end{cases}$$

Since, $g_i(\theta)$ is defined as $g_{k,s}(\theta) = 10\alpha \log_{10} d_k - 20 \log_{10} A_{k,s}(\phi)$ and unknown vector

parameter $\theta = [\theta_1, \theta_2, \theta_3]^T = [x, y, \alpha]$. The gradients of $g_i(\theta)$ can be extracted as given:

$$\begin{aligned}
\frac{\partial g_{k,s}(\theta)}{\partial x} &= -\frac{10\alpha}{\ln 10}\frac{u_{kx}}{d_k} - \frac{20}{\ln 10}\frac{\partial \ln A_{k,s}(x,y)}{\partial x} \\
\frac{\partial g_{k,s}(\theta)}{\partial y} &= -\frac{10\alpha}{\ln 10}\frac{u_{ky}}{d_k} - \frac{20}{\ln 10}\frac{\partial \ln A_{k,s}(x,y)}{\partial y} \\
\frac{\partial g_{k,s}(\theta)}{\partial \alpha} &= \frac{10}{\ln 10}\ln d_k
\end{aligned} \tag{6.6}$$

where u_{kx} and u_{ky} are defined $\frac{x_k - x}{d_k}$, $\frac{y_k - y}{d_k}$ respectively and $A_{k,s}(x,y) = exp[-a_{3dB}(\frac{|\Delta\phi_{k,s}(x,y)|}{\phi_{HBW}})^{\tau}]$

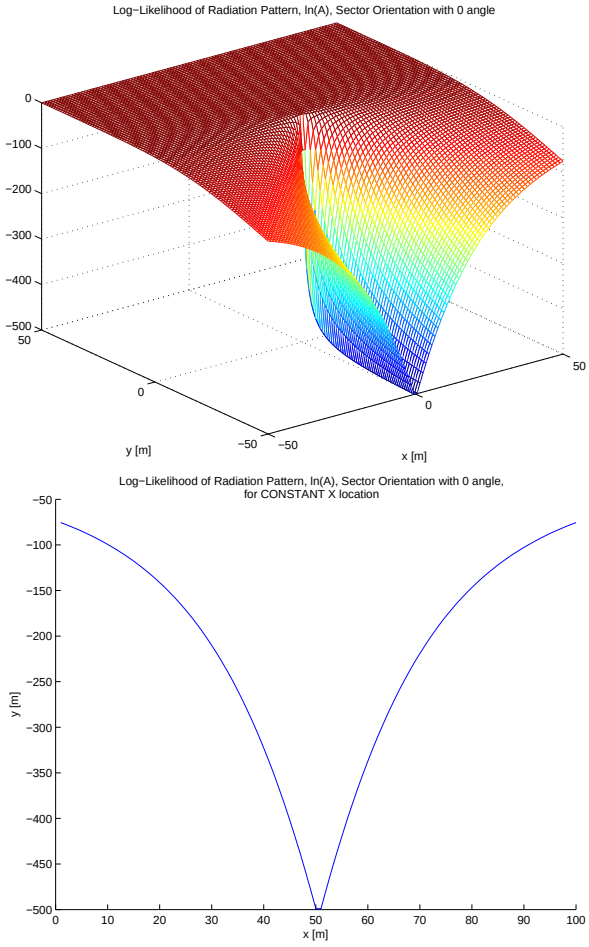

Figure 6.1. Plot of Log-Likelihood of Radiation pattern in field of [-50 50] m

As it is seen from the Fig.6.1, Log likelihood of radiation pattern is continuous but fails to be differentiable on the line which MS lies on direction of sector, since the

tangent slopes do not approach the same value from the left as they do from the right [Appendix C.1]. To avoid these cases, we make sure that MS is not in this locations:
Taking into account that $\phi_{k,s}(x,y) = arctan(\frac{y-y_k}{x-x_k})$ and definitions
$\frac{d}{dt}[|t|] = \frac{t}{|t|} = sgn(t)$, $\frac{d}{dt}(arctan(t)) = \frac{1}{1+t^2}$.

Thus, the partial derivatives of $A_{k,s}(x,y)$ can be expressed as follows:

$$\frac{\partial \ln A_{k,s}(x,y)}{\partial x} = D\frac{|\Delta\phi_{k,s}(x,y)|^\tau}{\Delta\phi_{k,s}(x,y)}\left(-\frac{u_{ky}}{d_k}\right) \tag{6.7}$$

$$\frac{\partial \ln A_{k,s}(x,y)}{\partial y} = D\frac{|\Delta\phi_{k,s}(x,y)|^\tau}{\Delta\phi_{k,s}(x,y)}\left(-\frac{u_{kx}}{d_k}\right) \tag{6.8}$$

where $D = a_{3dB}\frac{-\tau}{(\phi_{HBW})^\tau}$.

6.2. Accuracy Measures

Let $(\hat{x},\hat{y})$ be any unbiased location estimator. Then CRB in Eq.(6.3) gives lower bound on the variance of the unbiased estimator $(\hat{x},\hat{y})$; that is,

$$E[(\hat{x}-x)^2] \geq [\mathbf{F}^{-1}]_{11}, \qquad E[(\hat{y}-y)^2] \geq [\mathbf{F}^{-1}]_{22}, \tag{6.9}$$

In location estimation applications a more meaningful performance measure of location estimators is based on the geometric location estimation error $\epsilon = \sqrt{(\hat{x}-x_k)^2+(\hat{y}-y_k)^2}$.

The mean-squared error (MSE) of any unbiased location estimator is lower bounded as Eq.(6.9) describes:

$$\epsilon_{rms}^2 = E[\epsilon^2] \geq [\mathbf{F}^{-1}]_{11} + [\mathbf{F}^{-1}]_{22} \tag{6.10}$$

where ϵ_{rms} is defined as the root-MSE (RMSE) of location estimators.
Thus, from Eq.(6.10), we can determine the lower bound on the MSE of any unbiased

location estimator,

$$\epsilon_{rms}^2 \geq (F_{22}F_{33} - F_{23}^2 + F_{11}F_{33} - F_{13}^2)/|\mathbf{F}| \tag{6.11}$$

where $|\mathbf{F}|$ is the determinant of the Fisher information matrix. In the same way, we can determine the lower bound on the variance of any unbiased estimator of distance-power gradient α as:

$$\sigma_{\hat{\alpha}}^2 \geq (F_{11}F_{22} - F_{12}^2)/|\mathbf{F}| \tag{6.12}$$

So, the Fisher information matrix (3x3) is represented as follows:

$$\mathbf{F} = \begin{bmatrix} F_{11} & F_{12} & F_{13} \\ F_{21} & F_{22} & F_{23} \\ F_{31} & F_{32} & F_{33} \end{bmatrix}.$$

Since the FIM matrix is symmetric, $F_{12} = F_{21}$, $F_{13} = F_{31}$ and $F_{23} = F_{32}$; so, the

members are defined as:

$$F_{11} = \frac{1}{\sigma_v^2}\sum_{k=1}^{n}\sum_{s=1}^{3}\left(\frac{\partial g_{k,s}(\theta)}{\partial x}\right)^2$$
$$= \frac{1}{\sigma_v^2}\sum_{k=1}^{n}\sum_{s=1}^{3}\left(\frac{-10\alpha}{\ln 10}\frac{u_{kx}}{d_k} - \frac{20}{\ln 10}\frac{\partial \ln A_{k,s}(x,y)}{\partial x}\right)^2$$

$$F_{12} = \frac{1}{\sigma_v^2}\sum_{k=1}^{n}\sum_{s=1}^{3}\left(\frac{\partial g_{k,s}(\theta)}{\partial x}\right)\left(\frac{\partial g_{k,s}(\theta)}{\partial y}\right)$$
$$= \frac{1}{\sigma_v^2}\sum_{k=1}^{n}\sum_{s=1}^{3}\left(\frac{-10\alpha}{\ln 10}\frac{u_{kx}}{d_k} - \frac{20}{\ln 10}\frac{\partial \ln A_{k,s}(x,y)}{\partial x}\right)\left(\frac{-10\alpha}{\ln 10}\frac{u_{ky}}{d_k} - \frac{20}{\ln 10}\frac{\partial \ln A_{k,s}(x,y)}{\partial y}\right)$$

$$F_{13} = \frac{1}{\sigma_v^2}\sum_{k=1}^{n}\sum_{s=1}^{3}\left(\frac{\partial g_{k,s}(\theta)}{\partial x}\right)\left(\frac{\partial g_{k,s}(\theta)}{\partial \alpha}\right)$$
$$= \frac{1}{\sigma_v^2}\sum_{k=1}^{n}\sum_{s=1}^{3}\left(\frac{-10\alpha}{\ln 10}\frac{u_{kx}}{d_k} - \frac{20}{\ln 10}\frac{\partial \ln A_{k,s}(x,y)}{\partial x}\right)\left(\frac{10}{\ln 10}\ln d_k\right)$$

$$F_{21} = F_{12}$$
$$F_{22} = \frac{1}{\sigma_v^2}\sum_{k=1}^{n}\sum_{s=1}^{3}\left(\frac{\partial g_{k,s}(\theta)}{\partial y}\right)^2$$
$$= \frac{1}{\sigma_v^2}\sum_{k=1}^{n}\sum_{s=1}^{3}\left(\frac{-10\alpha}{\ln 10}\frac{u_{ky}}{d_k} - \frac{20}{\ln 10}\frac{\partial \ln A_{k,s}(x,y)}{\partial y}\right)^2$$
$$F_{23} = \frac{1}{\sigma_v^2}\sum_{k=1}^{n}\sum_{s=1}^{3}\left(\frac{\partial g_{k,s}(\theta)}{\partial y}\right)\left(\frac{\partial g_{k,s}(\theta)}{\partial \alpha}\right)$$
$$= \frac{1}{\sigma_v^2}\sum_{k=1}^{n}\sum_{s=1}^{3}\left(\frac{-10\alpha}{\ln 10}\frac{u_{ky}}{d_k} - \frac{20}{\ln 10}\frac{\partial \ln A_{k,s}(x,y)}{\partial y}\right)\left(\frac{10}{\ln 10}\ln d_k\right)$$
$$F_{31} = F_{13}$$
$$F_{32} = F_{23}$$
$$F_{33} = \frac{1}{\sigma_v^2}\sum_{k=1}^{n}\sum_{s=1}^{3}\left(\frac{\partial g_{k,s}(\theta)}{\partial \alpha}\right)\left(\frac{\partial g_{k,s}(\theta)}{\partial \alpha}\right)$$
$$= \frac{1}{\sigma_v^2}\sum_{k=1}^{n}\sum_{s=1}^{3}\left(\frac{10}{\ln 10}\ln d_k\right)^2$$

To evaluate RMSE

$$\epsilon_{rms}^2 \geq (F_{22}F_{33} - F_{23}^2 + F_{11}F_{33} - F_{13}^2)/|\mathbf{F}|$$

we have to find each multiplication and determinant of FIM matrix. However, the computation complexity can be reduced if we derive the interpretation of accuracy measures by utilizing the definitions of cross product and dot product of geometric vectors.

Given two geometric vectors $\mathbf{a} = a_x\mathbf{u_x} + a_y\mathbf{u_y}$ and $\mathbf{b} = b_x\mathbf{u_x} + b_y\mathbf{u_y}$, the cross product of two vectors can be written as:

$$\mathbf{a} \times \mathbf{b} = (a_x b_y - a_y b_x)\mathbf{u_z}$$

Where $\mathbf{u_z} = \mathbf{u_x} \times \mathbf{u_y}$ is the unit vector in the direction of z axis. If we further define the angle of a vector, denoted by ϕ, as the angle measured from x axis in counter-clockwise direction as in polar coordinate system, the cross product and dot product of two vectors becomes:

$$\mathbf{a} \times \mathbf{b} = |\mathbf{a}||\mathbf{b}| \sin\phi_{ab}\mathbf{u_z},$$
$$\mathbf{a} \bullet \mathbf{b} = |\mathbf{a}||\mathbf{b}| \cos\phi_{ab}$$

where $\phi_{ab} = \phi_b - \phi_a$, ϕ_a and ϕ_b being the angles of vectors $\mathbf{a}$ and $\mathbf{b}$.

Applying these definitions to two vectors, $\mathbf{u_i} = u_{ix}\mathbf{u_x} + u_{iy}\mathbf{u_y}$ and $\mathbf{u_j} = u_{jx}\mathbf{u_x} + u_{jy}\mathbf{u_y}$, we can derive that

$$\mathbf{u_i} \times \mathbf{u_j} = (u_{ix}u_{jy} - u_{iy}u_{jx})\mathbf{u_z} = \sin\phi_{ab}\mathbf{u_z},$$
$$\mathbf{u_i} \bullet \mathbf{u_j} = (u_{ix}u_{jx} + u_{iy}u_{jy}) = \cos\phi_{ij}$$

After some tedious derivation, the lower bound on the accuracy measures defined in

6.10 can be written as (see Appendix B.1)

$$\epsilon_{rms}^2 \geq (\sigma_v/\alpha)^2 . GDOP_{xy}^2 \tag{6.13}$$

Where $GDOP_{xy,u}$ is the geometric dilution of precision [32] and it is given as:

$$GDOPxy,u = \frac{\ln 10}{10}\frac{1}{3}\sqrt{\frac{\sum_{k=1}^{n-1}\sum_{t=k+1}^{n}[(\frac{\ln d_t}{d_k}-\frac{\ln d_k}{d_t})^2+2\frac{\ln d_t \ln d_k}{d_k d_t}(1-\cos\phi_{kt})]+ETerms*}{\sum_{m=1}^{n}[\sum_{k=1}^{n-1}\sum_{t=k+1}^{n}\frac{(\ln d_m)^2}{d_k^2 d_l^2}\sin^2\phi_{kl}+\sum_{k=1}^{n-1}\sum_{l=1}^{n}\frac{\ln d_l \ln d_m}{d_k^2 d_l d_m}\sin\phi_{kl}\sin\phi_{mk}]+ETerms^{**}}} \tag{6.14}$$

In fact, by defining GDOP, it will be easy to analyze the effect of environmental parameter, α and σ_v, and the geometric parameters, d_k and ϕ_k.
Actually, since $ETerms$ in GDOP is difficult to simplify with pure ϕ parameter, we will not analyse the angular distribution of Base stations on field. But numerical analyses will be in our study.

6.2.1. Accuracy Measures for Distinct PLE

In previous sections, we assumed that the Path loss exponent value is same for all base stations in our coverage area. However, in most cases, this assumption does not usually hold because of the environment dependency of PLE value. Thus, we are going to evaluate the performance of the model considering a scenario where each base station has a different PLE value.

In the general case, $g_i(\theta)$ is defined as $g_{k,s}(\theta) = 10\alpha_k \log_{10} d_k - 20\log_{10} A_{k,s}(\phi)$
Unknown vector paramater $\theta = [\theta_1, \theta_2, ..., \theta_k]^T = [x, y, \alpha_1, \alpha_2, ..., \alpha_k]^T$. The gradients

of $g_i(\theta)$ can be extracted as given:

$$\begin{aligned}
\frac{\partial g_{k,s}(\theta)}{\partial x} &= -\frac{10\alpha_k}{\ln 10}\frac{u_{kx}}{d_k} - \frac{20}{\ln 10}\frac{\partial \ln A_{k,s}(x,y)}{\partial x} \\
\frac{\partial g_{k,s}(\theta)}{\partial y} &= -\frac{10\alpha_k}{\ln 10}\frac{u_{ky}}{d_k} - \frac{20}{\ln 10}\frac{\partial \ln A_{k,s}(x,y)}{\partial y} \\
\frac{\partial g_{k,s}(\theta)}{\partial \alpha_1} &= \left(\frac{10}{\ln 10}\ln d_1\right)\delta_{k1} \\
\frac{\partial g_{k,s}(\theta)}{\partial \alpha_2} &= \left(\frac{10}{\ln 10}\ln d_2\right)\delta_{k2} \\
\frac{\partial g_{k,s}(\theta)}{\partial \alpha_3} &= \left(\frac{10}{\ln 10}\ln d_3\right)\delta_{k3} \\
&\vdots \\
\frac{\partial g_{k,s}(\theta)}{\partial \alpha_l} &= \left(\frac{10}{\ln 10}\ln d_k\right)\delta_{kl}
\end{aligned} \tag{6.15}$$

where u_{kx} and u_{ky} are defined $\frac{x_k - x}{d_k}$, $\frac{y_k - y}{d_k}$ respectively and $A_{k,s}(x,y) = exp[-a_{3dB}(\frac{|\Delta\phi_{k,s}(x,y)|}{\phi_{HBW}})^{\tau}]$ So, the size of fisher information matrix increases to k+2, and it can be represented as follows:

$$\mathbf{F}_{k+2,k+2} = \begin{bmatrix} F_{1,1} & F_{1,2} & \cdots & F_{1,k+2} \\ F_{2,1} & F_{2,2} & \cdots & F_{2,k+2} \\ \vdots & \vdots & \ddots & \vdots \\ F_{k+2,1} & F_{k+2,2} & \cdots & F_{k+2,k+2} \end{bmatrix}.$$

In case if number of base stations are 3, the FIM matrice reduces to $5x5$ and unknown vector paramater is given as $\theta = [x, y, \alpha_1, \alpha_2, \alpha_3]^T$.

The mean-squared error (MSE) of any unbiased location estimator is lower bounded as rewritting the equation (6.9) describes:

$$\epsilon^2_{rms} = E[(\epsilon^2] \geq [\mathbf{F}^{-1}]_{11} + [\mathbf{F}^{-1}]_{22} = \frac{\tilde{F}(1,1)}{det(F)} + \frac{\tilde{F}(2,2)}{det(F)} \tag{6.16}$$

We assume that path loss exponent value for each base station is independent of each other. Thus, FIM matrix elements include multiplicaton of partial derivatives of diffe-

rent α reduces to zero. $\tilde{F}$ is an $(k+1)$X$(k+1)$ matrix obtained by deleting the first or second row and the first or second column of $\mathbf{F}$, and it can be decomposed into matrices of a special sructure:

$$\tilde{\mathbf{F}} = \begin{bmatrix} a & f_1 & f_1 & f_3 & \cdots & f_n \\ e_1 & d_1 & 0 & 0 & \cdots & 0 \\ e_2 & 0 & d_2 & 0 & \cdots & 0 \\ \vdots & \vdots & \ddots & \ddots & \ddots & \vdots \\ e_n & 0 & 0 & \cdots & 0 & d_n \end{bmatrix}.$$

The computation complexity can be greatly reduced if we take advantage of the following relation:

$$det\tilde{\mathbf{F}} = \prod_{n=1}^{N} d_n . \left(a - \sum_{n=1}^{N} \frac{f_n e_n}{d_n} \right) \tag{6.17}$$

After some algepraic manipulation, $[F^{-1}]_{11}$ and $[F^{-1}]_{22}$ are expressed as:

$$\begin{aligned} [F^{-1}]_{11} &= (F_{22}F_{33}F_{44}F_{55} - F_{23}^2F_{44}F_{55} - F_{24}^2F_{33}F_{55} - F_{25}^2F_{33}F_{44})/|\mathbf{F}| \\ [F^{-1}]_{22} &= (F_{11}F_{33}F_{44}F_{55} - F_{13}^2F_{44}F_{55} - F_{14}^2F_{33}F_{55} - F_{15}^2F_{33}F_{44})/|\mathbf{F}| \end{aligned} \tag{6.18}$$

where $|\mathbf{F}|$ is the determinant of the Fisher information matrix and ϵ_{rms} is defined as the root-MSE (RMSE) of location estimators. Thus each member of the FIM matrix

can be given as:

$$
\begin{aligned}
F_{11} &= \frac{1}{\sigma_v^2}\sum_{k=1}^{n}\sum_{s=1}^{3}(\frac{\partial g_{k,s}(\theta)}{\partial x})^2 \\
&= \frac{1}{\sigma_v^2}\sum_{k=1}^{n}\sum_{s=1}^{3}(\frac{-10\alpha_k}{\ln 10}\frac{u_{kx}}{d_k} - \frac{20}{\ln 10}\frac{\partial \ln A_{k,s}(x,y)}{\partial x})^2 \\
F_{12} &= \frac{1}{\sigma_v^2}\sum_{k=1}^{n}\sum_{s=1}^{3}(\frac{\partial g_{k,s}(\theta)}{\partial x})(\frac{\partial g_{k,s}(\theta)}{\partial y}) \\
&= \frac{1}{\sigma_v^2}\sum_{k=1}^{n}\sum_{s=1}^{3}(\frac{-10\alpha_k}{\ln 10}\frac{u_{kx}}{d_k} - \frac{20}{\ln 10}\frac{\partial \ln A_{k,s}(x,y)}{\partial x})(\frac{-10\alpha_k}{\ln 10}\frac{u_{ky}}{d_k} - \frac{20}{\ln 10}\frac{\partial \ln A_{k,s}(x,y)}{\partial y}) \\
F_{13} &= \frac{1}{\sigma_v^2}\sum_{k=1}^{n}\sum_{s=1}^{3}(\frac{\partial g_{k,s}(\theta)}{\partial x})(\frac{\partial g_{k,s}(\theta)}{\partial \alpha_1}) \\
&= \frac{1}{\sigma_v^2}\sum_{s=1}^{3}(\frac{-10\alpha_1}{\ln 10}\frac{u_{1x}}{d_1} - \frac{20}{\ln 10}\frac{\partial \ln A_{1,s}(x,y)}{\partial x})(\frac{10}{\ln 10}\ln d_1), \\
F_{14} &= \frac{1}{\sigma_v^2}\sum_{k=1}^{n}\sum_{s=1}^{3}(\frac{\partial g_{k,s}(\theta)}{\partial x})(\frac{\partial g_{k,s}(\theta)}{\partial \alpha_2}) \\
&= \frac{1}{\sigma_v^2}\sum_{s=1}^{3}(\frac{-10\alpha_k}{\ln 10}\frac{u_{2x}}{d_2} - \frac{20}{\ln 10}\frac{\partial \ln A_{2,s}(x,y)}{\partial x})(\frac{10}{\ln 10}\ln d_2), \\
F_{15} &= \frac{1}{\sigma_v^2}\sum_{k=1}^{n}\sum_{s=1}^{3}(\frac{\partial g_{k,s}(\theta)}{\partial x})(\frac{\partial g_{k,s}(\theta)}{\partial \alpha_3}) \\
&= \frac{1}{\sigma_v^2}\sum_{s=1}^{3}(\frac{-10\alpha_3}{\ln 10}\frac{u_{3x}}{d_3} - \frac{20}{\ln 10}\frac{\partial \ln A_{3,s}(x,y)}{\partial x})(\frac{10}{\ln 10}\ln d_3), \\
F_{21} &= F_{12} \\
F_{22} &= \frac{1}{\sigma_v^2}\sum_{k=1}^{n}\sum_{s=1}^{3}(\frac{\partial g_{k,s}(\theta)}{\partial y})^2 \\
&= \frac{1}{\sigma_v^2}\sum_{k=1}^{n}\sum_{s=1}^{3}(\frac{-10\alpha_k}{\ln 10}\frac{u_{ky}}{d_k} - \frac{20}{\ln 10}\frac{\partial \ln A_{k,s}(x,y)}{\partial y})^2
\end{aligned}
$$

$$F_{23} = \frac{1}{\sigma_v^2}\sum_{k=1}^{n}\sum_{s=1}^{3}(\frac{\partial g_{k,s}(\theta)}{\partial y})(\frac{\partial g_{k,s}(\theta)}{\partial \alpha_k})$$

$$= \frac{1}{\sigma_v^2}\sum_{s=1}^{3}(\frac{-10\alpha_1}{\ln 10}\frac{u_{1y}}{d_1} - \frac{20}{\ln 10}\frac{\partial \ln A_{1,s}(x,y)}{\partial y})(\frac{10}{\ln 10}\ln d_1),$$

$$F_{24} = \frac{1}{\sigma_v^2}\sum_{k=1}^{n}\sum_{s=1}^{3}(\frac{\partial g_{k,s}(\theta)}{\partial y})(\frac{\partial g_{k,s}(\theta)}{\partial \alpha_2})$$

$$= \frac{1}{\sigma_v^2}\sum_{s=1}^{3}(\frac{-10\alpha_2}{\ln 10}\frac{u_{2y}}{d_2} - \frac{20}{\ln 10}\frac{\partial \ln A_{2,s}(x,y)}{\partial y})(\frac{10}{\ln 10}\ln d_2),$$

$$F_{25} = \frac{1}{\sigma_v^2}\sum_{k=1}^{n}\sum_{s=1}^{3}(\frac{\partial g_{k,s}(\theta)}{\partial y})(\frac{\partial g_{k,s}(\theta)}{\partial \alpha_3})$$

$$= \frac{1}{\sigma_v^2}\sum_{s=1}^{3}(\frac{-10\alpha_3}{\ln 10}\frac{u_{3y}}{d_3} - \frac{20}{\ln 10}\frac{\partial \ln A_{3,s}(x,y)}{\partial y})(\frac{10}{\ln 10}\ln d_3),$$

$$F_{31} = F_{13}$$

$$F_{32} = F_{23}$$

$$F_{33} = \frac{1}{\sigma_v^2}\sum_{k=1}^{n}\sum_{s=1}^{3}(\frac{\partial g_{k,s}(\theta)}{\partial \alpha_1})(\frac{\partial g_{k,s}(\theta)}{\partial \alpha_1})$$

$$= \frac{1}{\sigma_v^2}\sum_{s=1}^{3}(\frac{10}{\ln 10}\ln d_1)^2$$

$$F_{34} = 0, F_{35} = 0$$

$$F_{41} = F_{14}, F_{42} = F_{24}$$

$$F_{44} = \frac{1}{\sigma_v^2}\sum_{k=1}^{n}\sum_{s=1}^{3}(\frac{\partial g_{k,s}(\theta)}{\partial y})(\frac{\partial g_{k,s}(\theta)}{\partial \alpha_2})$$

$$= \frac{1}{\sigma_v^2}\sum_{s=1}^{3}(\frac{10}{\ln 10}\ln d_2)^2$$

$$F_{43} = 0, F_{45} = 0$$

$$F_{51} = F_{15}, F_{52} = F_{25}$$

$$F_{53} = F_{35} = 0, F_{54} = F_{45} = 0$$

$$F_{55} = \frac{1}{\sigma_v^2}\sum_{k=1}^{n}\sum_{s=1}^{3}(\frac{\partial g_{k,s}(\theta)}{\partial \alpha_3})(\frac{\partial g_{k,s}(\theta)}{\partial \alpha_3})$$

$$= \frac{1}{\sigma_v^2}\sum_{s=1}^{3}(\frac{10}{\ln 10}\ln d_3)^2,$$

The multiplications for CRLB evaluation are not given explicitly here, thus having only member is enough for numerical solution with MATLAB tool.

6.2.2. Smooth CRB Analysis

In GSM and UMTS, minimum detectable threshold value of received signal strength is -110 dBm and -120 dBm respectively. If received signal power is below the -110 dBm or -120 dBm , the data under threshold is not taking into computations. The probability $X > -110$ dBm with Q-function definition is performed to simulate this threshold.

In statistics, the Q-function is the tail probability of the standard normal distribution. In other words, Q(x) is the probability that a standard normal random variable will obtain a value larger than x. Other definitions of the Q-function, all of which are simple transformations of the normal cumulative distribution function, are also used occasionally.

If we have a normal variable X $N(\mu, \sigma^2)$, the probability that $X > a$:

$$P(X > a) = Q(\frac{a - \mu_x}{\sigma_x}), \qquad \frac{a - \mu_x}{\sigma_x} > 0$$

where Q-function is defined as $Q(x) = \frac{1}{\sqrt{2\pi}} \int_x^\infty exp(\frac{-z^2}{2})dz$, using the relation,
$Q(x) = \frac{1}{2}(1 - erf(\frac{x}{\sqrt{(2)}}))$, we are going to use following relation for our computations,
$P(X > a) = \frac{1}{2} + \frac{1}{2} erf\left(\frac{\mu_x - a}{\sqrt{2}\sigma_x}\right)$
where μ can be extracted from the our propagation model given in Eq.5.8, thus:

$$\mu_{k,s}(x, y) = 10 \log_{10}\left(\frac{PG}{\beta}\right) - 10\alpha \log_{10}\left(\frac{d(x, y)}{d_0}\right) + 20 \log_{10} A_{k,s}(x, y), \tag{6.19}$$

When MS lies under coverage area of n BSs, there are $3n$ possible RSS measurements that corresponds to the data point $p_{k,s}$ of sector s of BS k that can be used to estimate location. But any of the $3n$ data points $p_{k,s}$ could correspond to a power level less the

the sensitivity threshold a, which here is taken to be -110 dBm, in that case $p_{k,s}$ is an invalid RSS measurement.

To describe each possible case of the validity of measurments, define the validity matrix $\mathbf{V}$, where

$$V = \begin{cases} 1, & \text{if } p_{k,s} \geq a \\ 0, & \text{if } p_{k,s} < a \end{cases} \tag{6.20}$$

Since there are $3n$ entries in V which only take on values 1 and 0, these are 2^{3n} possible V configurations.
For each configuration, i.e., each MS point, , it is possible to calculate the CRB which is a lower bound for the RMSE (variances) of any unbiased estimator.

Therefore the expected value of the RMSE of any unbiased estimator will satisfy,

$$E[(\tilde{\theta} - \theta)^2 | \theta = (x, y)] \geq \sum_i CRB[\theta = (x, y), V_i] P[V = V_i | \theta = (x, y)] \tag{6.21}$$

where the index i spans all the 2^{3n} possible states of V. And P is given as:

$$P(V = V_i | \theta = (x, y)) = \prod_{k=1}^{M} \prod_{s=1}^{3} p(k, s, \theta, [V_i]_{k,s})$$

assuming that each measurement is independent

$$p(k, s, \theta, [V_i]_{k,s}) = \begin{cases} P(p_{k,s} \geq a | \theta), & \text{if } [V_i]_{k,s} = 1 \\ 1 - P(p_{k,s} \geq a | \theta), & \text{if } [V_i]_{k,s} = 0 \end{cases}$$

For each validity configuration case the CRB has been evaluated as given below:

$$CRB(\theta = (x, y), V_i) = \prod_{k=1}^{M} \prod_{s=1}^{3} FIM^{-}1 \approx \tilde{A}(k, s, \theta, [V_i]_{k,s})$$

where $\tilde{A}(k, s, \theta, [V_i]_{k,s})$ is defined as:

$$\tilde{A}(k, s, \theta, [V_i]_{k,s}) = \begin{cases} A_{k,s}, & \text{if } [V_i]_{k,s} = 1 \\ A_{k,s} = 0, & \text{if } [V_i]_{k,s} = 0 \end{cases}$$

In numerical results as given in next chapter, it is clearly seen that smooth CRB shows better performance as compared with conventional CRB method.

7. CRB NUMERICAL ANALYSIS and PERFORMANCE EVALUATION

The performance lower bounds of any unbiased RSS location estimator depends environmental parameters, α and σ_v, as well as geometric parameters d and ϕ. MATLAB tool has been used throughout our work to analyze the performance of the formulation in previous chapter. In this chapter, various simulation environments have been implemented and performance bounds are analyzed and presented.

7.1. Performance Comparison CRB versus RMSE

7.1.1. Global Parameters

It is assumed that all BSs in the network (7.1) have three sector configuration where each sector belongs to a cell with identical coverage area and transmit power, the input parameters are given in Table 7.1

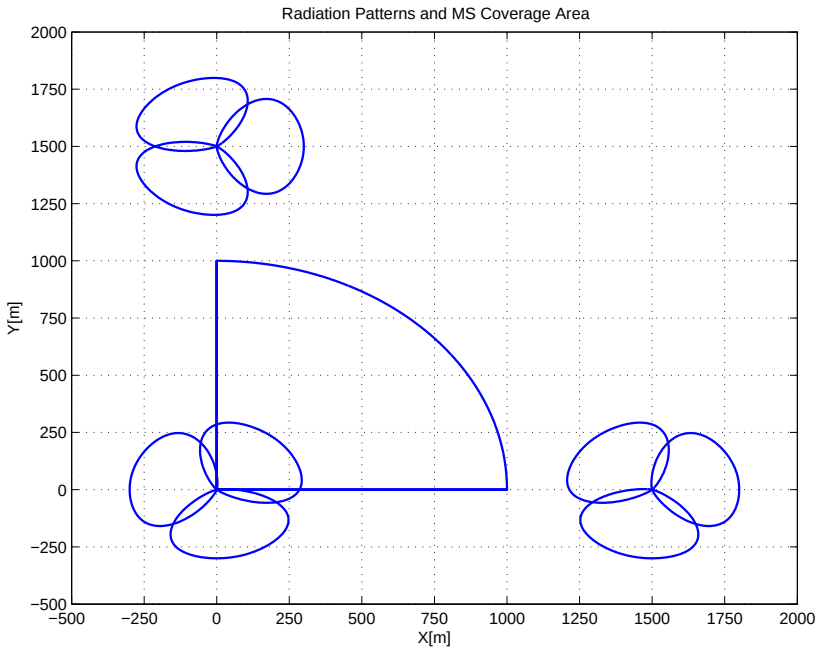

Figure 7.1. Radiation Pattern and Simulation Area

Parameter Name	Parameter Value	Unit
No of BSs	3	-
No of sector per BS	3	-
Min measurable RSS Value	-110(UMTS)	dBm
BS-1 Location	x=0,y=0	m
BS-2 Location	x=1500,y=0	m
BS-3 Location	x=0,y=1500	m
BS First sectoral orientation	$\pi/4$, $3\pi/4$ and 0	rad
BS RF Tx output power	50	dBm
Antenna HBW	$2\pi/3$	radians
Antenna Gain	25	dBi
σ_x	6	dBm
τ	6.639	-
Path Loss Exponent	3	-
Mobile Station Position	Uniform in coverage area with [0 1000] m	m

Table 7.1. Environment and Input Parameters for Analysing

7.1.2. Algorithm RMSE Results and CRLB Evaluation

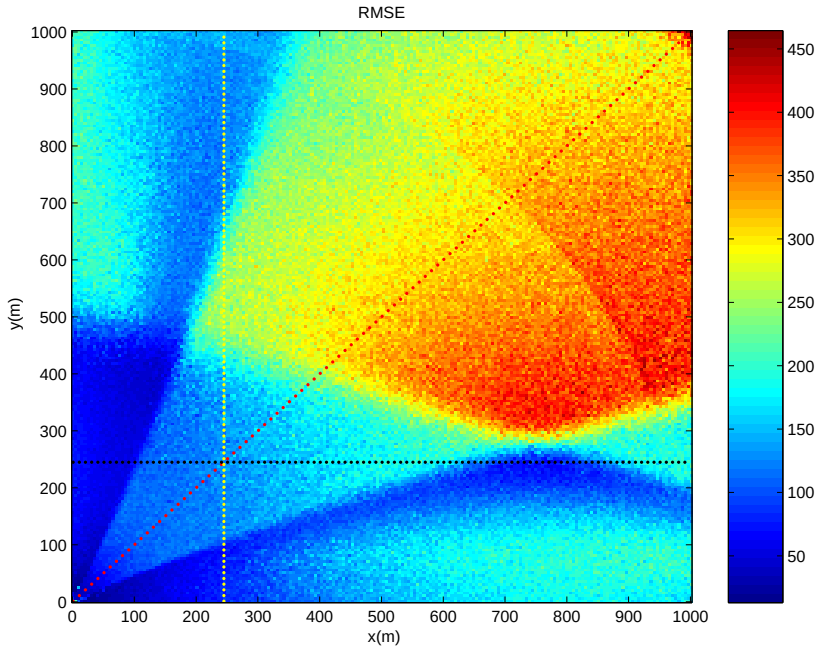

Figure 7.2. ALGORITHM RESULT: RMSE When RSS value is $\geq -110dBm$ [Error in Meter]

There is a transition seen from inside of quarter circle to outside which is caused of initialization of algorihtm done according to serving BS area restriction.

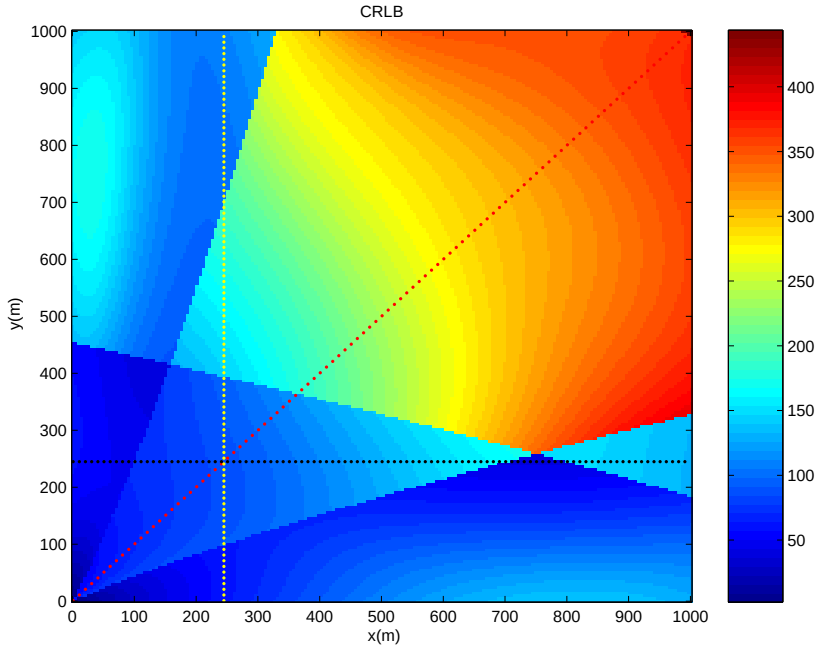

Figure 7.3. Cramer Rao Bound When RSS value is $\geq -110dBm$ [Error in Meter]

As it is seen from figures performance degrades up to 450 m in RMSE error, 400 m in CRB. CRB shows better performance in generally speaking. Moreover, it is clearly seen that Radiation Pattern has significant contributions to location estimation.

Three lines which are drawing on the images[Red,Yellow,Black] are taken for sampling to compare of CRB and RMSE as it is given figures below:

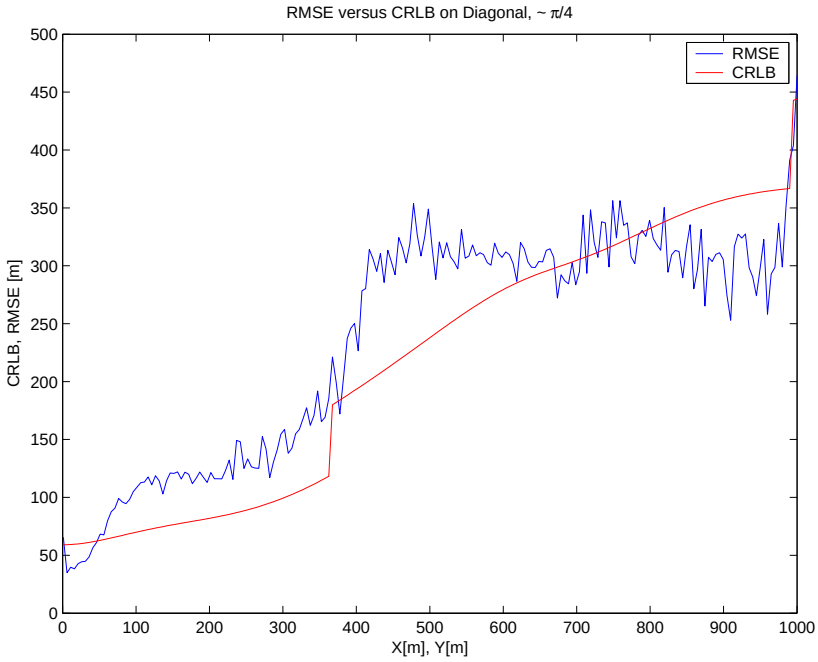

Figure 7.4. Plot of RMSE and CRB when MS is on the diagonal, as seen on diagonal line

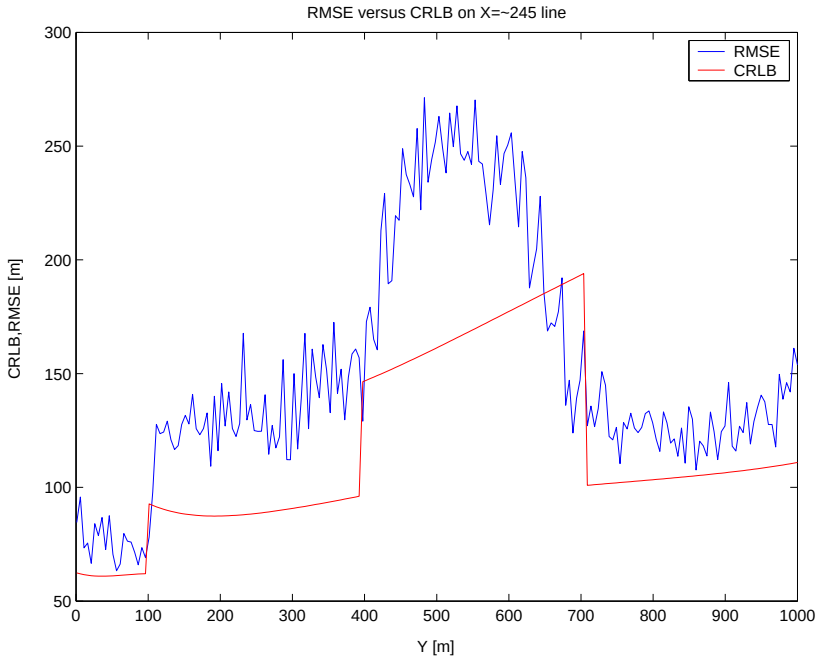

Figure 7.5. Plot of RMSE and CRLB when MS is on x=245 m line

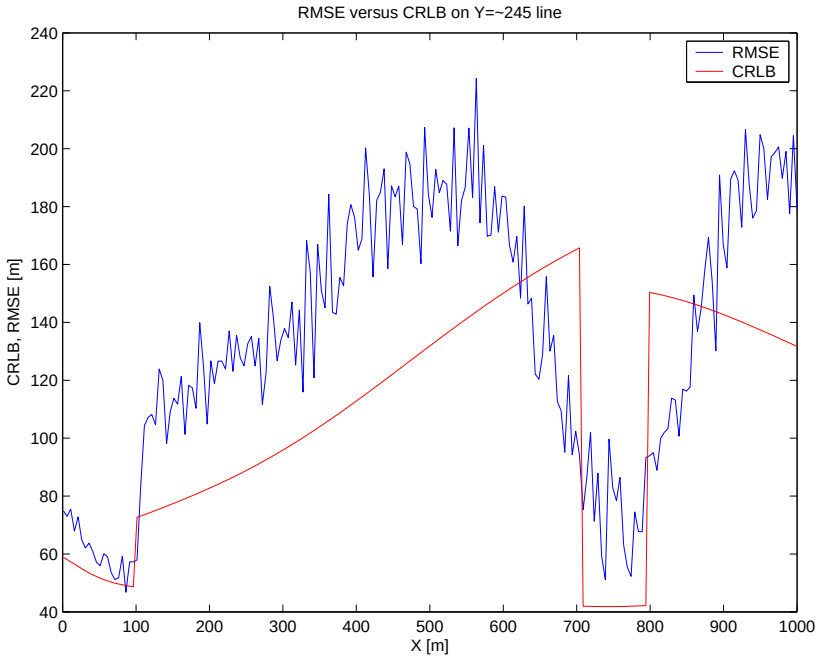

Figure 7.6. Plot of RMSE and CRLB when MS is on y=245 m line

Cramer-Rao Bound shows lower bound for algorithm RMSE in most cases . Thus, usually CRB gives better performance comparing RMSE of algorithm. There are some sharp transitions in CRB plot which is because of probability to decision signal strength threshold.

7.1.3. Smooth Transition Results

As it is stated in previous subsection, in CRB results there are sharp transitions in figures. Because, only one probability of sectoral existence taken in evaluation formulation for each MS[x,y] location in uniform area. However, if take all possibilities in our computation, there will more smooth transition betweenn edges. For instances, in our case, 3 base stations and 3 sectors for each, existence of one sector in one location may have $2^9 = 512$ possibilities. So, following this idea we got the results given below:

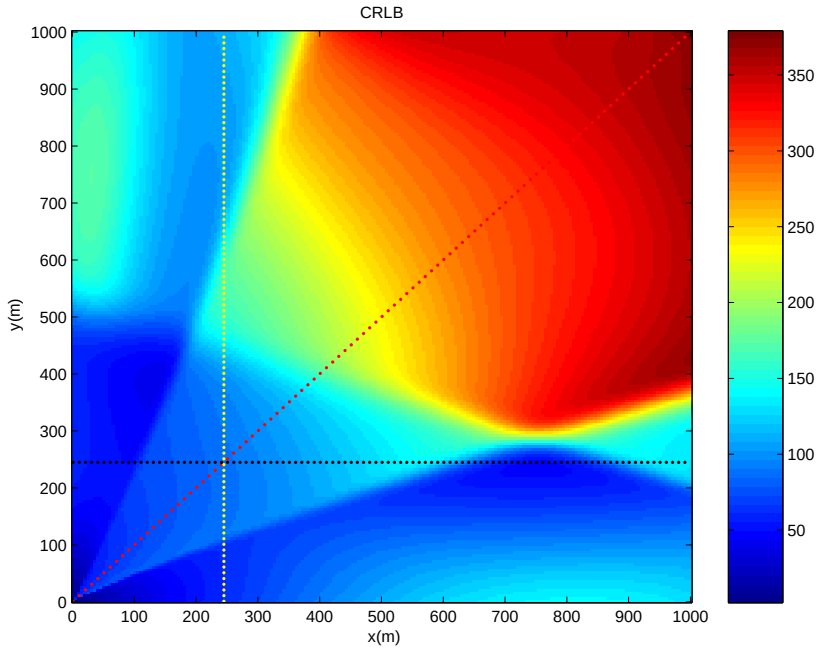

Figure 7.7. Smooth CRB When RSS value is $\geq -110dBm$-ALL CASES [Error in Meter]

The error decreases by 50 m comparing with sharp transition given in Fig.7.3. And it is easily seen that RMSE (Fig7.2)and CRB(Fig7.7) almost seem identical comparing figure overlay.

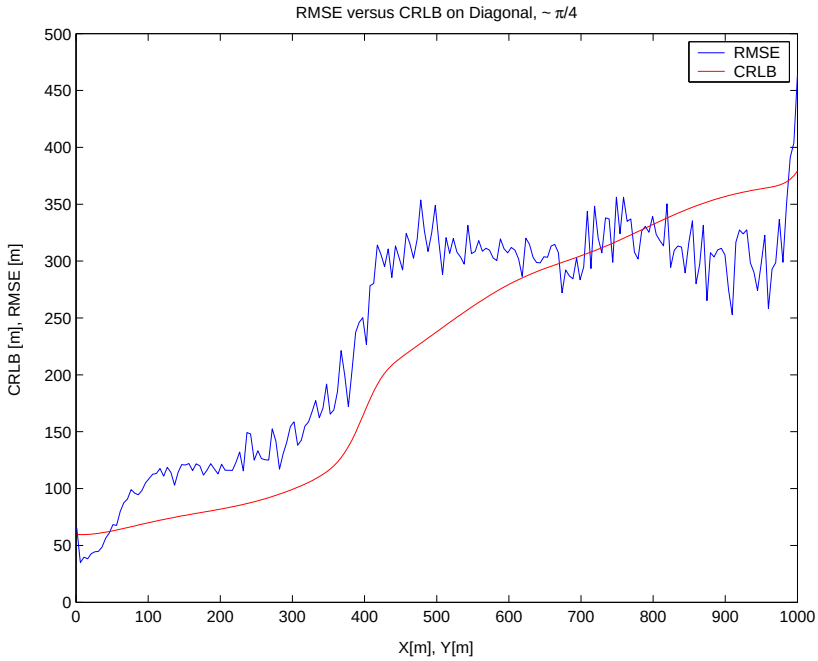

Figure 7.8. Plot of RMSE and CRB when MS is on the diagonal, as seen on diagonal line

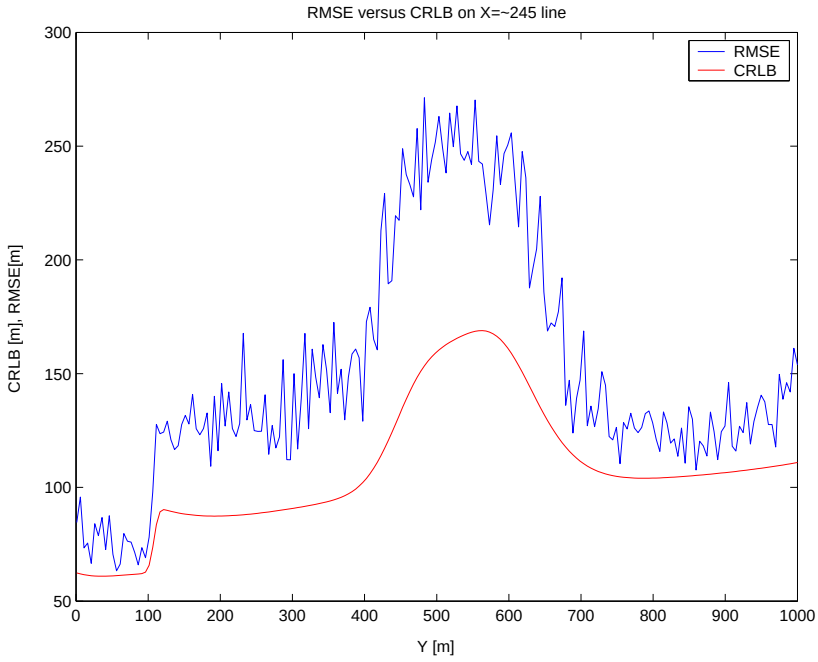

Figure 7.9. Plot of RMSE and CRLB when MS is on x=245 m line

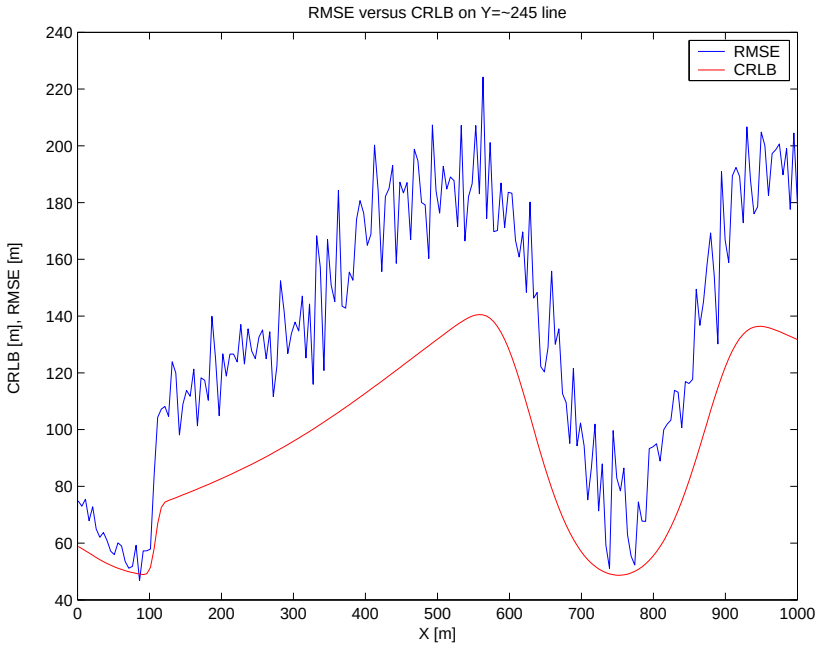

Figure 7.10. Plot of RMSE and CRLB when MS is on y=245 m line

CRB always follows the RMSE of algorithm and smoothly gives better performance in comparision.

7.1.4. Results for 4 BSs

In this section, our network consists of 4 Base Stations and radiation pattern given in Fig.7.11. The first sector of each BS $[BS1 = \pi/4, BS2 = 3\pi/4, BS3 = -\pi/4, BS4 = -3\pi/4]$ is directed to central point where MS lies.

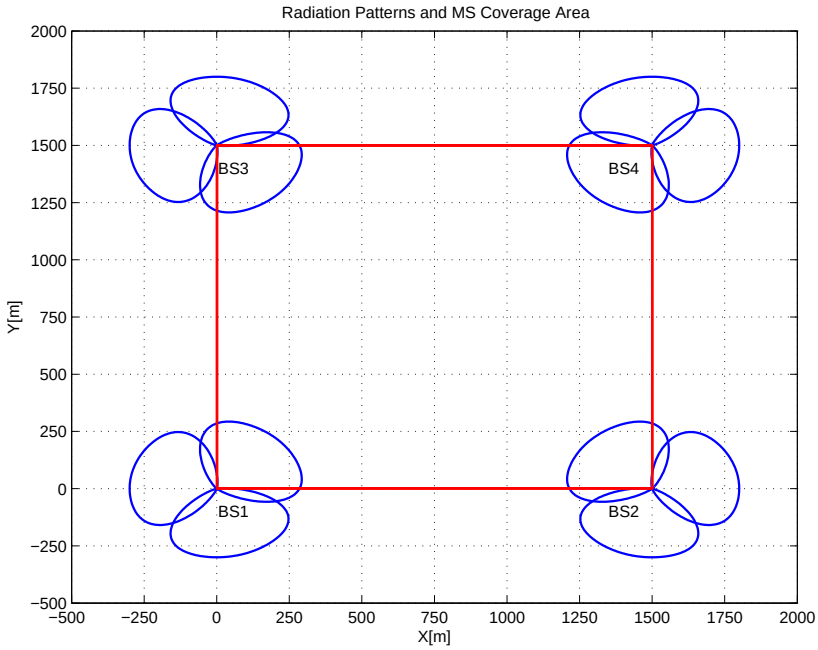

Figure 7.11. The Network Schema and Sectoral Orientation of BSs

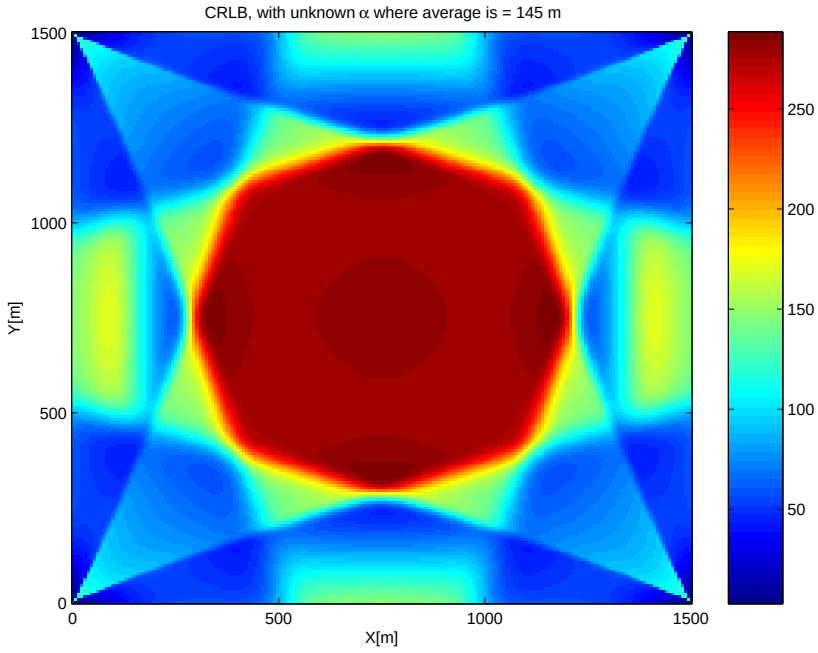

Figure 7.12. CRB Results: The sectoral orientation of BS#1 is 45 deg

It is clearly seen the symmetry of image in Fig.7.12 which naturally result of BSs location and sectoral planning in network. CRB values are poor in central areas and gives better where sectoral orientation of BSs intersects in boundary areas.

7.1.5. The Pure Pathloss Model Results/Omnidirectional Case

In this scenario, for a square field with sidess of Lenght 1500 m, the four BSs are placed at the corners of the field with some margin Δ=1. In this simulation scenario, positioning accuracy of the RSS based positioning algorithm which has only omnidirectional and does not have any directional antenna configuration [32] has been considered. From the results we can observe CRLB is small in the center of the field and becomes large as target node moves toward boundary areas.

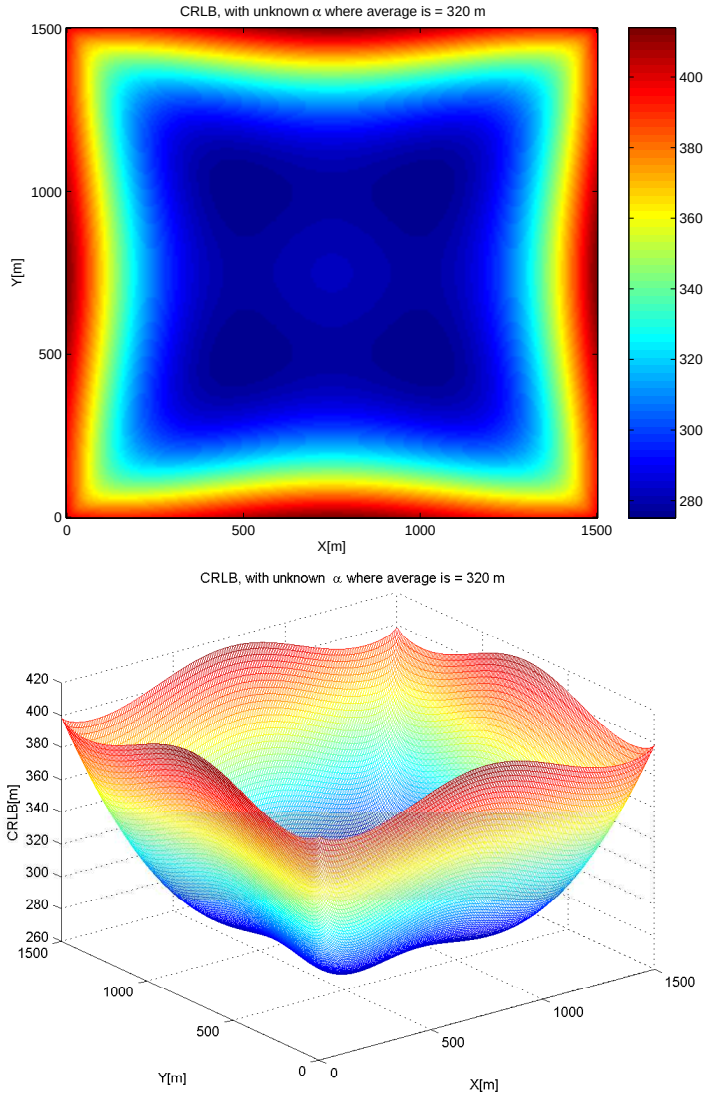

Itis clearly seen that the average CRLB Error for pure Log-normal pathloss model is 320 m while 145 m for our radiation pattern model from Figure 7.12. And additionally, the maximum error where worst case occur at boundary areas decreases in our model and gives better performance.

7.1.5.1. Effect of Base Station Sectoral Orientation. To analyse the sectoral orientation of BSs in CRB results, BS#1 is chosen as reference sample for testing. The sectoral direction of all BS are unchanged except BS#1 as starting $[0, 15, 30, 45, 60, 75, 90]deg$.

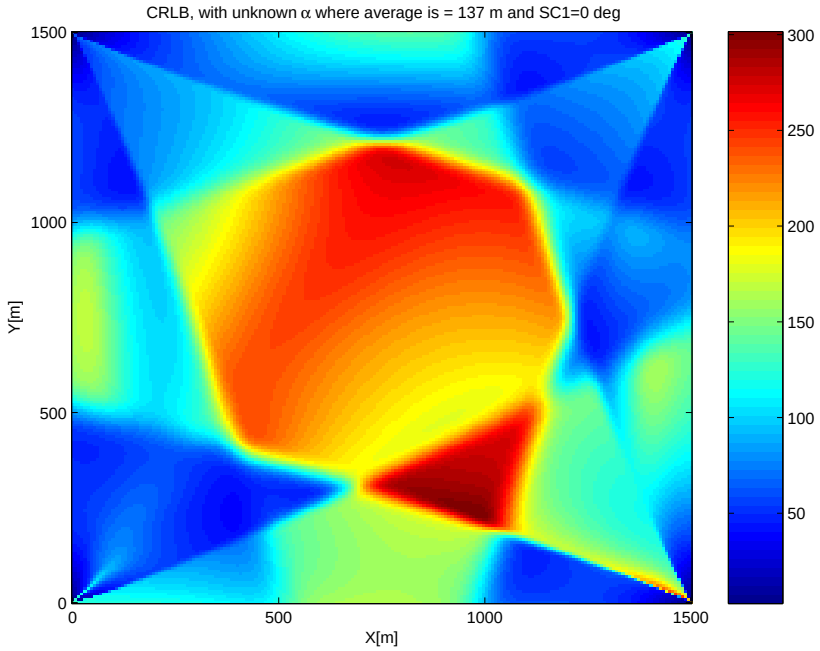

Figure 7.13. The sectoral orientation of BS#1 has been changed as 0 deg

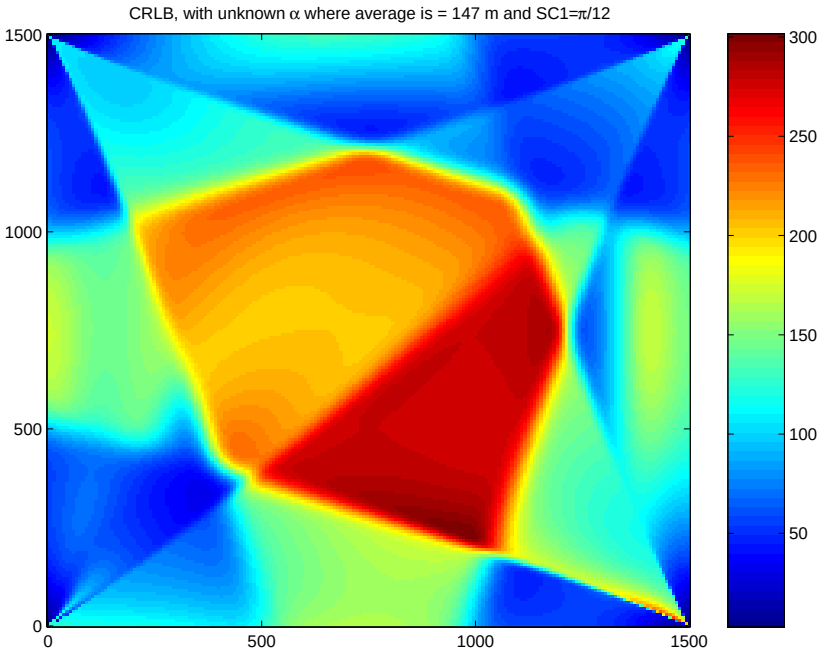

Figure 7.14. The sectoral orientation of BS#1 has been changed as 15 deg

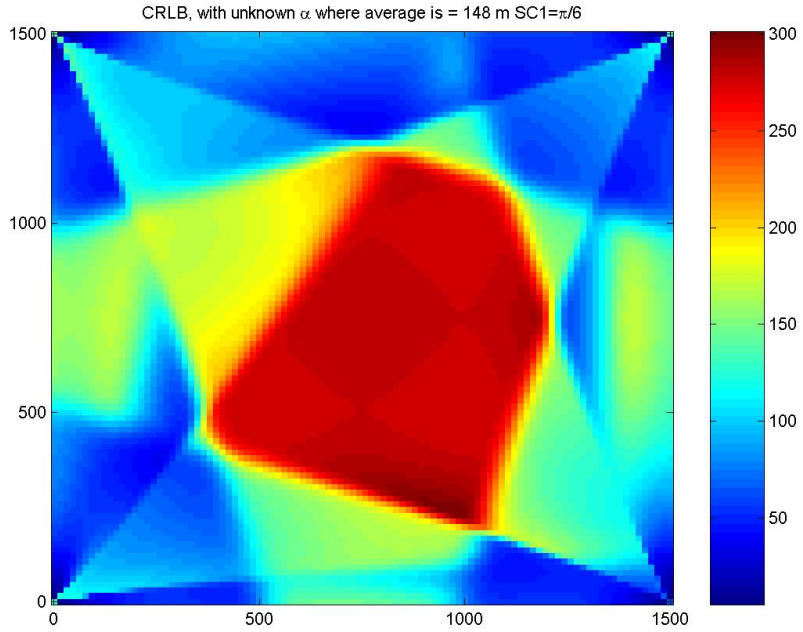

Figure 7.15. The sectoral orientation of BS#1 has been changed as 30 deg

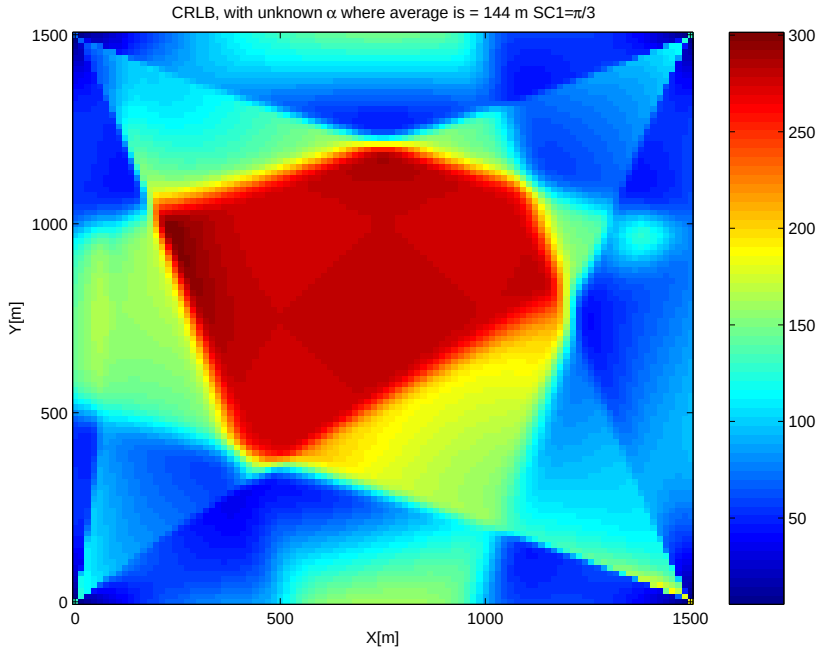

Figure 7.16. The sectoral orientation of BS#1 has been changed as 60 deg

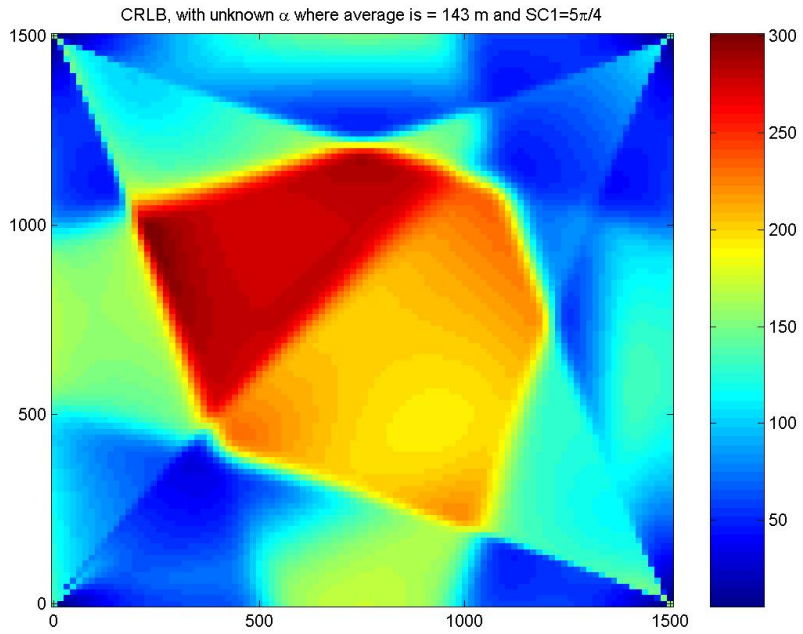

Figure 7.17. The sectoral orientation of BS#1 has been changed as 75 deg

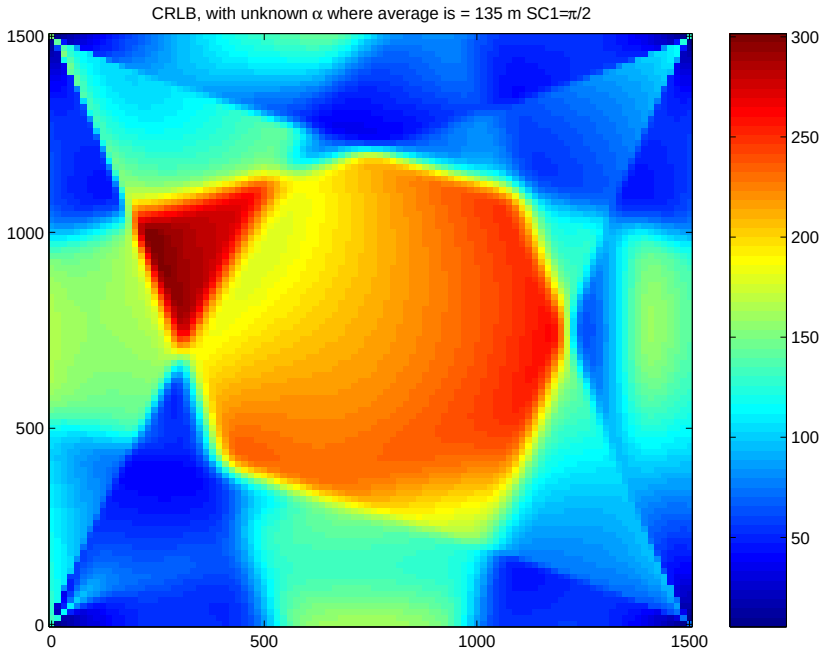

Figure 7.18. The sectoral orientation of BS#1 has been changed as 90 deg

It is clearly seen that sectoral orientation of BS#1 affect the image overlay of CRLB. As sectoral direction changes, the blind area where CRB worst shifts.

7.1.6. A Sample Scenario: Boshphorus and Affect of Different PLE

In previous sections, particularly, channels used by the cells that are served by the same BS are assumed the same PLE and this PLE is not necessarily the same for other channels. In addition, we assumed that PLE value of each base station is the same. However, in most cases channels used by the distant BSs have different propagation characteristics. Thus, in this section we consider the divergent PLEs in the signal model for channels that are used by the different BSs and evaluate CRLB for a particular scenario given in Fig.7.19.

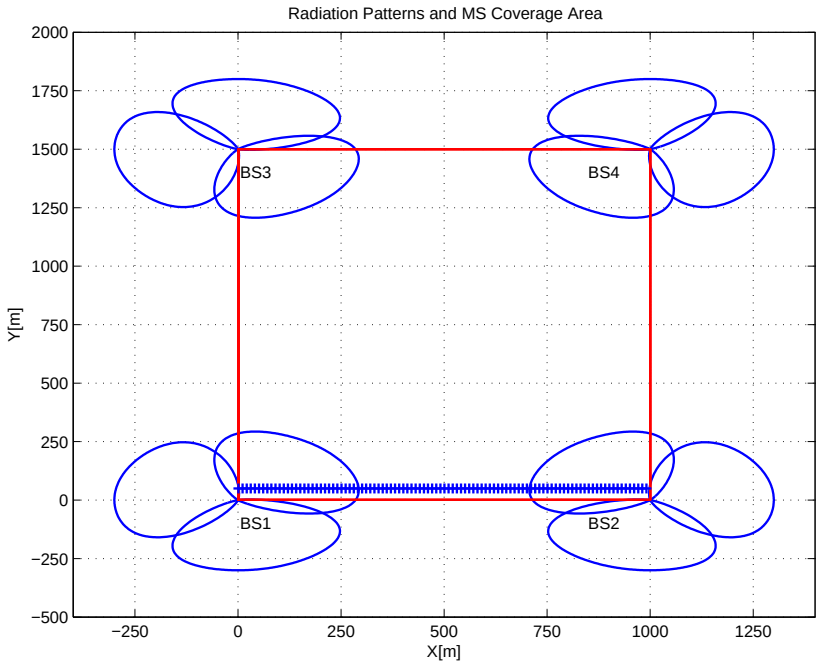

Figure 7.19. CRB Results for sample case: different PLEs

It is assumed that 4 BSs are located in the opposide side of bosphorus, the distance between BSs located on the edge is $1500m$ and distance $1000m$ is between BSs located on the same side. The PLE values of BS:1 and BS:2 are chosen as 3.2 and 2.7 for BS:3 and BS:4.

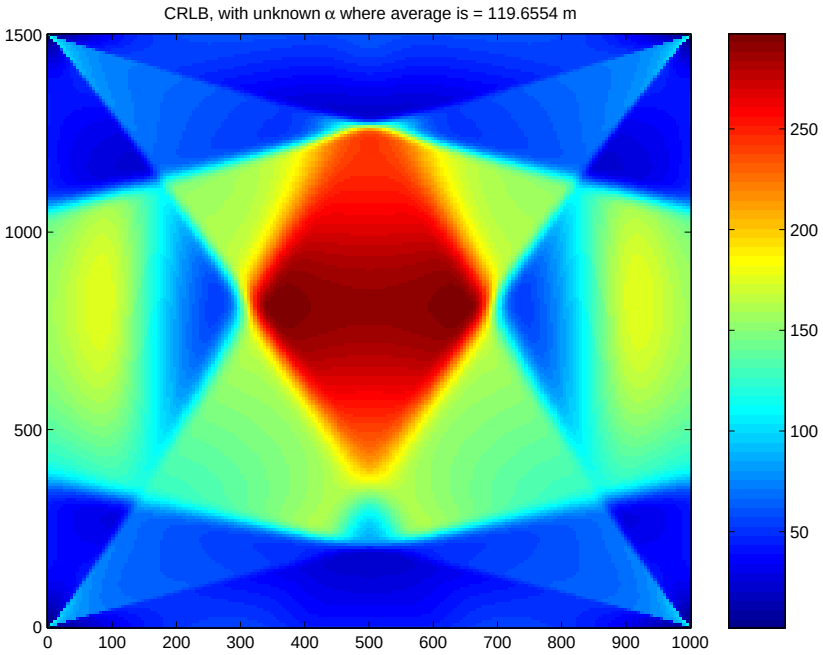

Figure 7.20. CRB Results

The Figure 7.20 shows us that CRB results where they are worst, i.e center area, gets better as BSs are getting closer and the area reduces.

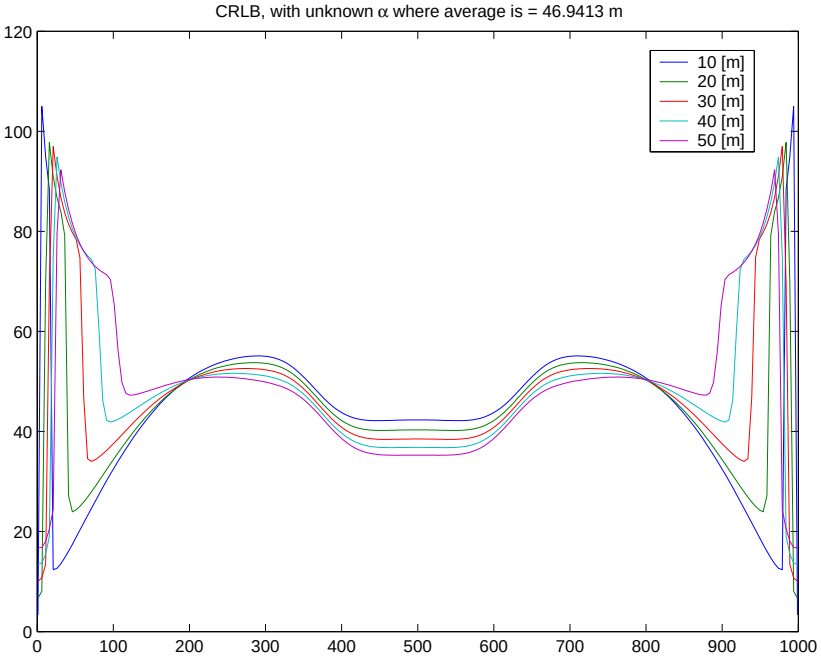

Figure 7.21. CRB Results

If MS is moving from BS:1 to BS:2 on the bank and taking different roads away

from straight line between BS:1 and BS:2, we got results given in Fig:7.21. The average error CRB shows is about $45m$ and it is quite acceptable for $1000m$ distance between both BSs. The fluctuation near the BSs are expected results since the values are very close to BS have significant bias, that is why CRB does not show real performance there.

7.1.7. Affect of Number of Base Station

To study the effects of the number of reference nodes which has significant effects on the performance of location estimators, the circular deployment of BS nodes has been considered in this section.

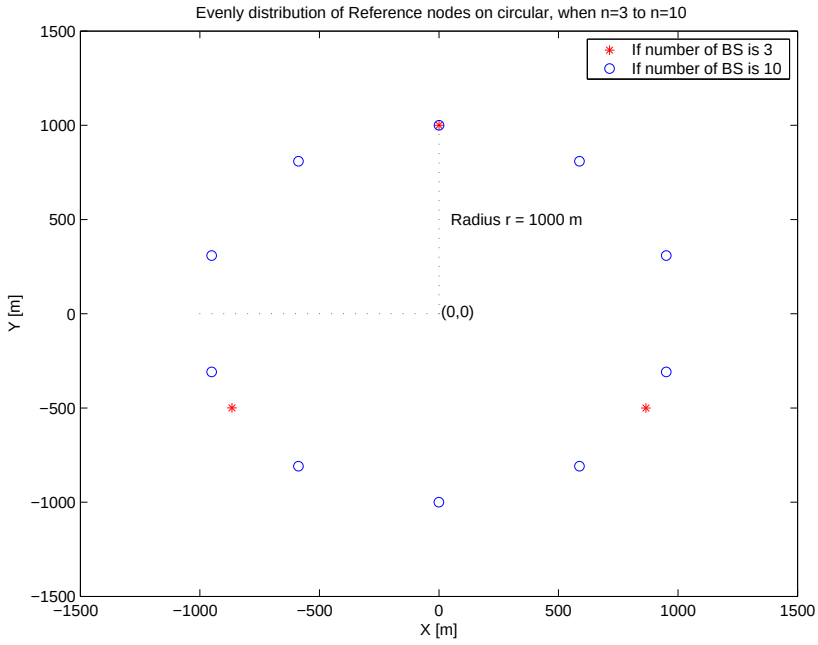

Figure 7.22. Circular Deployment of Reference Nodes in Simulations

In the circular deployment scheme, Base Stations are evenly spaced on a circle; the inside of the circle is considered as deployment field for Mobile Station. The center of the field is fixed at (0, 0) and the radius of the field is set to $1000m$. Random target node locations are uniformly sampled in the field. At each random location, it is determined CRB has been evaluated.

Figure 7.23 shows simulation results at two randomly selected Mobile Station locations (2, 0) and (200, 900), one close to the center of field and the other close to the edge.

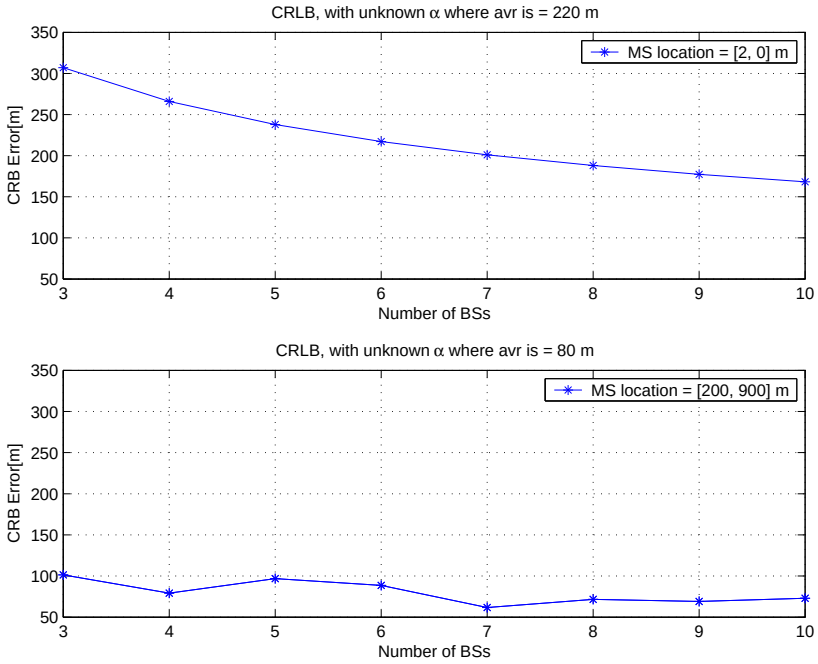

Figure 7.23. CRB versus Number of Base Station

It is clear that at location (2, 0) CRB performance increases as number of BS increases. That is expected result since log-normal model tells that as more measurement gives better result for location estimation. On the other hand, CRB result for the MS close to edge shows that there is no direct linear relation between number of BS and CRB. That is because, on the edge the sectoral orientation has significan contribution to CRB performance evaluations and correct information included on locations close to BS. From the Fig:7.23, location estimation close to BSs lower-bound under $100m$ comparing the location sample on the center which results $150m$ even with 10 BSs.

In order to exam the effects of noise level on the performance evaluation, we vary the standard deviation of log-normal fading variable σ_v, while Mobile station location is at (0,2) and (200,900) m. The sectoral antenna configuration model is compared to omnidirectional pure pathloss model as given in [32]. The results presented in Figure 7.24 show that the value of σ_v has significant effect on the center field while it does not

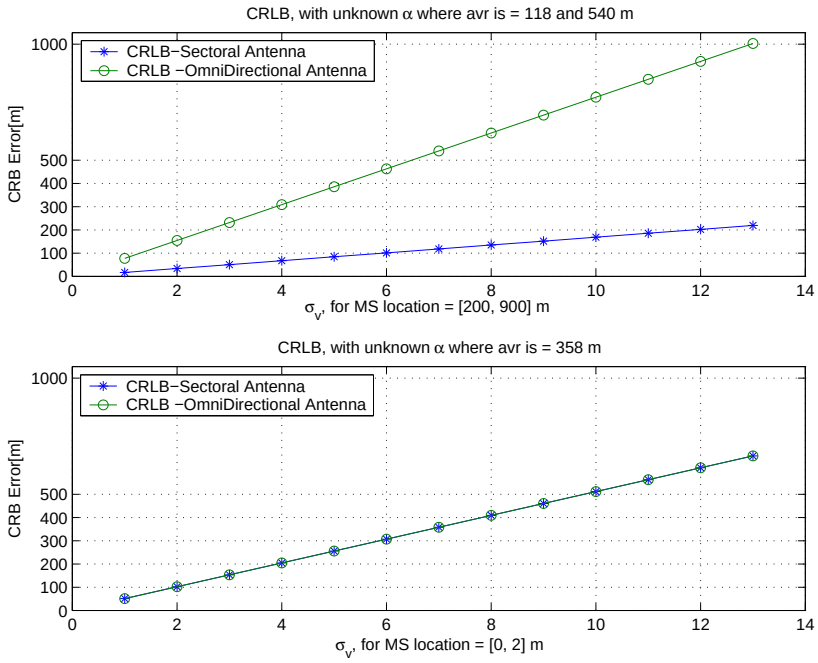

Figure 7.24. RMSE versus log-normal shadow fading variable σ_v[dB]

effect much at boundary area. In addition, it is observed that in center field sectoral antenna does not contribute in positioning accuracy as comparing with pure-pathloss model.

8. CONCLUSIONS

In this thesis, we have studied the performance bounds of RSS based localization using cramer-rao lower bound method. By using Cramer-Rao bound we have expressed a lower bound on the variance of estimator of the deterministic parameter in our location estimation model.

Throughout the study, we have concentrated on the RSS based positioning model which can be implemented in cellular networks with simple modifications in the existing infrastructure. This model is based on RSS mesurements which is easily can be obtained in cellular networks. This approach assumes path loss exponent value as an unknown variable, thus this assumption take the the model close to real environment where channel conditions can vary frequently. The most important part of the model is it incorporates the antenna radiation pattern information to supply additional improvement in positioning accuracy.

The estimation problem is first formulated into system of nonlinear equations and then performance of estimator studied based on CRB analysis and simulation results. Quantitative espressions of accuracy measures have been derived. Furthermore, smooth CRB is presented and compared to conventional CRB bound results.

The CRB results have been obtained under different scenarious and also compared the RMSE results obtained in an earlier study [14] uses RSS-MLE(Maximum Likelihood Estimation) method. It is obviously observed that CRB in most cases put lower-bound as comparing RMSE results. Based on CRB analysis, we have shown that the sectoral antenna planning has significant effect on location estimation error evaluation. With accurate sectoral planning on site, the estimation results where observed high can be eliminated. Moreover, Pure-Pathloss model is more sensitive to lognormal shadow fading variable than our sectoral RSS model.

APPENDIX A:

A.1. Fisher Information Matrix Derivation

Given the Joint distribution of observation in Equation 6.2 and propability density function in Equation 6.1

$$f(p_{k,s};\theta) = \frac{1}{\sqrt{2\pi}\sigma_v} exp(-\frac{(p_{k,s} - g_{k,s}(\theta))^2}{2\sigma_v^2})$$

$$f(\mathbf{p};\theta) = \prod_{k=1}^{n}\prod_{s=1}^{3} f(p_{k,s};\theta)$$

Rewritting the equation above:

$$f(\mathbf{p};\theta) = \prod_{k=1}^{n}\prod_{s=1}^{3} \frac{1}{\sqrt{2\pi}\sigma_v} exp(-\frac{(p_{k,s} - g_{k,s}(\theta))^2}{2\sigma_v^2})$$

Considering the natural logarithm of the PDF:

$$\begin{aligned}
\ln f(\mathbf{p};\theta) &= \ln\left[\prod_{k=1}^{n}\prod_{s=1}^{3} \frac{1}{\sqrt{2\pi}\sigma_v}\right] + \ln\left[\prod_{k=1}^{n}\prod_{s=1}^{3} exp(-\frac{(p_{k,s} - g_{k,s}(\theta))^2}{2\sigma_v^2})\right] \\
&= \ln(\frac{1}{\sqrt{2\pi}\sigma_v})^{3n} + \ln\left[exp(\sum_{k=1}^{n}\sum_{s=1}^{3} -\frac{(p_{k,s} - g_{k,s}(\theta))^2}{2\sigma_v^2})\right] \\
&= K - \frac{1}{2\sigma_v^2}\sum_{k=1}^{n}\sum_{s=1}^{3}(p_{k,s} - g_{k,s}(\theta))^2
\end{aligned}$$

where $K = \ln(\frac{1}{\sqrt{2\pi}\sigma_v})^{3n}$ and constant value, does not involve in derivative equations. Thus, we get the log-likelihood function in Equation 6.4:

$$l(\theta) = -\frac{1}{2\sigma_v^2}\sum_{k=1}^{n}\sum_{s=1}^{3}(p_{k,s} - g_{k,s}(\theta))^2$$

Recalling (6.5):

$$F_{ij} = [\mathbf{F}]_{ij} = -E[\frac{\partial^2 l(\theta)}{\partial\theta_i \partial\theta_j}]$$

Differentiating the log-likelihood function with respect to θ:

$$\begin{aligned}\frac{\partial l(\theta)}{\partial\theta_i} &= -\frac{1}{2\sigma_v^2}\sum_{k=1}^{n}\sum_{s=1}^{3}\frac{\partial}{\partial\theta_i}(p_{k,s} - g_{k,s}(\theta))^2 \\ &= -\frac{1}{2\sigma_v^2}\sum_{k=1}^{n}\sum_{s=1}^{3}2(p_{k,s} - g_{k,s}(\theta))(-\frac{\partial g_{k,s}(\theta)}{\partial\theta_i})\end{aligned}$$

if $i = j$, so the second derivative:

$$\begin{aligned}\frac{\partial^2 l(\theta)}{\partial\theta_i^2} &= -\frac{1}{\sigma_v^2}\sum_{k=1}^{n}\sum_{s=1}^{3}[\frac{\partial}{\partial\theta_i}(p_{k,s} - g_{k,s}(\theta))(-\frac{\partial g_{k,s}(\theta)}{\partial\theta_i}) + (p_{k,s} - g_{k,s}(\theta))(-\frac{\partial^2 g_{k,s}(\theta)}{\partial\theta_i^2})] \\ &= -\frac{1}{\sigma_v^2}\sum_{k=1}^{n}\sum_{s=1}^{3}[(\frac{\partial g_{k,s}(\theta)}{\partial\theta_i})^2 + (p_{k,s} - g_{k,s}(\theta))(-\frac{\partial^2 g_{k,s}(\theta)}{\partial\theta_i^2})]\end{aligned}$$

if $i \neq j$, so the second derivative:

$$\begin{aligned}\frac{\partial^2 l(\theta)}{\partial\theta_i\theta_j} &= -\frac{1}{\sigma_v^2}\sum_{k=1}^{n}\sum_{s=1}^{3}[\frac{\partial}{\partial\theta_j}(p_{k,s} - g_{k,s}(\theta))(-\frac{\partial g_{k,s}(\theta)}{\partial\theta_i}) + (p_{k,s} - g_{k,s}(\theta))(-\frac{\partial^2 g_{k,s}(\theta)}{\partial\theta_i\theta_j})] \\ &= -\frac{1}{\sigma_v^2}\sum_{k=1}^{n}\sum_{s=1}^{3}[(\frac{\partial g_{k,s}(\theta)}{\partial\theta_i}\frac{\partial g_{k,s}(\theta)}{\partial\theta_j}) + (p_{k,s} - g_{k,s}(\theta))(-\frac{\partial^2 g_{k,s}(\theta)}{\partial\theta_i\theta_j})]\end{aligned}$$

Taking the negative expected value yields,

$$-E\left[\frac{\partial^2 l(\theta)}{\partial \theta_i^2}\right] = \frac{1}{\sigma_v^2}\sum_{k=1}^{n}\sum_{s=1}^{3}(\frac{\partial g_{k,s}(\theta)}{\partial \theta_i})^2 \qquad \text{if } i = j;$$

$$-E\left[\frac{\partial^2 l(\theta)}{\partial \theta_i \theta_j}\right] = \frac{1}{\sigma_v^2}\sum_{k=1}^{n}\sum_{s=1}^{3}\frac{\partial g_{k,s}(\theta)}{\partial \theta_i}\frac{\partial g_{k,s}(\theta)}{\partial \theta_j} \qquad \text{if } i \neq j$$

and we get the result in Equations 6.1.2.

APPENDIX B:

B.1. Lower Bound Accuracy Measures Equations

The lower bound on the accuracy measures defined in 6.10, so the multiplications of members are given as follows:

$$F_{22}F_{33} = \underbrace{9C\sum_{k=1}^{n}\sum_{t=1}^{n}(\alpha^2\frac{u_{ky}^2}{d_k^2}(\ln d_t)^2)}_{c1} + ExtraTerms_1$$

$$F_{23}^2 = \underbrace{9C\sum_{k=1}^{n}\sum_{t=1}^{n}(\alpha^2\frac{u_{ky}u_{ty}}{d_k d_t}\ln d_k \ln d_t)}_{c2} + ExtraTerms_2$$

$$F_{11}F_{33} = \underbrace{9C\sum_{k=1}^{n}\sum_{t=1}^{n}(\alpha^2\frac{u_{kx}u_{tx}}{d_k d_t}\ln d_k \ln d_t)}_{c3} + ExtraTerms_3$$

$$F_{13}^2 = \underbrace{9C\sum_{k=1}^{n}\sum_{t=1}^{n}(\alpha^2\frac{u_{kx}u_{tx}}{d_k d_t}\ln d_k \ln d_t)}_{c4} + ExtraTerms_4$$

Where $C = (\frac{1}{\sigma_v^2}\frac{10}{ln_10})^4$ and ExtraTerms are multiplication of terms coming from radition pattern and path-loss terms.

Thus, $ExtraTerms$ can be explicitly given as:

$$ExtraTerms_1 = -3C\sum_{k=1}^{n}\sum_{t=1}^{n}\sum_{s=1}^{3}(2\alpha\frac{u_{ky}}{d_k}\frac{\partial \ln A_{k,s}(x,y)}{\partial y} - (\frac{\partial A_{k,s}(x,y)}{\partial y})^2)(\ln d_t)^2$$

$$\begin{aligned}ExtraTerms_2 = &-3C\sum_{k=1}^{n}\sum_{t=1}^{n}\sum_{z=1}^{3}\alpha\frac{u_{ky}}{d_k}\ln d_k \ln d_t\frac{\partial \ln A_{t,z}(x,y)}{\partial y}\\ &- 3C\sum_{k=1}^{n}\sum_{t=1}^{n}\sum_{s=1}^{3}\alpha\frac{u_{ty}}{d_t}\ln d_k \ln d_t\frac{\partial \ln A_{k,s}(x,y)}{\partial y}\\ &+ C\sum_{k=1}^{n}\sum_{t=1}^{n}\sum_{s=1}^{3}\sum_{z=1}^{3}\ln d_k \ln d_t\frac{\partial \ln A_{k,s}(x,y)}{\partial y}\frac{\partial \ln A_{t,z}(x,y)}{\partial y}\end{aligned}$$

$$ExtraTerms_3 = -3C\sum_{k=1}^{n}\sum_{t=1}^{n}\sum_{s=1}^{3}(2\alpha\frac{u_{kx}}{d_k}\frac{\partial \ln A_{k,s}(x,y)}{\partial x} - (\frac{\partial A_{k,s}(x,y)}{\partial x})^2)(\ln d_t)^2$$

$$\begin{aligned}ExtraTerms_4 = &-3C\sum_{k=1}^{n}\sum_{t=1}^{n}\sum_{z=1}^{3}\alpha\frac{u_{kx}}{d_k}\ln d_k \ln d_t\frac{\partial \ln A_{t,z}(x,y)}{\partial x}\\ &- 3C\sum_{k=1}^{n}\sum_{t=1}^{n}\sum_{s=1}^{3}\alpha\frac{u_{tx}}{d_t}\ln d_k \ln d_t\frac{\partial \ln A_{k,s}(x,y)}{\partial x}\\ &+ C\sum_{k=1}^{n}\sum_{t=1}^{n}\sum_{s=1}^{3}\sum_{z=1}^{3}\ln d_k \ln d_t\frac{\partial \ln A_{k,s}(x,y)}{\partial x}\frac{\partial \ln A_{t,z}(x,y)}{\partial x}\end{aligned}$$

So, $F_{22}F_{33} - F_{23}^2 + F_{11}F_{33} - F_{13}^2$ can simplified as follows and also verified in [32]:

$$= 9C(c_1 - c_2 + c_3 - c_4) + ExtraTerms* \tag{B.1}$$

$$= 9C\alpha^2\sum_{k=1}^{n-1}\sum_{t=k+1}^{n}[(\frac{\ln d_t}{d_k} - \frac{\ln d_k}{d_t})^2 + 2\frac{\ln d_t \ln d_k}{d_k d_t}(1-\cos\phi_{kt})] + ExtraTerms* \tag{B.2}$$

Similarly, detF is

$$\begin{aligned}|F| = &+F_{11}F_{22}F_{33} - F_{11}F_{23}F_{32}\\ &+F_{12}F_{23}F_{31} - F_{12}F_{21}F_{33}\\ &+F_{13}F_{21}F_{32} - F_{13}F_{22}F_{31}\end{aligned}$$

So, the multiplications are:

$$\begin{aligned}F_{11}F_{22}F_{33} = &(\frac{1}{\sigma_v^2}\frac{10}{\ln_1 0})^6 \sum_{k=1}^{n}\sum_{s=1}^{3}(-\alpha\frac{u_{kx}}{d_k} + \frac{\partial \ln A_{k,s}(x,y)}{\partial x})^2\\ &\cdot\sum_{k=1}^{n}\sum_{s=1}^{3}(-\alpha\frac{u_{ky}}{d_k} + \frac{\partial \ln A_{k,s}(x,y)}{\partial y})^2 \cdot \sum_{k=1}^{n}\sum_{s=1}^{3}(\ln d_k)^2\\ &= \underbrace{27B\sum_{k,l,m=1}^{n}\alpha^4\frac{u_{kx}^2}{d_k}\frac{u_{ly}^2}{d_l}\ln^2 d_m}_{C6} + ExtraTerms_5\end{aligned}$$

$$\begin{aligned}F_{11}F_{23}F_{32} = &B\sum_{k=1}^{n}\sum_{s=1}^{3}(-\alpha\frac{u_{kx}}{d_k} + \frac{\partial \ln A_{k,s}(x,y)}{\partial x})^2\\ &\cdot\sum_{k=1}^{n}\sum_{s=1}^{3}(-\alpha\frac{u_{ky}}{d_k} + \frac{\partial \ln A_{k,s}(x,y)}{\partial y})\\ &\cdot\sum_{k=1}^{n}\sum_{s=1}^{3}(-\alpha\frac{u_{ky}}{d_k} + \frac{\partial \ln A_{k,s}(x,y)}{\partial y})\ln d_k\\ &= \underbrace{27B\sum_{k,l,m=1}^{n}\alpha^4\frac{u_{kx}^2}{d_k^2}\frac{u_{ly}u_{my}}{d_l d_m}\ln d_m \ln d_l}_{C7} + ExtraTerms_6\end{aligned}$$

$$F_{12}F_{23}F_{31} = B\sum_{k=1}^{n}\sum_{s=1}^{3}(-\alpha\frac{u_{kx}}{d_k}+\frac{\partial \ln A_{k,s}(x,y)}{\partial x})(-\alpha\frac{u_{ky}}{d_k}+\frac{\partial \ln A_{k,s}(x,y)}{\partial y})$$
$$\cdot\sum_{k=1}^{n}\sum_{s=1}^{3}(-\alpha\frac{u_{ky}}{d_k}+\frac{\partial \ln A_{k,s}(x,y)}{\partial y})\ln d_k$$
$$\cdot\sum_{k=1}^{n}\sum_{s=1}^{3}(-\alpha\frac{u_{kx}}{d_k}+\frac{\partial \ln A_{k,s}(x,y)}{\partial x})\ln d_k$$
$$= \underbrace{27B\sum_{k,l,m=1}^{n}\alpha^4\frac{u_{kx}u_{ky}}{d_k^2}\frac{u_{ly}u_{mx}}{d_l d_m}\ln d_m \ln d_l}_{C8} + ExtraTerms_7$$

$$F_{12}F_{21}F_{33} = B[\sum_{k=1}^{n}\sum_{s=1}^{3}(-\alpha\frac{u_{kx}}{d_k}+\frac{\partial \ln A_{k,s}(x,y)}{\partial x})(-\alpha\frac{u_{ky}}{d_k}+\frac{\partial \ln A_{k,s}(x,y)}{\partial y})]^2$$
$$\cdot\sum_{k=1}^{n}\sum_{s=1}^{3}\ln^2 d_k$$
$$= \underbrace{27B\sum_{k,l,m=1}^{n}\alpha^4\frac{u_{kx}u_{ky}}{d_k^2}\frac{u_{my}u_{mx}}{d_m^2}\ln^2 d_l}_{C9} + ExtraTerms_8$$

$$F_{13}F_{21}F_{32} = B\sum_{k=1}^{n}\sum_{s=1}^{3}(-\alpha\frac{u_{kx}}{d_k}+\frac{\partial \ln A_{k,s}(x,y)}{\partial x})\ln d_k$$
$$\cdot\sum_{k=1}^{n}\sum_{s=1}^{3}(-\alpha\frac{u_{kx}}{d_k}+\frac{\partial \ln A_{k,s}(x,y)}{\partial x})(-\alpha\frac{u_{ky}}{d_k}+\frac{\partial \ln A_{k,s}(x,y)}{\partial y})$$
$$\cdot\sum_{k=1}^{n}\sum_{s=1}^{3}(-\alpha\frac{u_{ky}}{d_k}+\frac{\partial \ln A_{k,s}(x,y)}{\partial y})\ln d_k$$
$$= \underbrace{27B\sum_{k,l,m=1}^{n}\alpha^4\frac{u_{kx}u_{lx}}{d_l^2}\frac{u_{ly}u_{my}}{d_k d_m}\ln d_k \ln d_m}_{C10} + ExtraTerms_9$$

$$F_{13}F_{22}F_{31} = B\sum_{k=1}^{n}\sum_{s=1}^{3}(-\alpha\frac{u_{kx}}{d_k} + \frac{\partial \ln A_{k,s}(x,y)}{\partial x})\ln d_k$$
$$\cdot\sum_{l=1}^{n}\sum_{z=1}^{3}(-\alpha\frac{u_{lx}}{d_l} + \frac{\partial \ln A_{k,s}(l,z)}{\partial y})\ln d_l$$
$$\cdot\sum_{m=1}^{n}\sum_{\beta=1}^{3}(-\alpha\frac{u_{my}}{d_m} + \frac{\partial \ln A_{m,\beta}(x,y)}{\partial y})^2$$
$$= \underbrace{27B\sum_{k,l,m=1}^{n}\alpha^4\frac{u_{my}^2}{d_m^2}\frac{u_{lx}u_{kx}}{d_l d_k}\ln d_l \ln d_k}_{C11} + ExtraTerms_{10}$$

As the same way we derived the numerator, we get the following analytical representation for determinant and already verified the first part [32].

$$|F| = 27B\alpha^4(c_6 - c_7 + c_8 - c_9 + c_{10} - c_{11}+) + ExtraTerms^{**} \tag{B.3}$$
$$= 27B\alpha^4\sum_{m=1}^{n}[\sum_{k=1}^{n-1}\sum_{t=k+1}^{n}\frac{(\ln d_m)^2}{d^2kd^2l}\sin^2\phi kl + \sum_{k=1}^{n-1}\sum_{l=1}^{n}\frac{\ln d_l \ln d_m}{d_k^2 d_l d_m}\sin\phi_{kl}\sin\phi_{mk}] + ExtraTerms^{**} \tag{B.4}$$

Where $B = (\frac{1}{\sigma_v^2}\frac{10}{\ln_1 0})^6$.

Thus, $ExtraTerms*$ can be explicitly given as:

$$ExtraTerms_5 = 3B \sum_{k,l,m=1}^{n} \sum_{s,z=1}^{3} \alpha^2 \frac{u_{kx}^2}{d_k^2} \ln^2 d_m (-2\alpha \frac{u_{ly}}{d_l} \frac{\partial \ln A_{l,z}(x,y)}{\partial y} + (\frac{\partial \ln A_{l,z}(x,y)}{\partial y})^2)$$
$$+ 3B \sum_{k,l,m=1}^{n} \sum_{s,z=1}^{3} [-2\alpha \frac{u_{kx}}{d_k} \frac{\partial \ln A_{k,s}(x,y)}{\partial x} + (\frac{\partial \ln A_{l,z}(x,y)}{\partial x})^2] \ln^2 d_m$$
$$[\frac{\alpha^2 u_{l_y}^2}{d_l^2} \frac{-2\alpha u_{ly}}{d_l} \frac{\partial \ln A_{l,z}(x,y)}{\partial y} (\frac{\partial \ln A_{l,z}(x,y)}{\partial y})^2]$$

$$ExtraTerms_6 = B \sum_{k,l,m=1}^{n} \sum_{s,z,\beta=1}^{3} \alpha^2 \frac{u_{kx}^2}{d_k^2} \ln d_t \ln d_m [-\alpha \frac{u_{ly}}{d_l} \frac{\partial \ln A_{m,\beta}(x,y)}{\partial y} -$$
$$\alpha \frac{u_{my}}{d_m} \frac{\partial \ln A_{l,z}(x,y)}{\partial y} - \frac{\partial \ln A_{l,z}(x,y)}{\partial y} \frac{\partial \ln A_{m,\beta}(x,y)}{\partial y}]$$
$$+ B \sum_{k,l,m=1}^{n} \sum_{s,z,\beta=1}^{3} \ln d_t \ln d_m [(-2\alpha u_{kx} \frac{\partial \ln A_{k,s}(x,y)}{\partial x} + (\frac{\partial \ln A_{k,s}(x,y)}{\partial x})^2)$$
$$(-\frac{\alpha u_{ly}}{d_l} + \frac{\partial \ln A_{l,z}(x,y)}{\partial y})(-\frac{\alpha u_{my}}{d_m} + \frac{\partial \ln A_{m,\beta}(x,y)}{\partial y})^2)]$$

$$ExtraTerms_7 = B \sum_{k,l,m=1}^{n} \sum_{s,z,\beta=1}^{3} -\alpha^3 \frac{u_{kx} u_{ky}}{d_k^2} \frac{u_{ly}}{d_l} \ln d_t \ln d_m \frac{\partial \ln A_{m,\beta}(x,y)}{\partial y}$$
$$+ B \sum_{k,l,m=1}^{n} \sum_{s,z,\beta=1}^{3} [\alpha^2 \frac{u_{kx} u_{ky}}{d_k^2} \frac{\partial \ln A_{l,z}(x,y)}{\partial y}$$
$$+ (-\alpha \frac{u_{kx}}{d_k} \frac{\partial \ln A_{k,s}(x,y)}{\partial y} - \alpha \frac{u_{ky}}{d_k} \frac{\partial \ln A_{k,s}(x,y)}{\partial x} + \frac{\partial \ln A_{k,s}(x,y)}{\partial x} \frac{\partial \ln A_{k,s}(x,y)}{\partial y})$$
$$(-\alpha \frac{u_{ly}}{d_l} + \frac{\partial \ln A_{l,z}(x,y)}{\partial y})] \ln d_l \ln d_m [(-\alpha \frac{u_{mx}}{d_m} + \frac{\partial \ln A_{m,\beta}(x,y)}{\partial x}]$$

$$ExtraTerms_8 = 3B \sum_{k,l,m=1}^{n} \sum_{s,z,\beta=1}^{3} \alpha^2 \frac{u_{kx}u_{ky}}{d_k^2} \ln^2 d_l [-\alpha \frac{u_{mx}}{d_m} \frac{\partial \ln A_{m,z}(x,y)}{\partial y} -$$
$$\alpha \frac{u_{my}}{d_m} \frac{\partial \ln A_{m,z}(x,y)}{\partial x} - \frac{\partial \ln A_{m,z}(x,y)}{\partial x} \frac{\partial \ln A_{m,z}(x,y)}{\partial y}]$$
$$+ 3B \sum_{k,l,m=1}^{n} \sum_{s,z,\beta=1}^{3} \ln^2 d_l [(-\frac{\alpha}{d_k} u_{kx} \frac{\partial \ln A_{k,s}(x,y)}{\partial y} + \frac{\alpha}{d_k} u_{ky} \frac{\partial \ln A_{k,s}(x,y)}{\partial x})$$
$$+ \frac{\partial \ln A_{k,s}(x,y)}{\partial x} \frac{\partial \ln A_{k,s}(x,y)}{\partial y}$$
$$(-\frac{\alpha^2 u_{mx}u_{my}}{d_m^2} + -\frac{\alpha}{d_m} u_{mx} \frac{\partial \ln A_{m,z}(x,y)}{\partial y} - \frac{\alpha u_{my}}{d_m} \frac{\partial \ln A_{m,z}(x,y)}{\partial x}) +$$
$$\frac{\partial \ln A_{m,z}(x,y)}{\partial x} \frac{\partial \ln A_{m,z}(x,y)}{\partial y}]$$

$$ExtraTerms_9 = B \sum_{k,l,m=1}^{n} \sum_{s,z,\beta=1}^{3} -\alpha^3 \frac{u_{kx}u_{ky}}{d_k^2} \frac{u_{ly}}{d_l} \ln d_t \ln d_m \frac{\partial \ln A_{m,\beta}(x,y)}{\partial y}$$
$$+ B \sum_{k,l,m=1}^{n} \sum_{s,z,\beta=1}^{3} [\alpha^2 \frac{u_{kx}u_{ky}}{d_k^2} \frac{\partial \ln A_{l,z}(x,y)}{\partial y}$$
$$+ (-\alpha \frac{u_{kx}}{d_k} \frac{\partial \ln A_{k,s}(x,y)}{\partial y} - \alpha \frac{u_{ky}}{d_k} \frac{\partial \ln A_{k,s}(x,y)}{\partial x} + \frac{\partial \ln A_{k,s}(x,y)}{\partial x} \frac{\partial \ln A_{k,s}(x,y)}{\partial y})$$
$$(-\alpha \frac{u_{ly}}{d_l} + \frac{\partial \ln A_{l,z}(x,y)}{\partial y})] \ln d_l \ln d_m [(-\alpha \frac{u_{mx}}{d_m} + \frac{\partial \ln A_{m,\beta}(x,y)}{\partial x}]$$

$$ExtraTerms_{10} = B \sum_{k,l,m=1}^{n} \sum_{s,z,\beta=1}^{3} \alpha^2 \frac{u_{kx}^2}{d_k^2} \ln d_t \ln d_m [-\alpha \frac{u_{ly}}{d_l} \frac{\partial \ln A_{m,\beta}(x,y)}{\partial y} -$$
$$\alpha \frac{u_{my}}{d_m} \frac{\partial \ln A_{l,z}(x,y)}{\partial y} - \frac{\partial \ln A_{l,z}(x,y)}{\partial y} \frac{\partial \ln A_{m,\beta}(x,y)}{\partial y}]$$
$$+ B \sum_{k,l,m=1}^{n} \sum_{s,z,\beta=1}^{3} \ln d_t \ln d_m [(-2\alpha u_{kx} \frac{\partial \ln A_{k,s}(x,y)}{\partial x} + (\frac{\partial \ln A_{k,s}(x,y)}{\partial x})^2)$$
$$(-\frac{\alpha u_{ly}}{d_l} + \frac{\partial \ln A_{l,z}(x,y)}{\partial y})(-\frac{\alpha u_{my}}{d_m} + \frac{\partial \ln A_{m,\beta}(x,y)}{\partial y})^2)]$$

APPENDIX C:

C.1. Need for Four-Quadrant Inverse Tangent

The tangent function has a period of π, i.e. $tan(\phi + \pi) = tan(\phi)$. Consequently the inverse of the tangent function is not uniquely defined. However if we restrict the domain of tan to the interval between $-\pi/2$ and $\pi/2$ it becomes a continuous one to one map onto the real line. This makes it convenient to restrict the range of the inverse function to the interval between $-\pi/2$ and $\pi/2$. This gives a continuous function that is one to one on the whole real line. This inverse is called $arctan$.

Even though arctan is a convenient function it cannot give us the angular coordinate for some points in plane. For example consider the points (1, 1) and (-1,-1). They are collinear with the origin and the slope of this line is 1. We can substitute this slope into the arctan function to get the angular coordinate of (1, 1) (i.e. the angle that the ray starting at the origin and passing through (1, 1) makes with the positive x-axis). This angle is $\pi/4 = arctan(1)$. However the angular coordinate of (-1,-1) is $3\pi/4$ (or $5\pi/4$) which is outside of the range of $arctan$.

One way to avoid this problem is to define a function which makes use of both the horizontal and vertical coordinates of the point. That is the purpose of the $atan2$ function. Its range is the interval between $-\pi$ and π along with the value π. The $atan2$, equivalently $arctan_{4Q}$, function can be defined in terms of $arctan$ as follows:

$$arctan_{4Q}(y,x) = \begin{cases} arctan(y/x), & \text{if } x > 0 \\ \pi + arctan(y/x), & \text{if } y \geq 0, x < 0 \\ -\pi + arctan(y/x), & \text{if } y < 0, x < 0 \\ \pi/2, & \text{if } y > 0, x = 0 \\ -\pi/2, & \text{if } y < 0, x = 0 \\ undefined, & \text{if } y = 0, x = 0 \end{cases} \tag{C.1}$$

$arctan_{4Q}$ is left undefined for the point (0, 0). Note that it is conventional to put the y coordinate before the x coordinate in $arctan_{4Q}(y, x)$, but for easy use we will use in straight forward in our equations.

The diagram below show 3D view of $arctan_{4Q}(y, x)$ over a region of the plane.

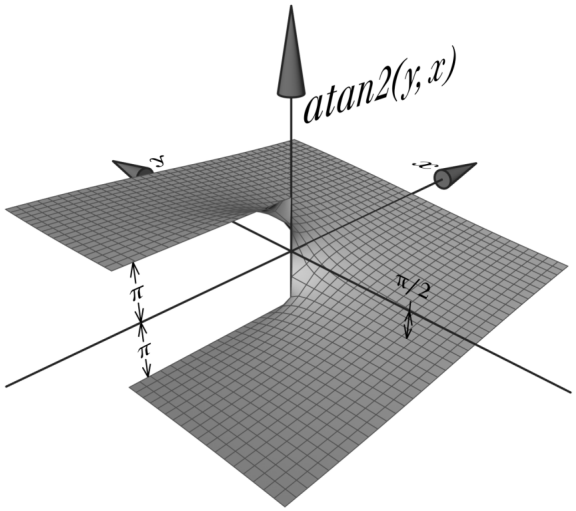

Figure C.1. 3D view of $arctan_{4Q}$

C.2. Limits and Continuity of Four-Quadrant Arc-Tangent

To discuss continuity of $arctan_4Q(x, y)$, lets look the values of the neighbourhood of the points given in the figure C.2.

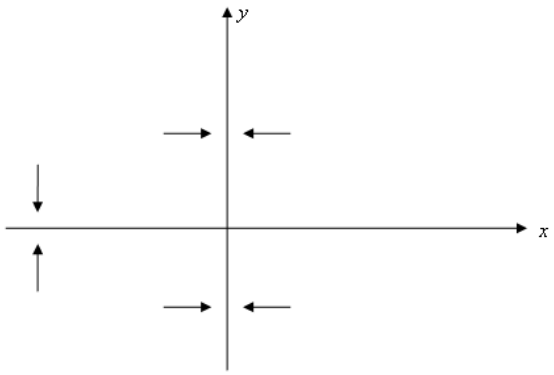

Figure C.2. continuity check points

1. $\boxed{x = 0,\ \ y > 0}$

- Right hand limit and Left hand limit:

$$\begin{aligned}
\lim_{x\to 0^+} arctan_{4Q}(x,y) &= \lim_{x\to 0^+} arctan(y/x), \quad since \;\; x>0, y>0 \\
&= \lim_{u\to +\infty} arctan(u) \\
&= \pi/2 \\
\lim_{x\to 0^-} arctan_{4Q}(x,y) &= \pi + \lim_{x\to 0^-} arctan(y/x), \quad since \;\; x<0, y>0 \\
&= \pi + \lim_{u\to -\infty} arctan(u) \\
&= \pi - \pi/2 \\
&= \pi/2
\end{aligned}$$

So, right hand limit and left hand limit are equal. Therefore,

$arctan_{4Q}(x,y)$ is continuous at $x=0$, $y>0$. $\surd$

2. $\boxed{x=0, \;\; y<0}$

- Right hand limit and Left hand limit:

$$\begin{aligned}
\lim_{x\to 0^+} arctan_{4Q}(x,y) &= \lim_{x\to 0^+} arctan(y/x), \quad since \;\; x>0, y<0 \\
&= \lim_{u\to -\infty} arctan(u) \\
&= -\pi/2 \\
\lim_{x\to 0^-} arctan_{4Q}(x,y) &= -\pi + \lim_{x\to 0^-} arctan(y/x), \quad since \;\; x<0, y<0 \\
&= -\pi + \lim_{u\to +\infty} arctan(u) \\
&= -\pi + \pi/2 \\
&= -\pi/2
\end{aligned}$$

Thus, $arctan_{4Q}(x,y)$ is continuous at $x=0$, $y<0$. $\surd$

3. $\boxed{x<0, \;\; y=0}$

- Right hand and Left hand limit:

$$\begin{aligned}
\lim_{y\to 0^+} arctan_{4Q}(x,y) &= \pi + \lim_{y\to 0^+} arctan(y/x), \quad since \;\; y>0, x<0 \\
&= \pi + \lim_{u\to 0^-} arctan(u) \\
&= \pi \\
\lim_{y\to 0^-} arctan_{4Q}(x,y) &= -\pi + \lim_{y\to 0^-} arctan(y/x), \quad since \;\; x<0, y<0 \\
&= -\pi + \lim_{u\to 0^+} arctan(u) \\
&= -\pi
\end{aligned}$$

So, right and left hand limit are not equal. Hence,

$$\Rightarrow \lim_{y\to 0^-} arctan_{4Q}(x,y) = -\pi = \pi = \lim_{y\to 0^+} arctan_{4Q}(x,y) \;\; \text{for} \;\; x<0$$

Thus, $arctan_{4Q}(x,y)$ is <u>discontinuous</u> at $y=0$, $x<0$.

C.3. Further Discussion: Continuity of Derivation of $arctan_{4Q}$

C.3.1. The Definitions:

$$tan(\phi) = u = \frac{sin\phi}{cos\phi}, \text{and} cos\phi = \frac{1}{sqrt(1+u^2)}$$

Taking derivative of u respect to ϕ, we get:

$$\begin{aligned}
\frac{du}{d\phi} &= \frac{sin'\phi cos\phi - cos'\phi sin\phi}{cos^2\phi} = \frac{cos^2\phi + sin^2\phi}{cos^2\phi} \\
\frac{du}{d\phi} &= \frac{1}{cos^2\phi} = 1+u^2 \quad \Rightarrow \frac{d\phi}{du} = \frac{1}{1+u^2}
\end{aligned}$$

Thus, replacing u with $\frac{y}{x}$, and derivative against x, and y respectively:

$$\frac{\partial}{\partial x} arctan(\frac{y}{x}) = \frac{1}{1+(y/x)^2}(\frac{-y}{x^2}) = \frac{-y}{x^2+y^2}$$
$$\frac{\partial}{\partial y} arctan(\frac{y}{x}) = \frac{1}{1+(y/x)^2}(\frac{1}{x}) = \frac{x}{x^2+y^2}$$

Therefore, the partial derivatives of x and y are continuous functions of x and y except at $x = y = 0$.

C.3.2. Partial Derivatives of $arctan$ wrt x

1. $\boxed{x < 0,\ \ y > 0}$

$$\begin{aligned}\frac{\partial}{\partial x}\left(arctan_{4Q}(x,y)\right) &= \frac{\partial}{\partial x}(\pi + arctan\frac{y}{x}) \\ &= \frac{-y}{x^2+y^2}\end{aligned}$$

2. $\boxed{x > 0,\ \ y > 0}$

$$\frac{\partial}{\partial x}\left(arctan_{4Q}(x,y)\right) = \frac{-y}{x^2+y^2}$$

3. $\boxed{x = 0,\ \ y > 0}$

$$\begin{aligned}
\frac{\partial}{\partial x}(arctan_{4Q}(x,y)|_{x=0} &= \lim_{\Delta x \to 0^+} (arctan_{4Q}(\Delta x, y) - arctan_{4Q}(0,y)) \\
&= \lim_{\Delta x \to 0^+} \frac{1}{\Delta x} (arctan(y/\Delta x) - \pi/2) \\
&= \lim_{\Delta x \to 0^+} \left(\frac{\frac{1}{1+(y/\Delta x)^2} \frac{-y}{(\Delta x)^2}}{1} \right) \\
&= \lim_{\Delta x \to 0^+} \frac{-y}{y^2 + (\Delta x)^2} = \lim_{\Delta x \to 0^+} \frac{-1}{y} = \frac{-1}{y} \surd
\end{aligned}$$

$$\begin{aligned}
&= \lim_{\Delta x \to 0^-} (arctan_{4Q}(\Delta x, y) - arctan_{4Q}(0,y)) \\
&= \lim_{\Delta x \to 0^-} \frac{1}{\Delta x} (arctan(y/\Delta x) - \pi/2) \\
&= \lim_{\Delta x \to 0^-} \left(\frac{\frac{1}{1+(y/\Delta x)^2} \frac{-y}{(\Delta x)^2}}{1} \right) \\
&= \lim_{\Delta x \to 0^-} \frac{-y}{y^2 + (\Delta x)^2} = \lim_{\Delta x \to 0^+} \frac{-1}{y} = \frac{-1}{y} \surd
\end{aligned}$$

Therefore for $x = 0$, and $y > 0$

$$\frac{\partial}{\partial x}(arctan_{4Q}(x,y)|_{x=0} = \frac{-1}{y}$$

exists and is continuous at $x = 0$, $y > 0$.

4. $\boxed{x = 0,\ \ y < 0}$

$$\begin{aligned}
\frac{\partial}{\partial x}(arctan_{4Q}(x,y)|_{x=0} &= \lim_{\Delta x\to 0^+}(arctan_{4Q}(\Delta x,y) - arctan_{4Q}(0,y)) \\
&= \lim_{\Delta x\to 0^+}\frac{1}{\Delta x}\left(arctan(y/\Delta x) - (-\pi/2)\right) \\
&= \lim_{\Delta x\to 0^+}\left(\frac{\frac{1}{1+(y/\Delta x)^2}\frac{-y}{(\Delta x)^2}}{1}\right) \\
&= \lim_{\Delta x\to 0^+}\frac{-y}{y^2+(\Delta x)^2} = \lim_{\Delta x\to 0^+}\frac{-1}{y} = -\frac{1}{y}\surd
\end{aligned}$$

$$\begin{aligned}
&= \lim_{\Delta x\to 0^-}(arctan_{4Q}(\Delta x,y) - arctan_{4Q}(0,y)) \\
&= \lim_{\Delta x\to 0^-}\frac{1}{\Delta x}\left(arctan(y/\Delta x) - (-\pi/2)\right) \\
&= \lim_{\Delta x\to 0^-}\left(\frac{\frac{1}{1+(y/\Delta x)^2}\frac{-y}{(\Delta x)^2}}{1}\right) \\
&= \lim_{\Delta x\to 0^-}\frac{-y}{y^2+(\Delta x)^2} = \lim_{\Delta x\to 0^+}\frac{-1}{y} = -\frac{1}{y}\surd
\end{aligned}$$

Therefore for $x = 0$, and $y < 0$

$$\Rightarrow \frac{\partial}{\partial x}(arctan_{4Q}(x,y)|_{x=0} = -\frac{1}{y}$$

exists and is continuous at $x = 0$, $y < 0$.

5. $\boxed{y = 0,\ \ x < 0}$

$$\begin{aligned}\frac{\partial}{\partial x}(arctan_{4Q}(x,y)|_{y=0} &= \frac{\partial}{\partial x}[\pi + arctan(y/x)]|_{y=0} \\ &= \frac{\partial}{\partial x}[\pi + arctan(y/x)]|_{y=0} \\ &= \frac{-y}{x^2+y^2}|_{y=0} \\ &= 0\end{aligned}$$

also for $y < 0,\ x < 0$

$$\begin{aligned}\frac{\partial}{\partial x}(arctan_{4Q}(x,y)|_{y=0} &= \frac{\partial}{\partial x}[-\pi + arctan(y/x)] \\ &= \frac{-y}{x^2+y^2}\end{aligned}$$

so for $x < 0$

$$\begin{aligned}\lim_{\Delta y \to 0^-} \frac{\partial}{\partial x}(arctan_{4Q}(x,y)|_{y=0} &= \lim_{\Delta y \to 0^-} \frac{-y}{x^2+y^2} \\ &= \frac{\partial}{\partial x}(arctan_{4Q}(y/x)|_{y=0} \\ &= 0\end{aligned}$$

Therefore $\frac{\partial}{\partial x}(arctan_{4Q}(y/x)$ exists and is continuous and exists at $y = 0,\ x < 0$.

$\frac{\partial}{\partial x}(arctan_{4Q}(y/x)$ does it exist everywhere, and is it continuous?

C.3.3. Partial Derivatives of $arctan_{4Q}$ wrt y

1. $\boxed{x = 0,\ y > 0}$

$$\begin{aligned}
\frac{\partial}{\partial y}(arctan_{4Q}(x,y)|_{x=0} &= \lim_{\Delta y\to 0}\frac{1}{\Delta y}\left(arctan_{4Q}(0,y+\Delta y) - arctan_{4Q}(0,y)\right)\\
&= \lim_{\Delta y\to 0}\frac{1}{\Delta y}(\pi/2-\pi/2)\\
&= 0\\
\lim_{x\to 0^+}\frac{\partial}{\partial y}arctan_{4Q}(x,y) &= \lim_{x\to 0^+}\frac{\partial}{\partial y}arctan(y/x)\\
&= \lim_{x\to 0^+}\frac{x}{x^2+y^2} = 0\\
\lim_{x\to 0^-}\frac{\partial}{\partial y}arctan_{4Q}(x,y) &= \lim_{x\to 0^-}\frac{\partial}{\partial y}(\pi + arctan(y/x))\\
&= \lim_{x\to 0^-}\frac{x}{x^2+y^2} = 0
\end{aligned}$$

$\Rightarrow \frac{\partial}{\partial y}arctan_{4Q}(x,y)$ exist and is continuous at $x=0$, $y>0$.

2. $\boxed{x=0,\ \ y<0}$

$$\begin{aligned}
\frac{\partial}{\partial y}(arctan_{4Q}(x,y)|_{x=0} &= \lim_{\Delta y\to 0}\frac{1}{\Delta y}\left(arctan_{4Q}(0,y+\Delta y) - arctan_{4Q}(0,y)\right)\\
&= \lim_{\Delta y\to 0}\frac{1}{\Delta y}(-\pi/2-(-\pi/2))\\
&= 0\\
\lim_{x\to 0^+}\frac{\partial}{\partial y}arctan_{4Q}(x,y) &= \lim_{x\to 0^+}\frac{\partial}{\partial y}arctan(y/x)\\
&= \lim_{x\to 0^+}\frac{x}{x^2+y^2} = 0\\
\lim_{x\to 0^-}\frac{\partial}{\partial y}arctan_{4Q}(x,y) &= \lim_{x\to 0^-}\frac{\partial}{\partial y}(-\pi + arctan(y/x))\\
&= \lim_{x\to 0^-}\frac{x}{x^2+y^2} = 0
\end{aligned}$$

$\Rightarrow \frac{\partial}{\partial y}arctan_{4Q}(x,y)$ exist and is continuous at $x=0$, $y<0$.

3. $\boxed{y=0,\ \ x<0}$

$\frac{\partial}{\partial y} arctan_{4Q}(x,y)$ undefined because $arctan_{4Q}(x,y)$ is discontinuous wrt y. But,

$$\begin{aligned}
\lim_{y\to 0^+} \frac{\partial}{\partial y} arctan_{4Q}(x,y) &= \lim_{y\to 0^+} \frac{\partial}{\partial y}(\pi + arctan(y/x)) \\
&= \lim_{y\to 0^+} \frac{x}{x^2+y^2} = \frac{1}{x} \\
\lim_{y\to 0^-} \frac{\partial}{\partial y} arctan_{4Q}(x,y) &= \lim_{y\to 0^-} \frac{\partial}{\partial y}(-\pi + arctan(y/x)) \\
&= \lim_{y\to 0^-} \frac{x}{x^2+y^2} = \frac{1}{x}
\end{aligned}$$

C.3.4. Continuity points of Log-Normal Model

Mean of our log-normal formula:

$$\mu_{k,s}(x,y) = L_o + 10\alpha \log_{10} d_{k,s}(x,y) - 20 \log_{10} A_{k,s}(x,y)$$

where

$$\begin{aligned}
&\Delta\phi_{k,s}(x,y) = f^*(\phi_k(x,y) - \phi_{k,s}) \\
&f^*(x) = ((x+\pi)_{mod 2\pi} - \pi) \\
&A_{k,s}(x,y) = exp\left(-a_{3dB}(\frac{|\Delta\phi_{k,s}(x,y)|}{\phi_{HBW}})^\tau\right)
\end{aligned}$$

More compact form of radiation pattern $A_{k,s}(x,y)$:

$$\begin{aligned}
20 \log_{10} A_{k,s}(x,y) &= 20\frac{\ln A_{k,s}(x,y)}{\ln 10} \\
&= \frac{20}{\ln 10}\left(-\frac{a_{3dB}}{(\phi_{HBW})^\tau}|\Delta\phi_{k,s}(x,y)|^\tau\right)
\end{aligned}$$

let $A_c = \frac{a_{3dB}}{(\phi_{HBW})^\tau}$

$$\ln A_{k,s}(x,y) = -A_c|\Delta\phi_{k,s}(x,y)|^\tau$$

let $f(u) = -A_c(|u|)^\tau$

$\Rightarrow f'(u) = -A_c\tau|u|^{\tau-1}sgn(u)$

since $\tau > 1$, $f'(u=0) = 0$ and $f'(u)$ is continuous at $u = 0$.

$\Rightarrow f'(u) = -A_c\tau|u|^{\tau-1}sgn(u)$ is continuous everywhere.

In case $\phi_{k,s}(x,y) = arctan_{4Q}(x - x_k, y - y_k)$

$$f^*(\phi) = (\phi + \pi)_{mod2\pi} - \pi$$

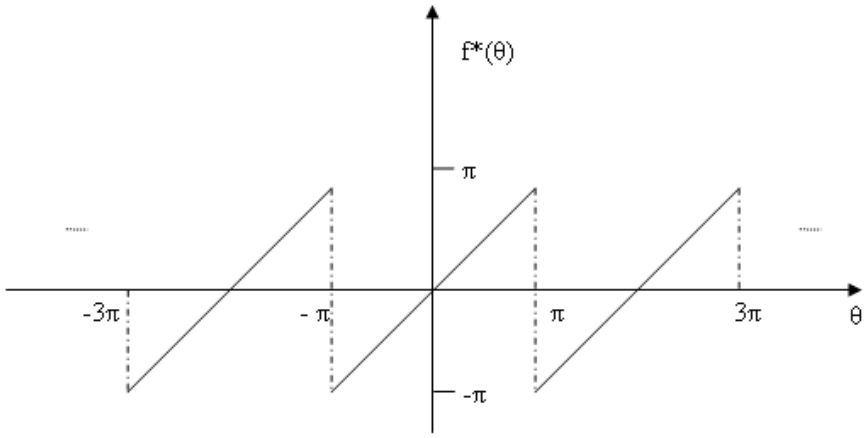

Figure C.3. f function definition

$$(f^*(\phi))' = 1 \quad \text{everywhere except at } \phi = \pi + k2\pi, \quad k \in Z$$

Taking the derivatives of radiation pattern ($A_{k,s}$) wrt x and y:

$$\frac{\partial}{\partial x}\ln A_{k,s}(x,y) = -A_c\tau|\Delta\phi_{k,s}(x,y)|^{\tau-1}sgn(\Delta\phi_{k,s}(x,y))(f^*(\phi_k(x,y) - \phi_{k,s}))'\frac{\partial}{\partial x}arctan_{4Q}(x - x_k, y - y_k)$$

$$\frac{\partial}{\partial y}\ln A_{k,s}(x,y) = -A_c\tau|\Delta\phi_{k,s}(x,y)|^{\tau-1}sgn(\Delta\phi_{k,s}(x,y))(f^*(\phi_k(x,y)-\phi_{k,s}))'\frac{\partial}{\partial y}arctan_{4Q}(x-x_k,y-y_k)$$

$\rightarrow$ What happens at $y - y_k = 0$, $x - x_k < 0$?,

$\rightarrow$ What happens at $\phi_k(x,y) = \phi_{k,s} + \pi$?

Conclusions:

- Discontinuities in derivatives wrt x and y exist because of the term $sgn(\phi_{k,s}(x,y))$ in both partial derivatives.
- Discontinuties in partial derivatives are on the line $|\phi_k(x,y) - \phi_{k,s}| = \pi$
- On the same line partial derivatives may not exist since $f^*(\phi_k(x,y) - \phi_{k,s}))'$ does not have a derivative.

REFERENCES

1. James J. Caffery. *Wireless location in CDMA cellular radio systems.* Springer, 2000.

2. *IEEE P802.15.4a/D4 (Amendment of IEEE Std 802.15.4), Part 15.4: Wireless medium access control(MAC) and physical layer (PHY) specifications for low-rate wireless personal area networks (LRWPANs)*, july 2006.

3. F. C. Commission. Revision of the commissions rules to insure compatibility with enhanced 911 emergency calling systems. *FCC Docket No. 94102.*, 1996.

4. J. Niemela, J. Lempiinen, and J. Borkowski. Cellular location techniques supporting agps positioning. In *Vehicular Technology Conference, 2005. VTC-2005-Fall. 2005 IEEE 62nd*, volume 1, pages 429–433, Sept. 2005.

5. Zhao Yilin. Standardization of mobile phone positioning for 3g systems. *Communications Magazine, IEEE*, 40(7):108 –116, Jul 2002.

6. K.W. Cheung, H.C. So, W.-K. Ma, and Y.T. Chan. Least squares algorithms for time-of-arrival-based mobile location. *Signal Processing, IEEE Transactions on*, 52(4):1121–1130, April 2004.

7. B.D.S. Lakmali and D. Dias. Database correlation for gsm location in outdoor and indoor environments. In *Information and Automation for Sustainability, 2008. ICIAFS 2008. 4th International Conference on*, pages 42–47, Dec. 2008.

8. S. Ahonen and H. Laitinen. Database correlation method for umts location. In *Vehicular Technology Conference, 2003. VTC 2003-Spring. The 57th IEEE Semiannual*, volume 4, pages 2696–2700 vol.4, April 2003.

9. M.A. Spirito. On the accuracy of cellular mobile station location estimation. *Ve-*

hicular Technology, IEEE Transactions on, 50(3):674–685, May 2001.

10. Mohamed Khalaf-Allah. Nonparametric bayesian filtering for location estimation, position tracking, and global localization of mobile terminals in outdoor wireless environments. *EURASIP J. Adv. Signal Process*, 2008:1–14, 2008.

11. G.M. Djuknic and R.E. Richton. Geolocation and assisted gps. *Computer*, 34(2):123 –125, Feb 2001.

12. P Rong and M.L. Sichitiu. Angle of arrival localization for wireless sensor networks. volume 1, pages 374 –382, Sept. 2006.

13. K. Raja, W.J. Buchanan, and J. Munoz. We know where you are [cellular location tracking]. *Communications Engineer*, 2(3):34–39, 2004.

14. Bora Zeytinci. Location estimation using rss measurements with unknown path loss exponents. Master's thesis, Bogazici University, Electrical and Electronics Engineering, 2009.

15. K.C. Budka, Doru Calin, Byron Chen, and D. Jeske. A bayesian method to improve mobile geolocation accuracy. In *Vehicular Technology Conference, 2002. Proceedings. VTC 2002-Fall. 2002 IEEE 56th*, volume 2, pages 1021–1025 vol.2, 2002.

16. K.M.K. Chu, K.R.P.H. Leung, J.K.-Y. Ng, and Chun Hung Li. Locating mobile stations with statistical directional propagation model. In *Advanced Information Networking and Applications, 2004. AINA 2004. 18th International Conference on*, volume 1, pages 230–235 Vol.1, 2004.

17. Yihong Qi and H. Kobayashi. On relation among time delay and signal strength based geolocation methods. In *Global Telecommunications Conference, 2003. GLOBECOM '03. IEEE*, volume 7, pages 4079–4083 vol.7, Dec. 2003.

18. R. Yamamoto, H. Matsutani, H. Matsuki, T. Oono, and H. Ohtsuka. Position location technologies using signal strength in cellular systems. In *Vehicular Technology*

Conference, 2001. VTC 2001 Spring. IEEE VTS 53rd, volume 4, pages 2570–2574 vol.4, 2001.

19. M. Aso, T. Saikawa, and T. Hattori. Maximum likelihood location estimation using signal strength and the mobile station velocity in cellular systems. In *Vehicular Technology Conference, 2003. VTC 2003-Fall. 2003 IEEE 58th*, volume 2, pages 742–746 Vol.2, Oct. 2003.

20. Junyang Zhou and Joseph Kee-Yin Ng. A data fusion approach to mobile location estimation based on ellipse propagation model within a cellular radio network. In *AINA '07: Proceedings of the 21st International Conference on Advanced Networking and Applications*, pages 459–466, Washington, DC, USA, 2007. IEEE Computer Society.

21. *Fact sheet: E-911 phase II decisions*, October 2001. `http://www.fcc.goc/Bureaus/Wireless/News_Releases/2001/nw10127a.txt`.

22. Jochen H. Schiller and Agne's Voisard. *Location-based services*. San Francisco, CA: Morgan Kaufmann Publishers, 2004.

23. J. Warrior, E. McHenry, and K. McGee. They know where you are [location detection]. *Spectrum, IEEE*, 40(7):20 – 25, july 2003.

24. *Location Based Services*, January 2003.

25. Editor-in-Chief Jerry D. Gibson. *The Communications Handbook,SECTION VI Wireless: Gordon L. Stiuber, James J. Caffery,Jr., Radiolocation Techniques,*. CRC Press LLC, 2002.

26. C. Drane, M. Macnaughtan, and C. Scott. Positioning gsm telephones. *Communications Magazine, IEEE*, 36(4):46 –54, 59, apr 1998.

27. Andrew Sage. Future positioning technologies and their application to the automotive sector. *The Journal of Navigation*, 54(03):321–328, 2001.

28. B. Hofmann-Wellenhof, K. Legat, and M. Wieser. *Navigation, Principles of Positioning and Guidance,*. Wien, 2003.

29. T. Kos, M. Grgic, and G. Sisul. Mobile user positioning in gsm/umts cellular networks. In *Multimedia Signal Processing and Communications, 48th International Symposium ELMAR-2006 focused on*, pages 185 –188, june 2006.

30. D.-B. Lin and R.-T. Juang. Mobile location estimation based on differences of signal attenuations for gsm systems. *Vehicular Technology, IEEE Transactions on*, 54(4):1447 – 1454, july 2005.

31. Sang Young Park, Hyo-Sung Ahn, and Wonpil Yu. Adaptive path-loss model-based indoor localization. pages 1 –2, jan. 2008.

32. Xinrong Li. Rss-based location estimation with unknown pathloss model. *Wireless Communications, IEEE Transactions on*, 5(12):3626–3633, December 2006.

33. J. Shirahama and T. Ohtsuki. Rss-based localization in environments with different path loss exponent for each link. pages 1509 –1513, may 2008.

34. Guoqiang Mao, Brian D. O. Anderson, and Barış Fidan. Path loss exponent estimation for wireless sensor network localization. *Comput. Netw.*, 51(10):2467–2483, 2007.

35. Joshua N. Ash and Lee C. Potter. Sensor network localization via received signal strength measurements with directional antennas. In *in Proceedings of the 2004 Allerton Conference on Communication, Control, and Computing*, pages 1861–1870, 2004.

36. K.W. Cheung, H.C. So, W.-K. Ma, and Y.T. Chan. Received signal strength based mobile positioning via constrained weighted least squares. In *Acoustics, Speech, and Signal Processing, 2003. Proceedings. (ICASSP '03). 2003 IEEE International Conference on*, volume 5, pages V – 137–40 vol.5, 6-10 2003.

37. A.J. Weiss. On the accuracy of a cellular location system based on rss measurements. *Vehicular Technology, IEEE Transactions on*, 52(6):1508 – 1518, nov. 2003.

38. R.W. Ouyang, A.K.-S. Wong, Chin-Tau Lea, and V.Y. Zhang. Received signal strength-based wireless localization via semidefinite programming. In *Global Telecommunications Conference, 2009. GLOBECOM 2009. IEEE*, pages 1 –6, nov. 2009.

39. Amer Catovic, Amer Catovic, Zafer Sahinoglu, and Zafer Sahinoglu. The cramer-rao bounds of hybrid toa/rss and tdoa/rss location estimation schemes. *IEEE Communications Letters*, 8:626–628, 2004.

40. T. Roos, P. Myllymaki, and H. Tirri. A statistical modeling approach to location estimation. *Mobile Computing, IEEE Transactions on*, 1(1):59 – 69, jan-mar 2002.

41. A.S. Soork, R. Saadat, and A.A. Tadaion. Cooperative mobile positioning based on received signal strength. In *Telecommunications, 2008. IST 2008. International Symposium on*, pages 273 –277, 27-28 2008.

42. I.G. Papageorgiou, C.D. Charalambous, and C. Panaviotou. An enhanced received signal level cellular location determination method via maximum likelihood and kalman filtering. In *Wireless Communications and Networking Conference, 2005 IEEE*, volume 4, pages 2524 – 2529 Vol. 4, 13-17 2005.

43. Kirk Martinez, Jane K. Hart, and Royan Ong. Environmental sensor networks. *Computer*, 37:50–56, 2004.

44. M. A. Alim, M. M. Rahman, M. M. Hossain, and A. Al-Nahid. Analysis of large-scale propagation models for mobile communications in urban area. *International Journal of Computer Science and Information Security*, 7(1), 2010.

45. T. Rappaport. *Wireless Communications*. Prentice Hall PTR, 2002.

46. M. Hata. Empirical formula for propagation loss in land mobile radio services. *Vehicular Technology, IEEE Transactions on*, 29(3):317 – 325, aug 1980.

47. V. et al Erceg. An empirically-based path loss model for wireless channels in suburban environments. volume 2, pages 922 –927 vol.2, 1998.

48. Kenneth M. K. et al Chu. A directional propagation model for locating mobile stations within a mobile phone network. *Int. J. Wire. Mob. Comput.*, 3(1/2):12–21, 2008.

49. A.A. Zavala and K. Koulinas. Antenna radiation pattern estimation in 3-d for indoor environments. pages 26 – 31, Feb. 2005.

50. V. Azman. Conformal antenna arrays for 3g cellular base stations. 2002.

51. Kenneth M. K. Chu, Karl R. P. H. Leung, Joseph Kee-Yin Ng, and Chun Hung Li. Locating mobile stations with statistical directional propagation model. *Advanced Information Networking and Applications, International Conference on*, 1:230, 2004.

52. D.L. Runyon. Optimum directivity coverage of fan-beam antennas. *Antennas and Propagation Magazine, IEEE*, 44(2):66–70, Apr 2002.

53. K. Pahlavan and A. Levesque. *Wireless Information Networks*. New York: John Wiley and Sons, Inc., 1995.

54. S. M. Kay. *Fundamentals of Statistical Signal Processing: Estimation Theory*. Upper Saddle River, NJ: Prentice Hall PTR, 1993.